REPORT NO.
UCB/EERC-79/04
FEBRUARY 1979

EARTHQUAKE ENGINEERING RESEARCH CENTER

A MATHEMATICAL MODEL OF MASONRY FOR PREDICTING ITS LINEAR SEISMIC RESPONSE CHARACTERISTICS

by

YALCIN MENGI
and
HUGH D. McNIVEN

Report to:
National Science Foundation
and the
North Atlantic Treaty Organization

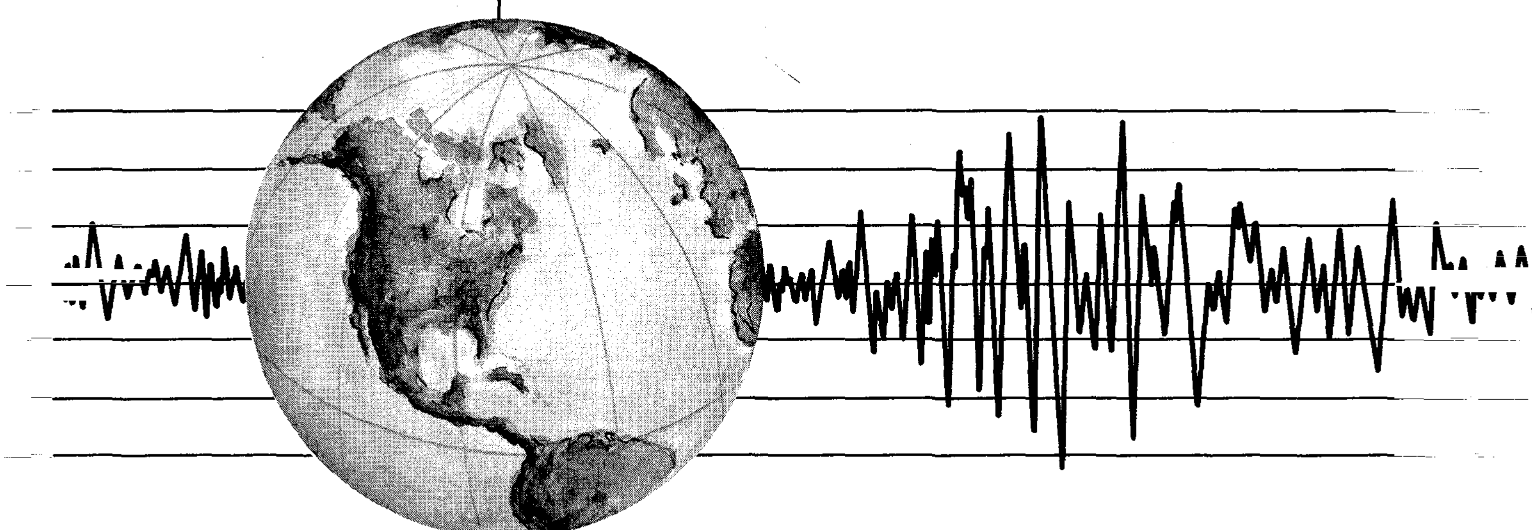

COLLEGE OF ENGINEERING

UNIVERSITY OF CALIFORNIA · Berkeley, California

BIBLIOGRAPHIC DATA SHEET	1. Report No. NSF/RA-790069	2.	3. Recipient's Accession No. PB298266

4. Title and Subtitle

A Mathematical Model of Masonry for Predicting its Linear Seismic Response Characteristics

5. Report Date: February 1979

6.

7. Author(s)

Y. Mengi and H.D. McNiven

8. Performing Organization Rept. No. UCB/EERC-79/04

9. Performing Organization Name and Address

Earthquake Engineering Research Center
University of California, Richmond Field Station
47th and Hoffman Blvd.
Richmond, California 94804

10. Project/Task/Work Unit No.

11. Contract/Grant No. ENV76-04265 and NATO No. 1446

12. Sponsoring Organization Name and Address

National Science Foundation
1800 G. Street, N.W.
Washington, D.C. 20550

13. Type of Report & Period Covered

14.

15. Supplementary Notes

16. Abstracts

This report represents work that is part of a study into the seismic behavior of masonry. The major part of the work is experimental, but this part is devoted to developing a mathematical model for masonry which could be used to derive the elastic stress field, in a wall or pier, when either is subjected to seismic loads.

Because masonry is made of two materials, and because its geometry is so complicated it is necessary, in studying stress fields that could arise, to replace the composite material by a homogeneous one. The model material must display the same constitutive characteristics as the prototype and must have the same wave dispersive properties. It is the mathematical model of such a homogeneous material that is developed in this report.

The development is made in three steps. In the first, a general theory is constructed for two phase materials. The method employed here uses the theory of mixtures applied to a two phase material in which the phases reflect a periodic structure and in which each phase is linearly elastic. Employing the fundamental equations of the theory of mixtures, the governing equations of a linear approximate theory are established. The theory, valid for an arbitrary direction of motion, replaces the composite by a homogeneous, two phase, anisotropic, elastic solid. It accommodates the dispersive nature of the composite by means of an elastodynamic operator, which is introduced into the constitutive relations of the linear momentum interactions.

The second step is to adapt the general theory to a particular geometry. The periodic material that we choose is made of alternate plane layers. This geometry is chosen for two reasons; first, the geometry of masonry can be accommodated within it, and second, because there is a wealth of material about the dynamic behavior of such materials, both analytical and experimental. The choice of geometry affects both the constitutive equations and the elastodynamic operators.

The theory for layered materials contains nineteen model constants and equations are developed from which these constants can be derived from the layered constants. The equations are derived partly using micro model analysis and partly by matching specific dynamic behaviors of the model and prototype. The ability with which the model predicts the dynamic response of the layered material is assessed in two ways. Both compare spectra reflecting the behavior of infinite trains of the principal kinds of waves. The first compares spectral lines from the model with those derived from the exact theory for layered

17c. COSATI Field/Group

18. Availability Statement	19. Security Class (This Report) UNCLASSIFIED	21. No. of Pages 115
Release Unlimited	20. Security Class (This Page) UNCLASSIFIED	22. Price A06 - A01

BIBLIOGRAPHIC DATA SHEET	1. Report No.	2.	3. Recipient's Accession No.
4. Title and Subtitle			5. Report Date
			6.
7. Author(s)			8. Performing Organization Rept. No.
9. Performing Organization Name and Address			10. Project/Task/Work Unit No.
			11. Contract/Grant No.
12. Sponsoring Organization Name and Address			13. Type of Report & Period Covered
			14.

15. Supplementary Notes

16. Abstracts

materials. The second compares lines from the model with those obtained from experiments. Predictions from the model prove to be quite accurate.

In the third phase we appraise the model by comparing the responses predicted by the model for a transient input with those observed experimentally. Experimental data allow us to make comparisons for the behavior of dilatational waves travelling both parallel and perpendicular to the layers in both plates and semi-infinite bodies. Where possible, comparison is also made with responses predicted by the exact theory. Responses in the model are found using the method of characteristics. Comparison is exhibited in a number of figures and shows that the responses predicted by the theory are quite accurate. The accuracy is not restricted to early arrival times but extends to behavior far behind the head of the pulse.

17b. Identifiers/Open-Ended Terms

17c. COSATI Field/Group

18. Availability Statement	19. Security Class (This Report) UNCLASSIFIED	21. No. of Pages
	20. Security Class (This Page UNCLASSIFIED	22. Price

A MATHEMATICAL MODEL OF MASONRY FOR PREDICTING ITS LINEAR SEISMIC RESPONSE CHARACTERISTICS

by

YALCIN MENGI

and

HUGH D. McNIVEN

Report to the

National Science Foundation

and the

North Atlantic Treaty Organization

Report No. UCB/EERC-79/04

Earthquake Engineering Research Center
College of Engineering
University of California
Berkeley, California

February 1979

ib

ABSTRACT

This report represents work that is part of a study into the seismic behavior of masonry. The major part of the work is experimental, but this part is devoted to developing a mathematical model for masonry which could be used to derive the elastic stress field, in a wall or pier, when either is subjected to seismic loads.

Because masonry is made of two materials, and because its geometry is so complicated it is necessary, in studying stress fields that could arise, to replace the composite material by a homogeneous one. The model material must display the same constitutive characteristics as the prototype and must have the same wave dispersive properties. It is the mathematical model of such a homogeneous material that is developed in this report.

The development is made in three steps. In the first, a general theory is constructed for two phase materials. The method employed here uses the theory of mixtures applied to a two phase material in which the phases reflect a periodic structure and in which each phase is linearly elastic. Employing the fundamental equations of the theory of mixtures, the governing equations of a linear approximate theory are established. The theory, valid for an arbitrary direction of motion, replaces the composite by a homogeneous, two phase, anisotropic, elastic solid. It accommodates the dispersive nature of the composite by means of an elastodynamic operator, which is introduced into the constitutive relations of the linear momentum interactions.

The second step is to adapt the general theory to a particular geometry. The periodic material that we choose is made of alternate plane layers. This geometry is chosen for two reasons; first, the geometry of

masonry can be accommodated within it, and second, because there is a wealth of material about the dynamic behavior of such materials, both analytical and experimental. The choice of geometry affects both the constitutive equations and the elastodynamic operators.

The theory for layered materials contains nineteen model constants and equations are developed from which these constants can be derived from the layered constants. The equations are derived partly using micro model analysis and partly by matching specific dynamic behaviors of the model and prototype. The ability with which the model predicts the dynamic response of the layered material is assessed in two ways. Both compare spectra reflecting the behavior of infinite trains of the principal kinds of waves. The first compares spectral lines from the model with those derived from the exact theory for layered materials. The second compares lines from the model with those obtained from experiments. Predictions from the model prove to be quite accurate.

In the third phase we appraise the model by comparing the responses predicted by the model for a transient input with those observed experimentally. Experimental data allow us to make comparisons for the behavior of dilatational waves travelling both parallel and perpendicular to the layers in both plates and semi-infinite bodies. Where possible, comparison is also made with responses predicted by the exact theory. Responses in the model are found using the method of characteristics. Comparison is exhibited in a number of figures and shows that the responses predicted by the theory are quite accurate. The accuracy is not restricted to early arrival times but extends to behavior far behind the head of the pulse.

ACKNOWLEDGMENTS

The research reported here was supported by Grant No. ENV76-04265 from the National Science Foundation to the University of California at Berkeley, and NATO Project No. 1446 with the Middle East Technical University in Ankara, Turkey and the University of California at Berkeley. The support is gratefully acknowledged.

Al Klash and his associates are responsible for the drafting, Judith Sanders and Shirley Edwards typed the manuscript.

TABLE OF CONTENTS

LIST OF FIGURES

LIST OF FIGURES (Cont'd)

CHAPTER 1

INTRODUCTION

This report, as the title implies, is devoted to developing a mathematical model that will predict the linear, dynamic response of masonry. The study is motivated by a need to gain insight into the stress fields developed in masonry when it is subjected to seismic forces. This theoretical development is part of a program the major part of which is devoted to the experimental response of masonry piers.

The experimental program has shown that there are essentially two global modes of failure of the piers, flexural and shear. Whether the pier fails in flexure or shear depends on a number of factors, but in each case failure begins with the formation of cracks demonstrating a failure of the masonry itself in tension. When the mode is flexural the direction of tensile stress causing failure is vertical and when the mode of failure is shear it is the principal tensile stress that causes failure, so that the direction is at an oblique angle to the vertical.

In order to be able to predict when the first cracking would begin for either case of gross behavior, a knowledge of the stress field in a pier would have to be known when it is created by the simultaneous impositions of a vertical load and a horizontal displacement at the top, which are the conditions imposed by experiments. As masonry consists of two materials, brick and mortar, and because the geometric array is complicated, it is virtually impossible to ascertain the stress field in masonry without replacing the prototype by a model. The material of the mathematical model that is developed here is homogeneous, and is designed so that it displays both the same constitutive properties as the prototype and its dispersive properties.

The development falls naturally into three parts which are covered successively in Chapters 2, 3 and 4. In the first part, Chapter 2, we call the masonry and the mortar each a "phase" and develop a mathematical model for two phase materials. We assume that both of the phases are linearly elastic and perfectly bonded at their interfaces and that the phases have a periodic structure.

In establishing the mathematical model, several approaches can be adopted. The first is the exact treatment which includes the field equations of elasticity for each phase and the equations of continuity at the interfaces. As this approach makes the analysis very complicated, it is not of practical interest, and thus the development of an approximate theory becomes a necessity.

During the last few years, a number of approximate theories have been proposed. In the first of these, the two phase composite is replaced by a homogeneous, anisotropic, elastic medium. As this theory, called effective modulus theory, does not accommodate any dispersion, it is valid only when the wave length is very large. As an example of this type of theory, we refer to a study by Rytov [1], where an effective modulus theory is developed for a layered composite. To compensate for the shortcomings of the effective modulus theory, another approximate theory, called effective stiffness theory, has been proposed for layered and fiber reinforced composites in Refs. [2-4]. In this theory the approximate governing equations are obtained by expanding the displacements for each constituent in power series and introducing the series into a variational functional. However, the possibility of extending this theory to composites containing the vertical layering does not appear to be fruitful, as the theory has rather complicated equations even for simple composites like layered and fiber reinforced materials. Hegemier et al [5,6] proposed another approach, which they call theory of interacting continua. The theory contains a micro-structure and is based on asymptotic expansions of the field variables with respect to the space variables. However, they developed the theory again for layered and fiber reinforced composites only. For waves propagating perpendicular to layering in a layered material, the exact spectrum has a banded structure with passing and stopping bands, which contain points governing harmonic waves which are propagated and attenuated respectively. Herrman, Kaul and Delph [7,8] have developed a one-dimensional approximate theory which they call effective dispersion theory, for waves propagating perpendicular to layering only. Their theory accommodates the first stopping band and approximates quite well the two lowest spectral lines over the first two Brillouin zones.

We adopt a different approach for establishing the mathematical model for two phase materials. In this study the material is considered as a mixture consisting of two phases and the theory of mixtures is used to obtain approximate equations governing its dynamic behavior. The resulting theory is a general one which would include the geometry of a masonry wall as a particular case. The only restrictions imposed by the theory are that the two phases exhibit a periodic form and that the material of each phase is linearly elastic.

The idea of treating composites as a mixture is not new. In fact, it has previously been used in Refs. [9,10] for developing approximate theories predicting the dynamic response of layer and fiber reinforced composites when the motion is in the direction of the layers or fibers. Later, Bedford [11] attempted to extend this theory to a general case where the motion could have an arbitrary direction. However, his method has some shortcomings as he did not take into account coupling in the stress-strain relations which would imply that the state of stress of one phase is affected by the deformation of the other.

The approximate theory we propose in this study for an arbitrary direction of motion replaces the heterogenous two phase composite by an homogeneous, anisotropic, elastic solid. In developing the theory, we have chosen the mixture approach for several reasons. First, this method leads to equations simple enough to be used in the dynamic analysis of complicated composite materials such as masonry walls. Second, since we account for linear momentum interactions between the phases, the resulting approximate equations not only exhibit anisotropy, but also accommodate dispersion. The dispersion is accounted for by a time dependent operator, which we call an elastodynamic operator. It relates the interaction forces to the difference of the average phase displacements. The introduction of this operator, which we believe is new, not only improves the matching of approximate fundamental spectral lines with exact ones, but also makes it possible to match the second approximate and exact cut-off frequencies. Thirdly, the mixture approach allows us to write the approximate equations of all two phase composites in a common form. The difference comes when we adapt this form to a particular geometry. The microstructure derived from the geometry governs specific forms of the interaction and stress constitutive equations of a given composite.

In Chapter 3 the general theory is modified for a specific periodic array, namely a layered material in which the phases appear as alternate plane layers. This geometry is chosen for two reasons; first, because it is close to the geometry displayed by masonry and, second, because there is a wealth of information about the dynamic response of such materials, both from experiments and predicted by an exact theory.

Both the constitutive equations and the equations of linear momentum are affected by this choice of geometry. The layered material displays hexagonal symmetry which reduces the number of independent constitutive constants from 78 to 15. The elastodynamic operators appear in the general theory in symbolic form needing a specific geometry for their formulation. These operators are constructed in Section 3.1 from a study of a micro model, or cell, of the layered material. This analysis is similar to one used by Biot for establishing a viscodynamic operator for a fluid-filled porous medium. The elastodynamic operators reflect the behaviors at the interfaces. We felt that as first constructed the operators would render the equations of linear momentum too complicated for realistic dynamic problems, so the final part of Section 3.1 is devoted to replacing them by simpler approximations. To this end the operators are expanded in power series of their argument, and the first three terms are retained. The resulting equations of linear momentum contain four constants to accommodate dispersion. The final theory which acts as a model for a two phase layered composite contains 19 model constants.

Section 3.3 is devoted to constructing equations relating these 19 model constants to the elastic constants of each of the two phases. The constants are adjusted so that the dynamic responses of model and prototype will match as extensively as possible. The wealth of information about the behavior of waves travelling in layered materials is extremely useful in this section. The characteristics of the dynamic behavior of layered materials are almost without limit, certainly far exceeding the 19 needed to establish the unknown constants. So the constants are not unique and will change according to which set of behaviors is chosen for matching. We discuss the choice at some length in Section 3.3 pointing out that the best set would be obtained using system identification in conjunction with response obtained from experiments. The method used here to derive the set of equations is, we think, the simplest. Some of the equations are found using micro model analysis, the remainder by matching properties of spectral lines which reflect the behavior of infinite trains of the principal types of waves as predicted by the model and the exact theory for layered materials. With the capability of establishing the 19 model constants from the phase constants, the model is complete.

In the final section, Section 3.4, we make a preliminary assessment of the model material. We consider it preliminary since, in Chapter 4, we make a much more demanding, and perhaps more realistic, appraisal of the theory. In this chapter we compare the behaviors of transient waves as they propagate in the model and as observed in experiments conducted on layered materials.

The assessment in Chapter 3 is made by comparing spectral lines derived from the model with comparable lines from the exact theory and from experiments. Comparison is shown in a number of figures, in which all spectral lines reflect the behavior of infinite trains of the principal types of waves. This preliminary assessment is valuable in that it shows that even with the simplest procedure for establishing the model constants the prediction of the way in which the principal waves propagate in the model material matches quite well the way in which comparable waves propagate in two phase layered materials.

In Chapter 4 we subject the theory to what seems to us to be the most demanding test. This is comparison of the responses predicted by the theory with experimental transient responses. We are fortunate in having available excellent experimental data for transient waves propagating both parallel and perpendicular to the layers.

The transient responses predicted by the theory are obtained using the method of characteristics. This method is chosen, first because the governing equations are hyperbolic, and second because symmetry reduces the number of independent variables to time and one space variable. Where it seems appropriate we also make comparisons with responses predicted by the exact theory and by another approximate theory.

The theory for the model we have developed is, we think, simple for such a problem, the method of finding the constants is simple, so we are gratified to find such extensive matching between the responses due to the theory and to experiments. The matching is displayed in a number of figures. Not only do the profiles match for early times after the arrival of the first disturbance at a number of stations in the material, they also match well at distances remote from the head of the pulse.

CHAPTER 2

A MATHEMATICAL MODEL FOR TWO PHASE COMPOSITES

In this chapter, masonry is considered as a mixture consisting of two phases and the theory of mixtures is used to obtain approximate equations governing its dynamic behavior. The resulting theory is a general one which would include the geometry of masonry as a particular case. The only restrictions imposed by the theory are that the two phases exhibit a periodic form and that the material of each phase is linearly elastic.

The approximate theory we propose in this study, for an arbitrary direction of motion, replaces the heterogenous two phase composite by an homogeneous, anisotropic, elastic solid. In developing the theory, we have chosen the mixture approach for several reasons. First this method leads to equations simple enough to be used in the dynamic analysis of complicated composite materials such as masonry walls. Second, since we account for linear momentum interactions between the phases, the resulting approximate equations not only exhibit anisotropy, but also accommodate dispersion. The dispersion is accounted for by a time dependent operator, which we call an elastodynamic operator. It relates the interaction forces to the difference of the average phase displacements. The introduction of this operator, which we believe is new, not only improves the matching of approximate fundamental spectral lines with exact ones, but also makes it possible to match the second approximate and exact cut-off frequencies. Third, the mixture approach allows us to write the approximate equations of all two phase composites in a common form.

This chapter is devoted to the derivation of this general set of equations.

2.1 Fundamental Equations

As we adopt the theory of mixtures for developing the theory, we first review the fundamental equations of a two phase mixture, which have been studied extensively by many researchers (see e.g., [12-17]). All the variables appearing in these equations are related to the average values of the quantities they represent.

The local forms of the fundamental equations for a two phase composite, which is referred to an (x_1, x_2, x_3) Cartesian coordinate system, are

conservation of mass

$$\frac{\partial \rho_\alpha}{\partial t} + \frac{\partial}{\partial x_i}(\rho_\alpha v_i^\alpha) = 0 \; ; \tag{2.1}$$

equations of linear momentum

$$\rho_\alpha \frac{D^\alpha v_i^\alpha}{Dt} = \frac{\partial \sigma_{ji}^\alpha}{\partial x_j} + \rho_\alpha F_i^\alpha + M_i^\alpha \; ; \tag{2.2}$$

balance of energy

$$\rho_\alpha r^\alpha - \frac{\partial q_i^\alpha}{\partial x_i} - \rho_\alpha \frac{D^\alpha \varepsilon^\alpha}{Dt} + \sigma_{ki}^\alpha \frac{\partial v_i^\alpha}{\partial x_k} + \psi^\alpha = 0 \; ; \tag{2.3}$$

the Clausius-Duhem inequality

$$\rho_\alpha \frac{D^\alpha s^\alpha}{Dt} - \rho_\alpha \frac{r^\alpha}{T^\alpha} + \frac{\partial}{\partial x_k}\left(\frac{q_k^\alpha}{T^\alpha}\right) + \beta^\alpha \geq 0. \tag{2.4}$$

The index α ranges from 1 to 2 and distinguishes the two phases. The subscripts (i, j, k,..) take the values 1, 2 and 3, and are subject to indicial notation. In this notation any repeated latin index implies summation over the range of that index. In Eqs. (2.1-2.4)

ρ_α	partial masses of phases, measured per unit volume of the composite
v_i^α	average velocity components for phases
σ_{ij}^α	partial stress components for phases, measured per unit area of the composite
$\rho_\alpha F_i^\alpha$	body force components for phases, measured per unit volume of the composite
M_i^α	interaction force components, measured per unit volume of the composite
$\rho_\alpha \varepsilon^\alpha$	internal energy densities for phases, measured per unit volume of the composite
$\rho_\alpha r^\alpha$	heat energy rates (due to heat sources) for phases, measured per unit volume of the composite
q_i^α	heat flux components for phases, measured per unit area of the composite
$\rho_\alpha S^\alpha$	entropy densities for phases, measured per unit volume of the composite
T^α	average absolute phase temperatures
ψ^α	energy interactions between phases, measured per unit volume of the composite
β^α	entropy interactions between phases, measured per unit volume of the composite.

In Eqs. (2.1-2.4) "t" denotes time and the operator $\frac{D^\alpha}{Dt}$ is defined by

$$\frac{D^\alpha}{Dt} = \frac{\partial}{\partial t} + v_i^\alpha \frac{\partial}{\partial x_i} \quad . \tag{2.5}$$

We note that in writing the equation of conservation of mass, Eq. (2.1), we neglect the mass transfer between the phases. We assume that there is no angular momentum interaction between the phases. This implies that the partial stress components, σ_{ij}^{α}, are symmetric. This assumption is consistent with the classical mixture theory which is used in this study. To take into account the angular momentum interaction between phases, one needs to use the micromorphic mixture theory by which anti-symmetric distributions of the field variables can be accommodated.

In accordance with the equations of the theory of mixtures [12-17], the interactions M_i^{α}, ψ^{α} and β^{α} satisfy the relations

$$\sum_{\alpha=1}^{2} M_i^{\alpha} = 0; \quad \sum_{\alpha=1}^{2} (M_i^{\alpha} v_i^{\alpha} + \psi^{\alpha}) = 0; \quad \sum_{\alpha=1}^{2} \beta^{\alpha} = 0. \tag{2.6}$$

If the mass densities of the phases are denoted by ρ_{α}^{R}, the partial masses ρ_{α} are related to ρ_{α}^{R} by

$$\rho_{\alpha} = n_{\alpha} \rho_{\alpha}^{R}, \tag{2.7}$$

where n_{α} is the volume fraction of the α-phase with the property

$$\sum_{\alpha=1}^{2} n_{\alpha} = 1 \tag{2.8}$$

Finally, an important comment regarding the Clausius-Duhem inequality is in order. The form of the Clausius-Duhem inequality for a mixture is still the subject of controversy. Even though the form, Eq. (2.4), used in this study is physically acceptable for two phase composites where the constituents are separate in microscale, it is by no means universally accepted.

2.2 Thermodynamic Analysis for Infinitesimal Deformations

In the literature, thermodynamic analysis is presented in general terms for various mixtures composed of nonlinear phases (see e.g., [15-17]). In these works a single common temperature is assumed for all phases. Here we present thermodynamic analysis for our specific mixture, i.e., for linear two phase composites, by using the Coleman-Noll procedure. Through this analysis, we establish the specific form of the stress constitutive relations and heat conduction equations for our particular material. Our analysis is based on the fundamental equations presented in the previous section and on the findings established in the area of the theory of mixtures. We assume that deformations are infinitesimal and both phases are elastic.

We begin the analysis by approximating the operator $\frac{D^{\alpha}}{Dt}$ by

$$\frac{D^{\alpha}}{Dt} \cong \frac{\partial}{\partial t}$$

for infinitesimal theory. If internal energy and entropy densities, and heat rates due to heat sources are redefined by

$$\dot{E}^{\alpha} = \rho_{\alpha}\dot{\varepsilon}^{\alpha};\ R^{\alpha} = \rho_{\alpha}r^{\alpha};\ \dot{\eta}^{\alpha} = \rho_{\alpha}\dot{S}^{\alpha}$$

per unit volume of the composite, the energy equation, Eq. (2.3), and the Clausius-Duhem inequality, Eq. (2.4), become

$$R^{\alpha} - \frac{\partial q_i^{\alpha}}{\partial x_i} - \dot{E}^{\alpha} + \sigma_{ki}^{\alpha}\dot{e}_{ki}^{\alpha} + \psi^{\alpha} = 0 \tag{2.9}$$

$$T^{\alpha}\dot{\eta}^{\alpha} - R^{\alpha} + \frac{\partial q_k^{\alpha}}{\partial x_k} - \frac{q_k^{\alpha}}{T^{\alpha}}\frac{\partial T^{\alpha}}{\partial x_k} + T^{\alpha}\beta^{\alpha} \geq 0, \tag{2.10}$$

respectively, where the dot indicates partial differentiation with respect to time, and the e_{ij}^{α}, defined by

$$e_{ij}^{\alpha} = \frac{1}{2}\left(\frac{\partial u_i^{\alpha}}{\partial x_j} + \frac{\partial u_j^{\alpha}}{\partial x_i}\right), \tag{2.11}$$

represent the infinitesimal strain components for the α-phase. In Eq. (3.3) the u_i^{α} are the average phase displacement components.

With the aid of the energy equation, Eq. (2.9), the Clausius-Duhem inequality, Eq.(2.10), takes the form

$$T^{\alpha}\dot{\eta}^{\alpha} - \dot{E}^{\alpha} + \sigma_{ki}^{\alpha}\dot{e}_{ki}^{\alpha} + \psi^{\alpha} - \frac{q_k^{\alpha}}{T^{\alpha}}\frac{\partial T^{\alpha}}{\partial x_k} + T^{\alpha}\beta^{\alpha} \geq 0. \tag{2.12}$$

When we write Eq.(2.12) for $\alpha = 1$ and $\alpha = 2$, and add (using Eqs. (2.6)) we get

$$\sum_{\alpha=1}^{2} T^{\alpha}\dot{\eta}^{\alpha} - \dot{E} + \sum_{\alpha=1}^{2} \sigma_{ki}^{\alpha}\dot{e}_{ki}^{\alpha} - \sum_{\alpha=1}^{2} \frac{q_k^{\alpha}}{T^{\alpha}} \frac{\partial T^{\alpha}}{\partial x_k} - M_i^1 (v_i^1 - v_i^2) + \beta^1 (T^1 - T^2) \geq 0, \tag{2.13}$$

which is the total entropy inequality written per unit volume of the composite. In Eq. (2.13) $E = \sum_{\alpha=1}^{2} E^{\alpha}$ describes the total internal energy density.

In accordance with the findings established in the theory of mixtures [10] we assume

$$E^{\alpha} = E^{\alpha} (e_{ij}^1, e_{ij}^2, \eta^{\alpha}). \tag{2.14}$$

Eq. (2.14) shows that the phase internal energy density E^{α} depends on the deformations of both phases. This,as it will be seen later, leads to a coupling in the stress-strain relations implying that the state of stress of one phase is influenced by the deformations of the other. We believe that this coupling, which is disregarded in Ref. [11],is crucial for an adequate description of a composite as a mixture. Using Eq. (2.14) and the definition of the total internal energy density, the total entropy inequality, Eq. (2.13), can be written in the form

$$\sum_{\alpha=1}^{2} (T^{\alpha} - \frac{\partial E}{\partial \eta^{\alpha}}) \dot{\eta}^{\alpha} + \sum_{\alpha=1}^{2} (\sigma_{ij}^{\alpha} - \frac{\partial E}{\partial e_{ij}^{\alpha}}) \dot{e}_{ij}^{\alpha} - \sum_{\alpha=1}^{2} \frac{q_k^{\alpha}}{T^{\alpha}} \frac{\partial T^{\alpha}}{\partial x_k} - M_i^1 (v_i^1 - v_i^2) + \beta^1 (T^1 - T^2) \geq 0. \tag{2.15}$$

Since η^{α} and e_{ij}^{α} are independent state variables, in order to satisfy this inequality we should have

$$T^\alpha = \frac{\partial E}{\partial \eta^\alpha} = \frac{\partial E^\alpha}{\partial \eta^\alpha}$$

$$\sigma^\alpha_{ij} = \frac{\partial E}{\partial e^\alpha_{ij}} = \sum_{\beta=1}^{2} \frac{\partial E^\beta}{\partial e^\alpha_{ij}} \quad . \tag{2.16}$$

When Eqs. (2.16) are taken into account the total entropy inequality reduces to

$$- \sum_{\alpha=1}^{2} \frac{q^\alpha_k}{T^\alpha} \frac{\partial T^\alpha}{\partial x_k} - M^1_i(v^1_i - v^2_i) + \beta^1(T^1 - T^2) \geq 0. \tag{2.17}$$

Introducing the Helmholtz free energy density ϕ^α

$$\phi^\alpha = E^\alpha - T^\alpha \eta^\alpha \tag{2.18}$$

and defining the total Helmholtz free energy density ϕ

$$\phi = \sum_{\alpha=1}^{2} \phi^\alpha = E - \sum_{\alpha=1}^{2} T^\alpha \eta^\alpha, \tag{2.19}$$

and using Eqs. (2.14) and (2.16), we obtain the relations

$$\phi^\alpha = \phi^\alpha(e^1_{ij}, e^2_{ij}, T^\alpha) \tag{2.20}$$

and

$$\eta^\alpha = - \frac{\partial \phi}{\partial T^\alpha} = - \frac{\partial \phi^\alpha}{\partial T^\alpha}$$

$$\sigma^\alpha_{ij} = \frac{\partial \phi}{\partial e^\alpha_{ij}} = \sum_{\beta=1}^{2} \frac{\partial \phi^\beta}{\partial e^\alpha_{ij}} \quad , \tag{2.21}$$

which imply

$$\eta^\alpha = \eta^\alpha(e^1_{ij}, e^2_{ij}, T^\alpha)$$

$$\sigma^\alpha_{ij} = \sigma^\alpha_{ij}(e^1_{ij}, e^2_{ij}, T^1, T^2). \tag{2.22}$$

We let the temperatures of both phases be T_o in the reference configuration of the two phase composite, which is assumed to be free of stresses. As we are dealing with an infinitesimal theory and are assuming small deviations from the reference temperature T_o, we expand the stresses and entropies about zero deformation and the reference temperature T_o using Taylor's formula, and retain only linear terms. When we use the symmetry conditions

$$\frac{\partial \eta^\alpha}{\partial e^\beta_{ij}} = - \frac{\partial \sigma^\beta_{ij}}{\partial T^\alpha} \; ; \; \frac{\partial \sigma^\alpha_{ij}}{\partial e^\beta_{mn}} = \frac{\partial \sigma^\beta_{mn}}{\partial e^\alpha_{ij}} \; (\alpha,\beta = 1,2), \tag{2.23}$$

which are the implications of Eqs. (2.21), we obtain

$$\begin{aligned} \eta^\alpha &= \eta^\alpha_o + \sum_{\beta=1}^{2} p^{\alpha\beta}_{ij} e^\beta_{ij} + \frac{c^\alpha}{T_o} \theta^\alpha \\ \sigma^\alpha_{ij} &= \sum_{\beta=1}^{2} C^{\alpha\beta}_{ijmn} e^\beta_{mn} - \sum_{\beta=1}^{2} p^{\beta\alpha}_{ij} \theta^\beta , \end{aligned} \tag{2.24}$$

where the coefficients $C^{\alpha\beta}_{ijmn}$ have the property

$$C^{\alpha\beta}_{ijmn} = C^{\beta\alpha}_{mnij} . \tag{2.25}$$

In Eqs. (2.24) θ^α, defined by

$$\theta^\alpha = T^\alpha - T_o ,$$

represents phase temperature deviations from the reference temperature T_o; η^α_o denotes the value of the phase entropy density η^α in the reference configuration; c^α is the specific heat at constant deformation for the α-phase, measured per unit volume of the composite, and is defined by

$$c^{\alpha} = T_o \frac{\partial \eta^{\alpha}}{\partial T^{\alpha}} \Bigg|_{\substack{e^1_{ij} = e^2_{ij} = 0. \\ T^{\alpha} = T_o}}$$

The coefficients $C^{\alpha\beta}_{ijmn}$ and $p^{\alpha\beta}_{ij}$ appearing in the second of Eqs. (2.24) denote the material constants of a linear two phase composite. The symmetry of strain and stress components further imposes the conditions

$$\begin{aligned} p^{\alpha\beta}_{ij} &= p^{\alpha\beta}_{ji} \\ C^{\alpha\beta}_{ijmn} &= C^{\alpha\beta}_{jimn} \\ C^{\alpha\beta}_{ijmn} &= C^{\alpha\beta}_{ijnm} \end{aligned} \tag{2.26}$$

on the material constants. The conditions, Eqs. (2.25) and (2.26), indicate that the number of independent material constants in the stress-strain relations, the second of Eqs. (2.24), is at most 102.

The coefficients $(C^{12}_{ijmn}, C^{21}_{ijmn})$ and $(p^{12}_{ij}, p^{21}_{ij})$ describe the coupling in the stress constitutive equations, the second of Eqs. (2.24). These terms respectively permit the state of stress of one phase to be affected by the deformation and temperature deviation of the other phase.

We now turn our attention to deriving the heat conduction equations for a two phase composite. We first notice that the energy equation, Eq. (2.9), when Eqs. (2.14) and (2.16) are used, reduces to

$$R^{\alpha} - \frac{\partial q^{\alpha}_i}{\partial x_i} - \sum_{\beta=1}^{2} \frac{\partial E^{\alpha}}{\partial e^{\beta}_{ij}} \dot{e}^{\beta}_{ij} - T^{\alpha}\dot{\eta}^{\alpha} + \sigma^{\alpha}_{ij}\dot{e}^{\alpha}_{ij} + \psi^{\alpha} = 0. \tag{2.27}$$

We assume that partial heat flux vectors are related to the gradients of the average phase temperatures by the Fourier equation

$$q_i^{\alpha} = - \sum_{\beta=1}^{2} k_{ij}^{\alpha\beta} \frac{\partial\theta^{\beta}}{\partial x_j} , \qquad (2.28)$$

where $k_{ij}^{\alpha\beta}$ are the coefficients of heat conduction defined per unit area of the composite. The coefficients k_{ij}^{12} and k_{ij}^{21} in Eq. (2.28) describe the thermal coupling between phases.

When the linear entropy relation, the first of Eqs. (2.24), and the Fourier equation, Eq. (2.28), are used and when the temperature deviation from the equilibrium state is assumed to be small, the energy equation, Eq. (2.27), becomes

$$R^{\alpha} + \sum_{\beta=1}^{2} \frac{\partial}{\partial x_i} (k_{ij}^{\alpha\beta} \frac{\partial\theta^{\beta}}{\partial x_j}) - c^{\alpha}\dot{\theta}^{\alpha} - T_o \sum_{\beta=1}^{2} p_{ij}^{\alpha\beta}\dot{e}_{ij}^{\alpha\beta} + \overset{*}{\psi}^{\alpha} + \psi^{\alpha} = 0, \qquad (2.29)$$

where

$$\overset{*}{\psi}^{\alpha} = \sigma_{ij}^{\alpha}\dot{e}_{ij}^{\alpha} - \sum_{\beta=1}^{2} \frac{\partial E^{\alpha}}{\partial e_{ij}^{\beta}} \dot{e}_{ij}^{\beta} . \qquad (2.30)$$

From the second of Eqs. (2.16) and Eq. (2.30) it follows that $\overset{*}{\psi}^{\alpha}$ satisfies $\sum_{\alpha=1}^{2} \overset{*}{\psi}^{\alpha} = 0$. Eq. (2.30) shows that, in the absence of the coupling introduced by Eq. (2.14), $\overset{*}{\psi}^{\alpha}$ separately vanishes for both phases. This means that the term $\overset{*}{\psi}^{\alpha}$ in Eq. (2.29) represents the energy interaction between the phases due to the coupling in stress constitutive equations.

We now separate the interaction due to heat exchange between the phases from the total interaction $(\psi^{\alpha} + \overset{*}{\psi}^{\alpha})$. To do this we let

$$\psi^{\alpha} + \overset{*}{\psi}{}^{\alpha} = \bar{\bar{\psi}}{}^{\alpha} + Q^{\alpha}, \tag{2.31}$$

where Q^{α} represents the heat exchange between the phases (defined per unit volume of the composite) and satisfies $\sum_{\alpha=1}^{2} Q^{\alpha} = 0$. When we substitute Eq. (2.31) into Eq. (2.29) we obtain the final form of the heat conduction equation

$$\sum_{\beta=1}^{2} \frac{\partial}{\partial x_i} \left(k_{ij}^{\alpha\beta} \frac{\partial \theta^{\beta}}{\partial x_j}\right) - c^{\alpha}\dot{\theta}^{\alpha} + Q^{\alpha} + R^{\alpha} = T_o \sum_{\beta=1}^{2} p_{ij}^{\alpha\beta}\dot{e}_{ij}^{\alpha\beta} - \bar{\bar{\psi}}{}^{\alpha}, \tag{2.32}$$

where the interaction term $\bar{\bar{\psi}}{}^{\alpha}$ satisfies the equation

$$\sum_{\alpha=1}^{2} (\bar{\bar{\psi}}{}^{\alpha} + M_i^{\alpha} v_i^{\alpha}) = 0 \tag{2.33}$$

in view of the second of Eqs. (2.6), Eq. (2.31), and the relations $\sum_{\alpha=1}^{2} \overset{*}{\psi}{}^{\alpha} = 0$ and $\sum_{\alpha=1}^{2} Q^{\alpha} = 0$.

2.3 Restrictions on Model Constants

For studying the constraints imposed on model constants we use an hypothesis which states that the strain energy function must be positive definite. For a two phase composite the strain energy function W per unit volume is defined by

$$dW = \sum_{\alpha=1}^{2} \sigma_{ij}^{\alpha} de_{ij}^{\alpha}. \tag{2.34}$$

By integrating Eq. (2.34) and using the second of Eqs. (2.24), disregarding thermal effects we get

$$W = \frac{1}{2} \sum_{\alpha=1}^{2} \sum_{\beta=1}^{2} C_{ijmn}^{\alpha\beta} e_{ij}^{\alpha} e_{mn}^{\beta}. \tag{2.35}$$

In the derivation of Eq. (2.35) we assumed that the strain energy is zero at reference configuration. Eq.(2.35) indicates that the strain energy function will be positive definite only if

$$\sum_{\alpha=1}^{2} \sum_{\beta=1}^{2} C_{ijmn}^{\alpha\beta} f_{ij}^{\alpha} f_{mn}^{\beta} \geq 0 \qquad (2.36)$$

is satisfied for all symmetric f_{ij}^{α}, where the equality holds only when $f_{ij}^{\alpha} = 0$. Eq. (2.36) governs all of the constraints imposed on the model constants $C_{ijmn}^{\alpha\beta}$.

The stress contitutive equations and the positive definiteness condition can be written alternatively in matrix form by using vector representations of the stress and strain tensors. These forms are presented in Appendix A.

2.4 Some Remarks on Interaction Constitutive Equations

For completing the theory we have to supply it with additional constitutive relations for the interaction terms appearing in the linear momentum and energy equations. To this end we postulate that the force and heat interactions between the phases are, through time dependent linear operators, related to the differences of phase displacements and temperatures respectively, i.e.,

$$\begin{aligned} M_i^1 &= - M_i^2 = \Gamma_{ij}^{t}(u_j^2 - u_j^1) \\ Q^1 &= - Q^2 = H^t(\theta^2 - \theta^1), \end{aligned} \qquad (2.37)$$

where Γ_{ij}^{t} denotes the operator for linear momentum interaction and H^t for the heat exchange. In view of Ref. 16 another term involving the gradient of phase temperatures can be added to the right-hand side of the first of Eq. (5.1). However, in order to keep the theory as simple as possible, this term representing the coupling between the linear momentum interaction and the temperature gradient is neglected. For a given composite, the forms of the operators in Eqs. (5.1) can be determined either experimentally or by using micro-modal analysis. For example, in a subsequent study, where we will develop the theory for a two phase layered composite, approximate forms of these operators will be established by using a procedure based on micro-model analysis, which is very similar to the one used by Biot [18,19]. He introduces a viscodynamic operator describing the friction between the fluid and solid phases of an isotropic porous material.

We believe that the inclusion of the operator Γ^t_{ij}, which we will call the elastodynamic operator in the theory, is important. In fact, the presence of this operator in the theory, which accounts for the dispersion of waves in composites, not only brings some improvement to the matching of the approximate fundamental spectral lines with the exact, but also makes it possible to match the second approximate and exact cut-off frequencies.

We have now completed the general formulation of the linear approximate theory developed for a two phase composite. Provided that the constitutive equation for $\bar{\bar{\psi}}^\alpha$ is known, the field variables u^α_i, e^α_{ij}, σ^α_{ij} and θ^α can be found by solving the linear momentum equations, Eq. (2.2), strain-displacement relations, Eq.(2.11), stress constitutive relations, the second of Eqs. (2.24), heat conduction equations, Eq. (2.32), and interaction constitutive relations, Eqs.(2.37), subject to appropriate initial and boundary conditions.

2.5 Completion of the Model for a Particular Two Phase Material

The approximate theory, just established, governs the dynamic response of a two phase composite. The theory not only accommodates the anisotropy of the composite, but also its dispersive characteristics caused by the interfaces separating the two phases.

When we say that the theory is complete, it must be understood that it is complete only in the general sense. The theory applies to all two phase materials with periodic structure and for materials in which each of the phases is linearly elastic. The model cannot be completed until a specific two phase material is defined, which entails specifying the geometry and the properties of each of the two phases.

The steps required in progressing from the general theory to a complete model replacing a specific two phase material are significant. They are described in detail in the chapter following this, but it seems appropriate here to describe in a qualitative way what those steps entail.

When the geometry of the two phase material is known, its influence on the model constants and the elastodynamic operator must first be explored. The geometry usually imposes symmetry restrictions which significantly reduce the number of these unknowns. It remains to establish the surviving unknowns.

The best set of values for the unknowns will be achieved by using a method known as system identification. It is used in conjunction with experimental data. System identification is a systematic method for estimating the set of unknowns that will minimize the differences between responses predicted by the model and those from experiments over some specified extent of the responses.

Experimental data may not be available, and even if they are, the method of system identification could be complex and require a great deal of computer time.

Other methods are available which may be used separately or together. The first employs micro-model analysis which is based on the deformation modes assumed for the phases. When the geometry of the two phase material is known, the micro-model can be constructed. The second method depends on having an exact theory for the two phase material. The product of the exact theory would be frequency spectra relating frequencies and wave lengths for infinite trains of waves. The unknowns could be established by matching the two sets of spectral lines for a specific set of properties of these lines. In this procedure special attention should be given to avoiding the violation of the model constraints imposed because the strain energy function is positive definite.

The approximate theory developed here is based on the theory of mixtures. With the object of keeping the theory as simple as possible, we have used the average values of the field variables. It may be that because of this simplication, an acceptable match between the responses predicted by this theory and experimental responses, or the responses from the exact theory, will not be possible. If such is the case, the theory can be improved, at the expense of complication, by employing micromorphic mixture theory. In that theory, antisymmetric distributions of the field variables are accommodated.

A last comment regarding the application of the mathematical model developed in this study to masonry walls is in order. We know that taking into account nonlinear and debonding effects in the response of masonry walls to dynamic inputs is important. The linear theory proposed in this study will form the basis for including these effects in the model. To explain this more explicitly, we refer to the third chapter where a constitutive relation for the linear momentum interaction for layered composites is established through the use of micromodel analysis. This analysis is based on displacement and stress continuity conditions at interfaces. By relaxing these continuity conditions, the debonding effect can be accommodated in the theory.

CHAPTER 3

A MIXTURE THEORY FOR ELASTIC LAMINATED COMPOSITES

In this chapter the general theory is modified for a specific periodic array, namely a layered material in which the phases appear as alternate plane layers. This geometry is chosen for two reasons; first, because it is close to the geometry displayed by masonry and, secondly, because there is a wealth of information about the dynamic response of such materials, both from experiments and predicted by an exact theory. In the equations which will follow, the thermal effects contained in the previous chapter are disregarded.

3.1 Homogeneous Model for a Two Layer Material

In this section we choose a specific two-phase material; that is we choose a particular periodic geometry for our medium. We trace the influences that this specified geometry has on the general two phase theory, and modify the theory to this geometry. We will find that changes are required in both the constitutive equations and the equations of linear momentum.

The material which we study is one in which the two materials alternate in plane layers. The materials are called phases and each is identified by so called "phase constants". Each phase is isotropically elastic, so Lamé's constants μ_α and λ_α (α = 1 or 2) and the mass densities ρ_α^R are the phase constants. The two layers have thicknesses $2h_1$ and $2h_2$ respectively.

In what follows the laminated composite is referred to a Cartesian coordinate system (x_1, x_2, x_3) in which the x_2 axis is perpendicular to the planes of layering (see Fig. 1). With respect to this reference frame the composite displays hexagonal symmetry, in which x_2 is the axis of symmetry. We first study the constitutive equations.

(a) Constitutive Equations

The hexagonal symmetry resulting from layered periodically results in a reduction in the number of model constants appearing in the constitutive equations. The stiffness matrices defined in Eq. (A.1) have the forms,

$$\underline{C}^{\alpha\beta} = \begin{bmatrix} C_{11}^{\alpha\beta} & C_{12}^{\alpha\beta} & C_{13}^{\alpha\beta} & 0 & 0 & 0 \\ C_{12}^{\alpha\beta} & C_{22}^{\alpha\beta} & C_{12}^{\alpha\beta} & 0 & 0 & 0 \\ C_{13}^{\alpha\beta} & C_{12}^{\alpha\beta} & C_{11}^{\alpha\beta} & 0 & 0 & 0 \\ 0 & 0 & 0 & C_{44}^{\alpha\beta} & 0 & 0 \\ 0 & 0 & 0 & 0 & C_{55}^{\alpha\beta} & 0 \\ 0 & 0 & 0 & 0 & 0 & C_{44}^{\alpha\beta} \end{bmatrix} \quad (\text{for } \alpha = \beta), \quad (3.1)$$

where $C_{55}^{\alpha\beta} = \frac{1}{2}(C_{11}^{\alpha\beta} - C_{13}^{\alpha\beta})$, and

$$\underline{C}^{12} = \begin{bmatrix} C_{11}^{12} & C_{12}^{12} & C_{11}^{12} & 0 & 0 & 0 \\ C_{21}^{12} & C_{22}^{12} & C_{21}^{12} & 0 & 0 & 0 \\ C_{11}^{12} & C_{12}^{12} & C_{11}^{12} & 0 & 0 & 0 \\ 0 & 0 & 0 & C_{44}^{12} & 0 & 0 \\ 0 & 0 & 0 & 0 & 0 & 0 \\ 0 & 0 & 0 & 0 & 0 & C_{44}^{12} \end{bmatrix} \quad (3.2)$$

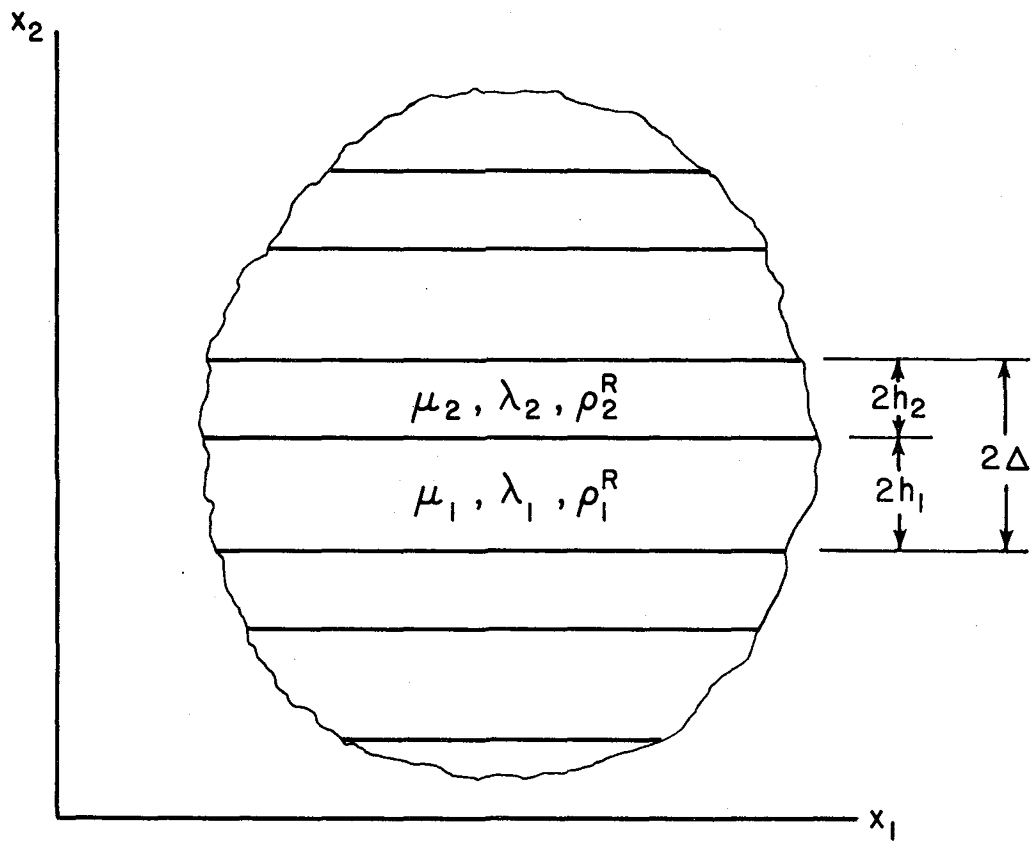

FIG. 1. A LAYERED COMPOSITE MATERIAL

Examination of Eqs. (3.1) and (3.2) shows that the number of independent constants has been reduced to fifteen. This reduction results from symmetry and also from recognizing that $C_{55}^{12} = 0$. The latter is obtained by integrating the constitutive relation $\overset{*}{\sigma}{}_{13}^{\alpha} = 2\mu_{\alpha}\, \overset{*}{e}{}_{13}^{\alpha}$ (where $\overset{*}{\sigma}{}_{13}^{\alpha}$ and $\overset{*}{e}{}_{13}^{\alpha}$ are the actual shear stress and strain distributions for the α phase) over the thickness of the α phase.

(b) Equations of Linear Momentum

First we write the linear momentum equations, Eq. (2.2), for each phase separately. They are

$$\begin{aligned} \frac{\partial \sigma_{ji}^{1}}{\partial x_j} + \rho_1 F_i^1 + \Gamma_{ij}^{t}(u_j^2 - u_j^1) &= \rho_1 \dot{v}_i^1 \\ \frac{\partial \sigma_{ji}^{2}}{\partial x_j} + \rho_2 F_i^2 + \Gamma_{ij}^{t}(u_j^1 - u_j^2) &= \rho_2 \dot{v}_i^2 \end{aligned} \tag{3.3}$$

In formulating the linear momemtum equations for the general two phase theory, interaction between the phases was accounted for by the term Γ_{ij}^{t}, which we called an elastodynamic operator. With the hexagonal symmetry of the layered material, the operator has the form

$$(\Gamma_{ij}^{t}) = \begin{bmatrix} \Gamma_1^t & 0 & 0 \\ 0 & \Gamma_2^t & 0 \\ 0 & 0 & \Gamma_1^t \end{bmatrix} \tag{3.4}$$

The physical meaning of the components is derived from a study of Eqs. (3.3). The first, Γ_1^t , describes the linear momentum interaction parallel to layering caused by the shear stresses at the interfaces, Γ_2^t accounts for interaction normal to layering caused by the normal, interface stresses. To gain insight into the forms of these two operators we analyze a micro model of the layered material. The analysis, which is based on assumed deformation modes for the phases, was previously used by Biot [8,9] for constructing a viscodynamic operator for fluid filled porous media.

Micro model analysis consists of a study of a unit cell of the composite material. The unit cell consists of one layer of the first constituent bounded by two half layers of the second (see Fig. 2). We refer the cell to a Cartesian coordinate system (x_1, x_2, x_3) so that the x_1-x_3 plane coincides with the mid-plane of the first constituent and the x_2 axis is perpendicular to the layers. The analysis is approximate in that a number of simplifying assumptions are made pertaining to the state variables involved. First, the variables are assumed to depend only on the thickness variable and time, so that the displacement, for example, $\overset{*}{u}{}_i^\alpha = \overset{*}{u}{}_i^\alpha(x_2,t)$, where the asterisk is used to denote actual distributions. In the general micro model theory, the same quantities are assumed to be distributed symmetrically about the midplane of each layer. If this simple theory proves to be inadequate, we would have to employ micromorphic mixture theory which accommodates antisymmetric distributions. The results of the theory are expressed in terms of the average values of the variables over the thickness. The average value of the variable $\overset{*}{u}{}_i^\alpha$ is denoted by u_i^α (no asterisk).

The derivation of expressions for Γ_1^t and Γ_2^t begins by substituting the displacements

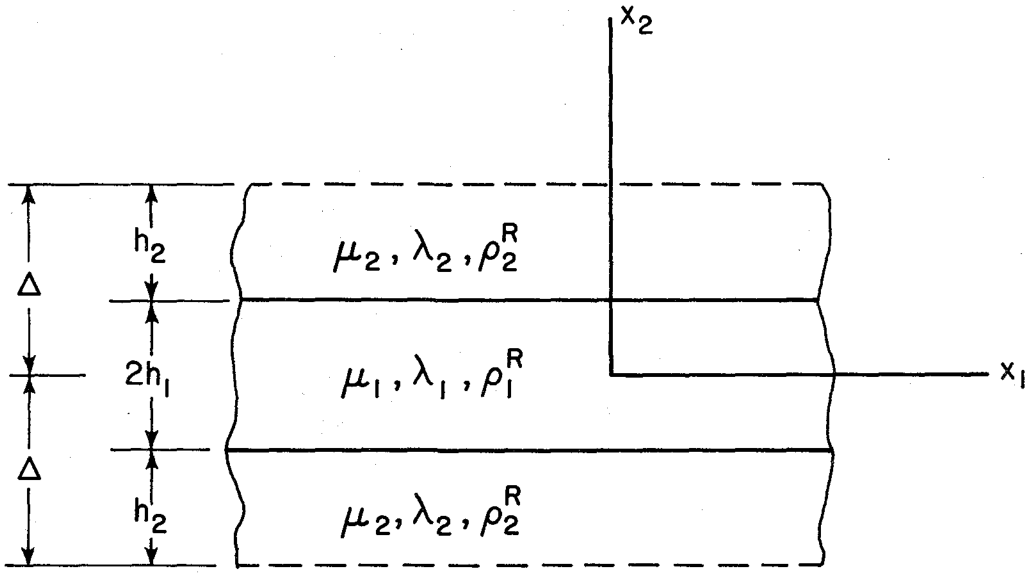

FIG. 2. A UNIT CELL

$$\overset{*}{u}{}_i^{\alpha} = \overset{*}{u}{}_i^{\alpha}(x_2,t) \tag{3.5}$$

into the field equations of elasticity. The restricted space dependency leads to the equations

$$\begin{aligned}
\mu_\alpha \frac{\partial^2 \overset{*}{u}{}_1^{\alpha}}{\partial x_2^2} + \overset{*}{F}{}_1^{\alpha} &= \rho_\alpha^R \ddot{\overset{*}{u}}{}_1^{\alpha} \\
(2\mu_\alpha + \lambda_\alpha) \frac{\partial^2 \overset{*}{u}{}_2^{\alpha}}{\partial x_2^2} + \overset{*}{F}{}_2^{\alpha} &= \rho_\alpha^R \ddot{\overset{*}{u}}{}_2^{\alpha} \\
\mu_\alpha \frac{\partial^2 \overset{*}{u}{}_3^{\alpha}}{\partial x_2^2} + \overset{*}{F}{}_3^{\alpha} &= \rho_\alpha^R \ddot{\overset{*}{u}}{}_3^{\alpha} ,
\end{aligned} \tag{3.6}$$

where $\alpha = 1, 2$ represents quantities in layers 1 and 2 respectively; and $\overset{*}{F}{}_i^{\alpha}$ are the components of the body force.

In what follows, we develop an expression for Γ_1^t; the method is the same for Γ_2^t . The form of Γ_1^t is governed by the interface shear stresses. For the assumed displacement field, these stresses are related only to the displacement parallel to the layers and the relationships are

$$\overset{*}{\sigma}{}_{21}^{\alpha} = \mu_\alpha \frac{\partial \overset{*}{u}{}_1^{\alpha}}{\partial x_2} ; \quad \overset{*}{\sigma}{}_{23}^{\alpha} = \mu_\alpha \frac{\partial \overset{*}{u}{}_3^{\alpha}}{\partial x_2} . \tag{3.7}$$

In our study of Γ_1^t , we may pursue either $\overset{*}{u}{}_1^{\alpha}$ or $\overset{*}{u}{}_3^{\alpha}$ as both will lead to the same expression. We choose the first, which is governed by the first of Eqs. (3.6), and continue by taking the Laplace transform of each side of this equation. The result of this operation is the equation

$$\frac{d^2 \overset{*}{u}{}_1^{\alpha L}}{dx_2^2} - m_\alpha^2 \overset{*}{u}{}_1^{\alpha L} = \frac{-\overset{*}{F}{}_1^{\alpha L}}{\mu_\alpha} , \tag{3.8}$$

where the superscript L denotes the Laplace transform of the quantity and

$$m_\alpha^2 = \frac{\rho_\alpha^R}{\mu_\alpha} p^2$$

in which p is the Laplace transform parameter.

In the integration of Eq. (3.8) we exploit the symmetry of $\overset{*}{u}{}_1^\alpha$ and $\overset{*}{F}{}_1^\alpha$, already discussed, and further we make the same assumption as made by Biot [13], that $\overset{*}{F}{}_1^\alpha$ depends on time only. Integration leads to the equation

$$\overset{*}{u}{}_1^{\alpha L} = A_\alpha \sinh m_\alpha x_2 + B_\alpha \cosh m_\alpha x_2 + G_\alpha \ , \qquad (3.9)$$

where

$$G_\alpha = \frac{\overset{*}{F}{}_1^{\alpha L}}{\mu_\alpha m_\alpha^2} \ . \qquad (3.10)$$

The four integration constants, A_α and B_α, appearing in Eq. (3.9),can be determined by using the continuity condition at the interface $x_2 = h_1$,

$$(\overset{*}{u}{}_1^1) = (\overset{*}{u}{}_1^2) \ ; \ (\overset{*}{\sigma}{}_{21}^1) = (\overset{*}{\sigma}{}_{21}^2) \ , \qquad (3.11)$$

and the conditions at the mid-planes $x_2 = 0$ and $x_2 = \Delta = h_1 + h_2$

$$(\overset{*}{\sigma}{}_{21}^1)_{x_2=0} = 0 \ ; \ (\overset{*}{\sigma}{}_{21}^2)_{x_2=\Delta} = 0 \qquad (3.12)$$

which are imposed by the symmetry of $\overset{*}{u}{}_1^\alpha$. After some manipulation, the final form of $\overset{*}{u}{}_1^{\alpha L}$ is found to be

$$\overset{*}{u}{}_1^{1L} = \frac{C}{D} (G_1 - G_2) \cosh m_1 x_2 + G_1 \qquad (3.13)$$

$$\overset{*}{u}{}_1^{2L} = \frac{1}{D} (G_1 - G_2)(\cosh m_2 x_2 - \tanh m_2 \Delta \sinh m_2 x_2) + G_2 \ ,$$

where

$$C = \frac{\mu_2 m_2}{\mu_1 \; m_1 \; \sinh m_1 h_1} (\sinh m_2 h_1 - \tanh m_2 \Delta \cosh m_2 h_1)$$

$$D = (F-C) \cosh m_1 h_1 \qquad (3.14)$$

$$F = \frac{1}{\cosh m_1 h_1} (\cosh m_2 h_1 - \tanh m_2 \Delta \sinh m_2 h_1) .$$

To determine the interface shear stress we substitute Eqs. (3.13) into Eqs. (3.7), and obtain

$$(\overset{*}{\sigma}{}^{1L}_{21})_{x_2=h_1} = (\overset{*}{\sigma}{}^{2L}_{21})_{x_2=h_1} = \frac{C}{D} \mu_1 \; m_1 (G_1 - G_2) \sinh m_1 h_1 . \qquad (3.15)$$

Our objective is to relate the interface shear stress to the difference of the average horizontal displacements. We formulate the averages

$$u_1^{1L} = \frac{1}{h_1} \int_0^{h_1} \overset{*}{u}{}_1^{1L} \, dx_2 \; ; \; u_1^{2L} = \frac{1}{h_2} \int_{h_1}^{\Delta} \overset{*}{u}{}_1^{2L} \, dx_2 \; , \qquad (3.16)$$

using $\overset{*}{u}{}_1^{\alpha L}$ from Eq. (3.13) and obtain an expression for their difference

$$u_1^{2L} - u_1^{1L} = -(G_1 - G_2) \left[\frac{C}{D} \left(\frac{m_1 \mu_1}{m_2 \mu_2} \frac{1}{m_2 h_2} + \frac{1}{m_1 h_1}\right) \sinh m_1 h_1 + 1\right] (3.17)$$

By eliminating the factor (G_1-G_2) between Eqs. (3.15) and (3.17), after some manipulation, we get

$$(\overset{*}{\sigma}{}^{1L}_{21})_{x_2=h_1} = (\overset{*}{\sigma}{}^{2L}_{21})_{x_2=h_1} = \frac{3 r_1 r_2}{r \Delta} L_1(\kappa_1^1, \kappa_2^1)(u_1^{2L} - u_1^{1L}), \qquad (3.18)$$

where

$$L_1(\kappa_1^1, \kappa_2^1) = \frac{r}{3} \frac{\kappa_1^1 \kappa_2^1 \sinh\kappa_1^1 \sinh\kappa_2^1}{r_1 \kappa_1^1 \sinh\kappa_1^1 \cosh\kappa_2^1 + r_2 \kappa_2^1 \cosh\kappa_1^1 \sinh\kappa_2^1 - (r_1 \frac{\kappa_1^1}{\kappa_2^1} + r_2 \frac{\kappa_2^1}{\kappa_1^1}) \sinh\kappa_1^1 \sinh\kappa_2^1} \qquad (3.19)$$

and the arguments κ_1^1 and κ_2^1 are defined by

$$\kappa_\alpha^1 = \Delta \sqrt{\frac{\rho_\alpha}{r_\alpha}}\; p, \qquad (3.20)$$

and

$$r_\alpha = \frac{\mu_\alpha}{n_\alpha} \;; \quad r = \sum_{\alpha=1}^{2} r_\alpha \,, \qquad (3.21)$$

where $n_\alpha = h_\alpha/\Delta$.

Even though Eq. (3.18) is written in the Laplace transform domain it can be interpreted from operational calculus as given in the real time domain provided that the Laplace transform parameter p is replaced by the operator $\frac{\partial}{\partial t}$. In our analysis we adopt this interpretation and accordingly drop the superscript L in Eq. (3.18). In this case $L_1(\kappa_1^1, \kappa_2^1)$ in Eq. (3.19) becomes an operator relating the relative average horizontal displacement to the interface shear stress. It should be noted the operator $L_1(\kappa_1^1,\kappa_2^1)$ is normalized so that $L_1(0,0) = 1$.

We now turn our attention to relating the elastodynamic operator Γ_1^t to the operator L_1. We first note that the x_1 component of the linear momentum interaction M_1^1 acting on the first constituent and defined per unit volume of composite is related to the interface shear stress by

$$M_1^1 = \frac{(\overset{*}{\sigma}{}_{21}^{1})_{x_2=h_1}}{\Delta} \;. \qquad (3.22)$$

On the other hand, we see from Eqs. (3.3) and (3.4) that in our general formulation the same interaction is given by

$$M_1^1 = \Gamma_1^t(u_1^2 - u_1^1). \qquad (3.23)$$

Considering Eq. (3.18), and comparing Eqs. (3.22) and (3.23) we finally obtain the form of the horizontal component of the elastodynamic operator as

$$\Gamma_1^t = K_1 L_1(\kappa_1^1, \kappa_2^1) , \tag{3.24}$$

where the constant K_1 is given by

$$K_1 = \frac{3r_1 r_2}{\Delta^2 r} \tag{3.25}$$

The operator Γ_2^t, which governs the vertical linear momentum interaction, can be obtained in a similar way. In the derivation of this operator, the terms $\overset{*\alpha}{u_1}$ and $\overset{*\alpha}{\sigma_{21}}$ appearing in Eqs. (3.10) and (3.11) must be replaced by $\overset{*\alpha}{u_2}$ and $\overset{*\alpha}{\sigma_{22}}$, respectively. The result is

$$\Gamma_2^t = K_2 L_2(\kappa_1^2 , \kappa_2^2) \tag{3.26}$$

where the constant K_2 and the operator $L_2(\kappa_1^2,\kappa_2^2)$ can again be defined by Eqs. (3.25) and (3.19), respectively, if the terms $(r_1,r_2,r,\kappa_1^1,\kappa_2^1)$ in these equations are replaced by $(E_1,E_2,E,\kappa_1^2,\kappa_2^2)$, respectively, where

$$E_\alpha = \frac{2\mu_\alpha + \lambda_\alpha}{n_\alpha} ; \quad E = \sum_{\alpha=1}^{2} E_\alpha , \tag{3.27}$$

and

$$\kappa_\alpha^2 = \Delta \sqrt{\frac{\rho_\alpha}{E_\alpha}} \quad p. \tag{3.28}$$

We recognize at this point in the development that the elastodynamic operators will make the equations of linear momentum too complicated for practical use. Accordingly, we replace each of the operators by an approximation derived by expanding the operators $L_1(\kappa_1^1, \kappa_2^1)$ and $L_2(\kappa_1^2, \kappa_2^2)$, defined by Eq. (3.19), in power series expansions of their arguments, and retain the first three terms. This procedure yields

$$\Gamma_1^t = K_1 + q_1 \frac{\partial^2}{\partial t^2}$$

$$\Gamma_2^t = K_2 + q_2 \frac{\partial^2}{\partial t^2} \tag{3.29}$$

where

$$q_1 = \frac{\rho_1 r_2^2 + \rho_2 r_1^2}{5r^2} \; ; \quad q_2 = \frac{\rho_1 E_2^2 + \rho_2 E_1^2}{5E^2} \, . \tag{3.30}$$

Here we first note that Eq. (3.29) is valid when the Laplace transform parameter is small. This means that Eq. (3.29) represents an asymptotic form for the operators valid for large times. Secondly, we note that Eq. (3.29) implies that the linear momentum interaction involves the constituent relative acceleration. This violates the principle of material indifference because the constituent relative acceleration is not an objective quantity. This point is discussed in [20] where the author states that this violation can be disregarded in linear theories.

When the expressions for Γ_1^t and Γ_2^t are introduced into the equations for linear momentum, Eqs. (2.1), we obtain the approximate form of these equations,

$$\frac{\partial \sigma_{ji}^1}{\partial x_j} + \rho_1 F_i^1 + K_{ij}(u_j^2 - u_j^1) = m_{ij}^1 \dot{v}_j^1 - q_{ij} \dot{v}_j^2$$

$$\frac{\partial \sigma_{ji}^2}{\partial x_j} + \rho_2 F_i^2 + K_{ij}(u_j^1 - u_j^2) = -q_{ij} \dot{v}_j^1 + m_{ij}^2 \dot{v}_j^2 \, , \tag{3.31}$$

where

$$(K_{ij}) = \begin{bmatrix} K_1 & 0 & 0 \\ 0 & K_2 & 0 \\ 0 & 0 & K_1 \end{bmatrix} \; ; \quad (q_{ij}) = \begin{bmatrix} q_1 & 0 & 0 \\ 0 & q_2 & 0 \\ 0 & 0 & q_1 \end{bmatrix} \; ; \tag{3.32}$$

$$(m_{ij}^{\alpha}) = \begin{bmatrix} (\rho_\alpha+q_1) & 0 & 0 \\ 0 & (\rho_\alpha+q_2) & 0 \\ 0 & 0 & (\rho_\alpha+q_1) \end{bmatrix}. \qquad (3.32)$$

Eqs. (3.31) along with the constitutive equation Eqs. (A.1), (3.1), (3.2) make up the model theory governing the homogeneous material which replaces the two layer material. It remains to establish the nineteen model constants of the theory in terms of the mechanical properties μ_α, λ_α, and ρ_α^R of each of the two constituents.

3.2 Comments on the Theory

Before establishing equations giving the model constants in terms of the phase constants, some comments on the theory are in order. There has already been work towards developing the same kind of theory. For example, Bedford and Stern [9] using a quasi-static analysis, found the same expression for K_1, Eq. (3.25). They proposed a special mixture theory for a layered composite valid only for dilatational waves propagating parallel to the layers. Their theory takes into account only the first term in the expansion of Γ_1^t and neglects the coupling in the stress-strain relations.

In the development of the equations of linear momentum in Section (3.1), the components of the elastodynamic operator Γ_{ij}^t, derived using a micro model analysis, are replaced by approximate forms. One might suspect that this step could make the resulting theory valid only when the relative phase displacements vary slowly with changes in time. This restriction would not be real if the frequency range of the theory accommodates the first nonzero cut-off frequencies in spectra representing the behavior of dilatational and shear waves propagating in the principal directions. Fortunately, this is the case for the present theory. In fact the operators contain model constants that can be adjusted to make these cut-off frequencies from the exact and model theories match. In the section which follows, the constants are used for this purpose. In the last section on the assessment of the theory we show convincingly that the approximations used for the elastodynamic operator are appropriate.

We end this section with two general remarks on the theory developed in Section (3.1). The first is that we feel the equations of linear momentum, Eqs.(3.31), even though they were developed for a layered two phase material, are appropriate for all periodic, two phase materials. We will use these same equations, for example, when developing a theory to represent a homogeneous model for masonry walls, which have vertical layers in addition to horizontal. The difference between the masonry model and that in which vertical layering is neglected will be reflected in the forms for K_{ij} and q_{ij} and the values of the constants in the matrices.

The last comment has to do with the model constants K_1, K_2, q_1 and q_2. We have already found these in terms of the phase constants as given by equations (3.25) and (3.30). These equations are found by using micro model analysis which is based on assumed deformation modes for the phases. It might well be that in producing a model that will behave like its prototype it is more appropriate to assign other values to the constants. It seems sensible when starting the process of establishing the set of model constants, to abandon the values of K_1, K_2, q_1 and q_2 established by Eqs. (3.25) and (3.30) and have them unassigned as are the remaining fifteen. Thus the two steps, the derivation of the forms of the equations of the model and the establishment of the model constants, are clearly separated.

3.3 Evaluation of the Constants

The theory just completed describes a homogeneous, dispersive material with hexagonal symmetry, that will be used to act as a model or replacement of a two phase material composed of alternating plane layers, each made up of an isotropically elastic material. The effectiveness of the model can be judged only when it has been decided what behavior of the prototype it is that we wish to mimic. In this study we will use the new material to predict the dynamic behavior of the layered material. We have at our disposal nineteen constants that we can use to this end.

We can establish the constants by matching the dynamic behaviors of the model and prototype but the possible matching phenomena are almost without limit, certainly far beyond nineteen, so that there is no unique set of constants or no unique material to be established. By the dynamic behavior of the layered material we could mean dilatational waves parallel to the layers, or shear waves normal to the layers or other variations; we could be referring to infinite trains of waves or transient wave behavior of each type; and the behavior we are considering could be that predicted by exact theories of layered materials, behavior of the model, or behavior observed from experiments.

Our choice of a layered material as a special case of a two phase, periodic material was made partly because a layered material is close to masonry but, equally important, the choice was made because there is a rich supply of information about the dynamic behavior of layered materials. We have at hand spectra developed from the exact theory for various types of trains of waves, which can be adapted to any layer properties; experimental data describing the behavior of both trains of waves and transient waves in several different two layer materials.

We can say unequivocally that the best set of constants would be those found using system identification to match some experimental behavior, either steady state or transient. If we used system identification we would have to decide at the beginning what few among the variety of experimental behaviors it is that we choose to match. If it is the behavior of infinite trains of waves in a variety of directions as reflected in spectral lines representing phase velocity vs. wave number then a criterion function would be chosen which would represent the accumulation of least squared errors between experimental points and model points on the spectra over whatever length of spectral lines we choose. An optimization algorithm would then be constructed from which the nineteen constants are established that would minimize the criterion function. We have had considerable experience with system identification, enough to know, that with nineteen parameters involved, the problem in using this method would be formidable. Accordingly, we leave this to a future study.

The method we use here to establish the nineteen constants in terms of the layer properties, (which turns out to be successful) is a mixture of micro model analysis and matching of specific properties of spectra from the exact theory reflecting the behavior of infinite trains of particular types of waves. The method described in what follows is, we think, the simplest.

As we will be matching spectra for infinite trains of waves, we require the velocity equation, and subsequently the frequency equation, which govern infinite trains of waves travelling in our model material. To this end we adopt the trial solution

$$u_j^{\alpha} = A_j^{\alpha} e^{ik(e_p x_p - ct)} \tag{3.33}$$

in which A_j^α are the amplitudes, $\underline{e}$ is the unit normal denoting the direction of propagation, k is the wave number and c the phase velocity. When we substitute (3.33) into the constitutive relations, Eqs. (A.1), and the equations of linear momentum, Eqs.(3.31), and use the strain-displacement relations,Eq.(2.11), the condition for which a nontrivial solution will exist gives the equation

$$[(\rho_1\rho_2+\rho q)k^2]c^4 - [(\rho_1 S_{22} + \rho_2 S_{11} + qS)k^2 + \rho K]c^2$$

$$+ [(S_{11}S_{22} - S_{12}S_{12})k^2 + SK] = 0 \qquad (3.34)$$

for waves propagating in the x_1 and x_2 directions.

Equation (3.34) relates the phase velocity c to the wave number k and it should be noted that for each k there are two phase velocities leading to two spectral lines on the k-c plane. Equation (3.34) will be used in the next section to trace out the spectral lines for a variety of types of waves, but in this section we are primarily interested in the case where k is zero or approaches zero. Study of Eq.(3.34) shows that as k approaches zero, one value of c approaches infinity, and the other approaches the cut-off velocity

$$c^2 = \frac{S}{\rho} \qquad (3.35)$$

where $\rho = \sum_{\alpha=1}^{2} \rho_\alpha$; $S = \sum_{\alpha=1}^{2} \sum_{\beta=1}^{2} S_{\alpha\beta}$.

The values of $S_{\alpha\beta}$, K and q appearing in Eqs.(3.34) and (3.35) differ for each type of principal wave. They are

for dilatational waves in the x_1 direction

$$S_{\alpha\beta} = C_{11}^{\alpha\beta} \; ; \; K = K_1 \; ; \; q = q_1 \qquad (3.36)$$

for S_V waves in the x_1 direction

$$S_{\alpha\beta} = C_{44}^{\alpha\beta} \; ; \quad K = K_2 \; ; \quad q = q_2 \tag{3.37}$$

for S_H waves in the x_1 direction

$$S_{\alpha\beta} = C_{55}^{\alpha\beta} \; ; \quad K = K_1 \; ; \quad q = q_1 \tag{3.38}$$

for dilatational waves in the x_2 direction

$$S_{\alpha\beta} = C_{22}^{\alpha\beta} \; ; \quad K = K_2 \; ; \quad q = q_2 \tag{3.39}$$

for shear waves in the x_2 direction

$$S_{\alpha\beta} = C_{44}^{\alpha\beta} \; ; \quad K = K_1 \; ; \quad q = q_1 \; . \tag{3.40}$$

The phase velocity of the second branch goes to infinity as the wave number approaches zero, so additional insight can be gained by studying the frequency equation. This is easily obtained from Eq.(3.34) when we recognize that the circular frequency ω is related to k and c according to $\omega = kc$. The frequency equation becomes

$$[(\rho_1\rho_2 + \rho q)]\omega^4 - [(\rho_1 S_{22} + \rho_2 S_{11} + qS)k^2 + \rho K]\omega^2$$

$$+ [(S_{11}S_{22} - S_{12}S_{12})k^4 + SKk^2] = 0 \tag{3.41}$$

When k = 0, the equation becomes

$$(\rho_1\rho_2 + \rho q)\omega^4 - \rho K \, \omega^2 = 0 \tag{3.42}$$

so that the lowest spectral line emanates from the origin of the ω - k plane, and the second has the cut-off frequency

$$\omega_\alpha^2 = \frac{\rho K_\alpha}{(\rho_1\rho_2 + \rho q_\alpha)} \; . \tag{3.43}$$

The frequency ω_1 is the cut-off for P and S_H waves propagating in the x_1 direction, and S_V waves propagating in the x_2 direction; ω_2 for S_V waves in the x_1 direction and P waves in the x_2 direction.

We now are in a position to begin the process of establishing equations that relate the model constants to the properties of each of the two layers in the prototype.

Determination of K_α and q_α

We first establish equations from which K_1, K_2, q_1 and q_2, the constants appearing in the equations of linear momentum, can be found. In the previous section while developing the form for the elasto-dynamic operator using micro-model analysis, we found values for K_1 and K_2. These values were temporarily abandoned to leave all constants free for evaluation by other matching, but now we again adopt these equations. Accordingly, we establish K_1 and K_2 from Eq. (3.25).

On the other hand, we do not use our previous equations to establish q_1 and q_2. These constants determine directly the cut-off frequencies of infinite trains of waves, so we adjust them so that the cut-off frequencies of P and S_V waves in the x_2 direction predicted by the model are the same as those predicted by the exact theory.

The cut-off frequencies $\bar{\omega}_1$ and $\bar{\omega}_2$ from the exact theory are the lowest nonzero roots respectively of the equations

$$\begin{aligned} &\cos \xi_1 \cos \xi_2 - \frac{1+p_1^2}{2p_1} \sin \xi_1 \sin \xi_2 = 1 \\ &\cos \eta_1 \cos \eta_2 - \frac{1+p_2^2}{2p_2} \sin \eta_1 \sin \eta_2 = 1 \ . \end{aligned} \qquad (3.44)$$

In Eqs. (3.44)

$$\xi_\alpha = 2h_\alpha \bar{\omega}_1/C_T^\alpha \quad ; \quad \eta_\alpha = 2h_\alpha \bar{\omega}_2/C_L^\alpha$$

$$C_T^\alpha = \sqrt{\frac{\mu_\alpha}{\rho_\alpha^R}} \quad ; \quad p_1 = \frac{\mu_1}{\mu_2} \frac{C_T^{\ 2}}{C_T^{\ 1}} \tag{3.45}$$

$$C_L^\alpha = \sqrt{\frac{\lambda_\alpha + 2\mu_\alpha}{\rho_\alpha^R}} \quad ; \quad p_2 \quad \frac{\mu_1 + 2\mu_1}{\lambda_2 + 2\mu_2} \frac{C_L^2}{C_L^1} .$$

The constants q_1 and q_2 are obtained by equating the ω_α^2 in Eq. (3.43) to the $\bar{\omega}_\alpha^2$ obtained from Eqs. (3.44).

Determination of $C_{11}^{\alpha\beta}$, $C_{12}^{\alpha\beta}$ and $C_{13}^{\alpha\beta}$

All of the equations establishing these constants are derived using micro model analysis. We present the derivation of the equations from which the $C_{11}^{\alpha\beta}$ are found, and then state the comparable equations for the $C_{12}^{\alpha\beta}$ and $C_{13}^{\alpha\beta}$.

We assume a quasi-longitudinal deformation state parallel to layering, see Fig. 2, so that distance between the mid-planes of layers remain unchanged. If the lateral expansion (or contraction) of the first constituent is δ, that of the second will be $(-\delta)$.

When we average the constitutive relations for $\overset{*}{\sigma}{}_{11}^{\alpha}$ and $\overset{*}{\sigma}{}_{22}^{\alpha}$

$$\overset{*}{\sigma}{}_{11}^{\alpha} = (\lambda_\alpha + 2\mu_\alpha)\, \overset{*}{e}{}_{11}^{\alpha} + \lambda_\alpha\, \overset{*}{e}{}_{22}^{\alpha}$$

$$\overset{*}{\sigma}{}_{22}^{\alpha} = (\lambda_\alpha + 2\mu_\alpha)\, \overset{*}{e}{}_{22}^{\alpha} + \lambda_\alpha\, \overset{*}{e}{}_{11}^{\alpha} \tag{3.46}$$

over the thickness of the αth constituent by using the formulas

$$\bar{\sigma}^1_{11} = \frac{1}{2h_1} \int_{-h_1}^{h_1} \overset{*}{\sigma}{}^1_{11} \, dx_2$$

$$\bar{\sigma}^2_{11} = \frac{1}{2h_2} \int_{h_1}^{\Delta+h_2} \overset{*}{\sigma}{}^2_{11} \, dx_2 \text{ ; etc.} \tag{3.47}$$

we obtain

$$\bar{\sigma}^1_{11} = n_1 E_1 \, \bar{e}^1_{11} + \lambda_1 \frac{\delta}{2h_1}$$

$$\bar{\sigma}^2_{11} = n_2 E_2 \, \bar{e}^2_{11} - \lambda_2 \frac{\delta}{2h_2} \tag{3.48}$$

and

$$\bar{\sigma}^1_{22} = \lambda_1 \bar{e}^1_{11} + n_1 E_1 \frac{\delta}{2h_1}$$

$$\bar{\sigma}^2_{22} = \lambda_2 \bar{e}^2_{11} - n_2 E_2 \frac{\delta}{2h_2} \quad . \tag{3.49}$$

At the interfaces of layers $\overset{*}{\sigma}{}^{\alpha}_{22}$ should be continuous. In the micro model we assume that this continuity is approximately satisfied by that of the average $\bar{\sigma}^{\alpha}_{22}$. By using Eqs. (3.49) and the continuity of $\overset{*}{\sigma}{}^{\alpha}_{22}$, the term δ appearing in Eqs. (3.48) can be eliminated. This yields

$$\bar{\sigma}^1_{11} = (n_1 E_1 - \frac{\lambda_1^2}{n_1 E})\bar{e}^1_{11} + \frac{\lambda_1 \lambda_2}{n_1 E} \bar{e}^2_{11}$$

$$\bar{\sigma}^2_{11} = \frac{\lambda_1 \lambda_2}{n_2 E} \bar{e}^1_{11} + (n_2 E_2 - \frac{\lambda_2^2}{n_2 E}) \bar{e}^2_{11} . \tag{3.50}$$

When we use the equation $\sigma_{11}^{\alpha} = n_{\alpha}\, \bar{\sigma}_{11}^{\alpha}$ which relates the partial stress σ_{11}^{α} to the average stress $\bar{\sigma}_{11}^{\alpha}$ and note that $e_{11}^{\alpha} = \bar{e}_{11}^{\alpha}$, we finally obtain

$$
\begin{aligned}
\sigma_{11}^{1} &= (n_1^2 E_1 - \frac{\lambda_1^2}{E})\, e_{11}^{1} + \frac{\lambda_1 \lambda_2}{E}\, e_{11}^{2} \\
\sigma_{11}^{2} &= \frac{\lambda_1 \lambda_2}{E}\, e_{11}^{1} + (n_2^2 E_2 - \frac{\lambda_2^2}{E})\, e_{11}^{2} .
\end{aligned}
\tag{3.51}
$$

To obtain the constants $C_{11}^{\alpha\beta}$ in terms of the properties of the layers we compare the expressions for σ_{11}^{1} and σ_{22}^{2} given by Eqs. (3.51) with those from the constitutive relations Eqs. (A.1). The comparable stresses are equal when

$$
C_{11}^{11} = n_1^2 E_1 - \frac{\lambda_1^2}{E} ; \quad C_{11}^{22} = n_2^2 E_2 - \frac{\lambda_2^2}{E} ; \quad C_{11}^{12} = C_{11}^{21} = \frac{\lambda_1 \lambda_2}{E} . \tag{3.52}
$$

The relations, Eqs. (3.52), were obtained previously in [10], where a mixture theory, valid only for dilatational waves propagating parallel to layering, was proposed.

Here we also note that a similar procedure to that described above was previously used by Stern and Bedford [21] to establish all of the constants of a model which they proposed by using the theory of mixtures. In that work Stern and Bedford did not take into account the coupling in the stress-strain relations which would imply that the state of stress of one phase is affected by the deformation of the other.

Using the same method as for $C_{11}^{\alpha\beta}$, we find

$$
\begin{aligned}
C_{12}^{11} &= n_1 \lambda_1 \frac{E_2}{E} ; \quad C_{12}^{22} = n_2 \lambda_2 \frac{E_1}{E} ; \quad C_{12}^{12} = n_2 \lambda_1 \frac{E_2}{E} \\
C_{12}^{21} &= C_{21}^{12} = n_1 \lambda_2 \frac{E_1}{E}
\end{aligned}
\tag{3.53}
$$

and

$$C_{13}^{11} = n_1\lambda_1 - \frac{\lambda_1^2}{E}\ ; \quad C_{13}^{22} = n_2\lambda_2 - \frac{\lambda_2^2}{E}\ . \tag{3.54}$$

We note from Ref. 1 that the constants found using Eqs.(3.52-3.54) are identical with those that will allow the cut-off phase velocities of P and S_H waves in the x_1 direction from the model to match those given by the exact theory. The last analysis also gives $C_{13}^{12} = C_{13}^{21} = \frac{\lambda_1\lambda_2}{E}$, but each of these is equal to C_{11}^{12}, already established, so these equalities do not provide independent information.

It only remains to establish $C_{22}^{\alpha\beta}$ and $C_{44}^{\alpha\beta}$, and we choose to find these sets of constants by adjusting the cut-off and asymptotic phase velocities of infinite trains of waves of two specific types.

Determination of $C_{22}^{\alpha\beta}$ and $C_{44}^{\alpha\beta}$

We find three independent constants C_{22}^{11}, C_{22}^{22} and C_{22}^{12} (= C_{22}^{21}) by matching three properties of the spectral lines representing the relationship between phase velocity and wave numbers for dilatational waves traveling perpendicular to layering. A similar procedure was previously used by Mindlin and McNiven [22] who matched cut-off frequencies to establish adjustment factors as part of an approximate theory governing the vibrations of rods. We first match the cut-off velocity of the lowest branch. We already have the velocity for the model from Eqs. (3.35) and (3.39). The same velocity from the exact theory is

$$\bar{c}^2 = \frac{E_1E_2}{\rho E}\ . \tag{3.55}$$

Matching gives the equation

$$C_{22}^{11} + C_{22}^{22} + 2C_{22}^{12} = \frac{E_1E_2}{E}\ . \tag{3.56}$$

The other two equations are obtained by matching the asymptotic phase velocities for the lowest and second lines, respectively.

We know from the exact theory that the asymptotic phase velocity of the lowest branch is zero. When we derive this same velocity for the model from Eq. (3.34) and set it equal to zero, we get

$$C_{22}^{11}\,C_{22}^{22} - C_{22}^{12}\,C_{22}^{12} = 0. \tag{3.57}$$

Finally, from the exact theory we have the expression for the fastest transmitted wave velocity.

$$c_{\infty} = \frac{\sqrt{\frac{E_1}{\rho_1}}\;\sqrt{\frac{E_2}{\rho_2}}}{\sqrt{\frac{E_1}{\rho_1}} + \sqrt{\frac{E_2}{\rho_2}}} \tag{3.58}$$

When the velocity is equated to the second asymptotic phase velocity for the model derived from Eq. (5.2), we get a third independent equation

$$\rho_1 C_{22}^{22} + \rho_2 C_{22}^{11} = (\rho_1\rho_2 + \rho q_2)c_{\infty}^2 - q_2\,\frac{E_2E_1}{E} \tag{3.59}$$

Comparable equations are obtained by matching the same quantities, this time for S_v waves propagating in the x_2 direction. The equations are

$$C_{44}^{11} + C_{44}^{22} + 2C_{44}^{12} = \frac{r_1r_2}{r} \tag{3.60}$$

$$C_{44}^{11}\,C_{44}^{22} - C_{44}^{12}\,C_{44}^{12} = 0 \tag{3.61}$$

$$\rho_1 C_{44}^{22} + \rho_2 C_{44}^{11} = (\rho_1\rho_2 + \rho q_1)c_{\infty}^2 - q_1\,\frac{r_1r_2}{r} \tag{3.62}$$

In Eq. (3.62)

$$c_{\infty} = \frac{\sqrt{\frac{r_1}{\rho_1}} \sqrt{\frac{r_2}{\rho_2}}}{\sqrt{\frac{r_1}{\rho_1}} \sqrt{\frac{r_2}{\rho_2}}} \tag{3.63}$$

With the set of equations established in this section, one is able to calculate the nineteen model constants for a particular layered material for which the phase constants are specified. This completes the formulation of the theory governing the model material.

3.4 Assessment of the Model

The final step in completing a theory is to ascertain how well it works. Here, we have available a wealth of material describing three types of dynamic behavior of various layered materials. The first is theoretical and consists of phase velocity and frequency spectra that predict the behavior of infinite trains of waves from the exact theory. The second displays the same behavior from experimental observations, and the third describes transient wave behavior from experiments.

The use of this transient wave behavior to assess the approximate theory is probably the most demanding and the most satisfying, but since it requires additional theoretical development this assessment is left to the next chapter.

We compare spectra derived from the model theory with the exact theory spectra of Sun et al. [2] which they used to assess a first order effective stiffness theory for a layered composite. The phase constants assumed by Sun and the comparable model constants are shown in Table 1. The experimental results used here are due to Whittier et al [23]. They established spectral lines representing the relationship between phase velocity and frequency for waves propagating parallel to layering. The spectral lines are for two different layered materials; thornel reinforced carbon phenolic and boron reinforced carbon phenolic. The elastic properties of each of these materials are shown in Tables 2 and 3, along with their respective model constants that are needed.

Comparisons with the exact theory are displayed in Figures (3-9). In these Figures, the dimensionless wave number ξ, the phase velocity β and the normalized frequency Ω are given by

$$\xi = 2h_1k \; ; \; \beta = c/(\mu_2/\rho_2^R)^{\frac{1}{2}} \; ; \; \Omega = 2h_1\omega/(\mu_2/\rho_2^R)^{\frac{1}{2}} \tag{3.64}$$

TABLE 1.
PROPERTIES OF SUN'S MATERIAL

SPECIFIED LAYER PROPERTIES							
n_1	n_2	$\bar{\rho}_1^R$	$\bar{\rho}_2^R$	$\bar{\mu}_1$	$\bar{\mu}_2$	$\bar{\lambda}_1$	$\bar{\lambda}_2$
0.8	0.2	3	1	100	1	150	2.333
COMPUTED MODEL CONSTANTS							
$\bar{K}_1$	$\bar{K}_2$	$\bar{q}_1$	$\bar{q}_2$				
36.923	158.550	0.041	0.040				
$\bar{C}_{11}^{11}$	$\bar{C}_{11}^{22}$	$\bar{C}_{11}^{12}$	$\bar{C}_{12}^{11}$	$\bar{C}_{12}^{22}$	$\bar{C}_{12}^{12}$	$\bar{C}_{21}^{12}$	
230.998	0.855	0.762	5.663	0.445	1.416	1.778	
$\bar{C}_{13}^{11}$	$\bar{C}_{13}^{22}$	$\bar{C}_{22}^{11}$	$\bar{C}_{22}^{22}$	$\bar{C}_{22}^{12}$	$\bar{C}_{44}^{11}$	$\bar{C}_{44}^{22}$	$\bar{C}_{44}^{12}$
70.998	0.455	44.076	4.389	-13.908	10.686	1.158	-3.517

THE DIMENSIONLESS QUANTITIES APPEARING IN THIS TABLE ARE DEFINED BY

$$\bar{\rho}_\alpha^R = \rho_\alpha^R / \rho_2^R \; ; \; \bar{\mu}_\alpha = \mu_\alpha / \mu_2 \; ; \; \bar{\lambda}_\alpha = \lambda_\alpha / \mu_2$$

$$\bar{K}_\alpha = \frac{(2h_1)^2 K_\alpha}{\mu_2} \; ; \; \bar{q}_\alpha = q_\alpha / \rho_2^R \; ; \; \bar{C}_{ij}^{\alpha\beta} = C_{ij}^{\alpha\beta} / \mu_2 .$$

TABLE 2.

PROPERTIES OF THORNEL REINFORCED CARBON PHENOLIC

SPECIFIED LAYER PROPERTIES							
h_1	h_2	ρ_1^R	ρ_2^R	μ_1	μ_2	λ_1	λ_2
cm		$\frac{\text{dyne-}\mu\text{sec}^2}{\text{cm}^4}$		dyne/cm^2		dyne/cm^2	
0.0032	0.0279	1.47 x10^{12}	1.42 x10^{12}	0.756 x10^{12}	0.0662 x10^{12}	0.756 x10^{12}	0.114 x10^{12}

COMPUTED MODEL CONSTANTS				
K_1	q_1	C_{11}^{11}	C_{11}^{22}	C_{11}^{12}
dyne/cm^4	$\frac{\text{dyne-}\mu\text{sec}^2}{\text{cm}^4}$	dyne/cm^2	dyne/cm^2	dyne/cm^2
227.213x10^{12}	0.399x10^{12}	0.210x10^{12}	0.220x10^{12}	0.0039x10^{12}

TABLE 3.

PROPERTIES OF BORON REINFORCED CARBON PHENOLIC

SPECIFIED LAYER PROPERTIES							
h_1	h_2	ρ_1^R	ρ_2^R	μ_1	μ_2	λ_1	λ_2
cm		$\frac{\text{dyne-}\mu\text{sec}^2}{\text{cm}^4}$		dyne/cm^2		dyne/cm^2	
0.0052	0.026	2.37 x10^{12}	1.42 x10^{12}	0.951 x10^{12}	0.0662 x10^{12}	0.806 x10^{12}	0.114 x10^{12}

COMPUTED MODEL CONSTANTS				
K_1	q_1	C_{11}^{11}	C_{11}^{22}	C_{11}^{12}
dyne/cm^4	$\frac{\text{dyne-}\mu\text{sec}^2}{\text{cm}^4}$	dyne/cm^2	dyne/cm^2	dyne/cm^2
239.387x10^{12}	0.280x10^{12}	0.410x10^{12}	0.204x10^{12}	0.0055x10^{12}

Figures 3-8 show comparisons between spectral lines representing phase velocities for waves travelling in principal directions. The matching is remarkably good. Figure 9 shows the same comparison for waves propagating parallel to the x_1-x_2 plane at an angle of 45 degrees with the x_1 axis. In Figures 3 and 7 comparison is made not only with the exact theory but with spectral lines derived from both first and second order effective stiffness theories [2,4]. From both figures we may conclude that the theory presented here is superior to the first order theory. In Figure 3, the present theory and the second order theory are about equally effective; while for P waves travelling in the x_2 direction shown in Figure 7, the second order effective stiffness theory is superior to the present theory. However, it is important to point out that this preferable performance is obtained at the expense of a considerable increase in complication. Even though the dispersion introduced by the lower approximate spectral line appears to be slight, we can report that the transient wave behavior, predicted by the present theory, of P waves propagating in the x_2 direction agrees well with the behavior reported from experiments. This comparison will be presented in the next chapter.

In all of these Figures the spectral lines give the relationship between phase velocity and wave number. Since the second spectral line extends toward infinite phase velocity as the wave number approaches zero, very little insight into the behavior of this higher mode is gained from these Figures for small wave numbers. Accordingly, for this mode, a comparison is made of spectral lines reflecting the relationship between frequency and wave number; these lines have finite cut-offs. Frequency spectra for this higher mode for P waves and S_H waves propagating parallel to layering are shown in Figures 4 and 6, respectively.

The last two figures, Figures 10 and 11, are devoted to thornel and boron reinforced carbon phenolic laminates, respectively. In the Figures we compare the first spectral lines found using the present theory with the exact and experimental ones for dilatational waves propagating parallel to layering. The comparisons are made on the (f-c) plane, where f is the cyclic frequency, related to the angular frequency ω by $f = \omega/2\pi$. The Figures indicate that agreement between experimental and theoretical data is remarkably good.

Finally, an important point should be noted. For waves propagating perpendicular to layering, the exact spectrum has a banded structure with passing and stopping bands. These bands are regions of the spectrum representing harmonic waves that propagate and attenuate respectively. The present approximate theory and others, except those proposed by Herrmann, Kaul and Delph [7,8], do not predict the stopping bands. In these papers the authors have developed a one-dimensional approximate theory, which they call effective dispersion theory, for waves propagating perpendicular to layering only. Their theory accommodates the first stopping band and approximates quite well the two lowest spectral lines over the first two Brillouin zones. A refined three-dimensional approximate theory based on micromorphic mixture theory is being developed for two phase composites by the authors of the present work and will be reported soon. In that work it is found that the refined theory, which accommodates both the symmetric and antisymmetric displacement distributions, within phases, predicts the stopping bands for waves propagating perpendicular to layering.

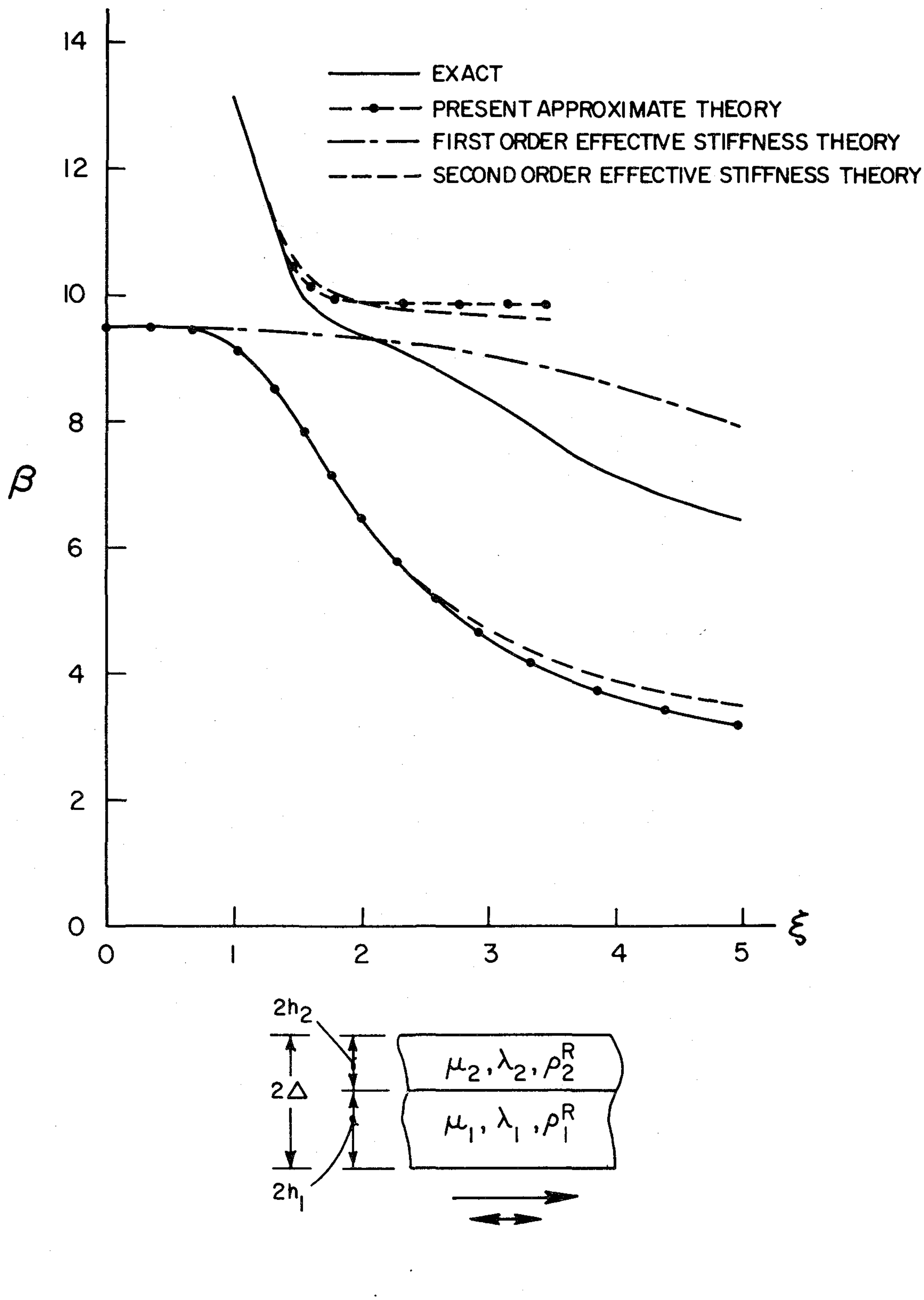

FIG. 3. SPECTRUM FOR DILATATIONAL WAVES PROPAGATING PARALLEL TO LAYERING (SUN'S MATERIAL)

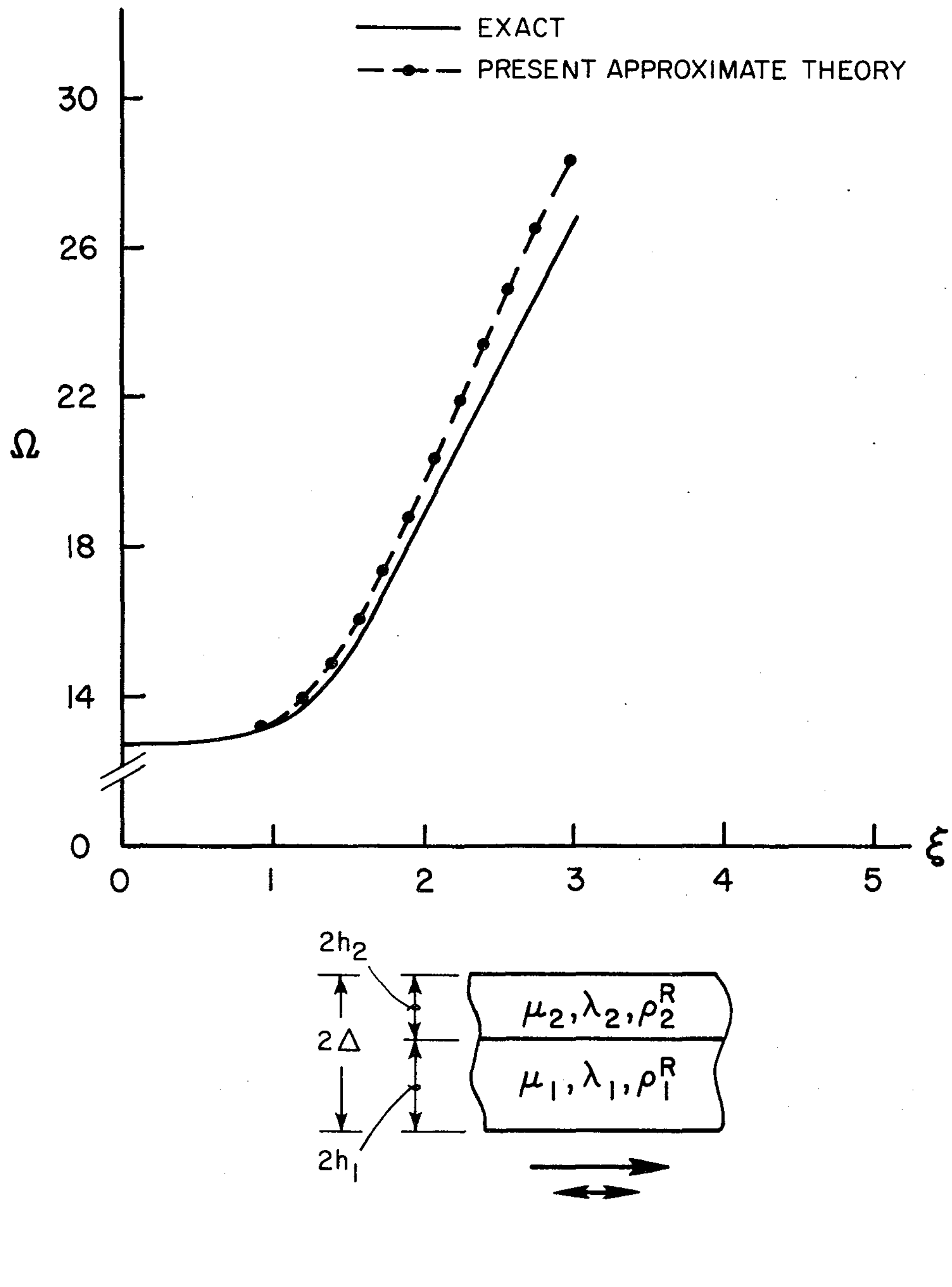

FIG. 4. THE SECOND SPECTRAL LINE ON THE FREQUENCY-WAVE NUMBER PLANE FOR DILATATIONAL WAVES PROPAGATING PARALLEL TO LAYERING (SUN'S MATERIAL)

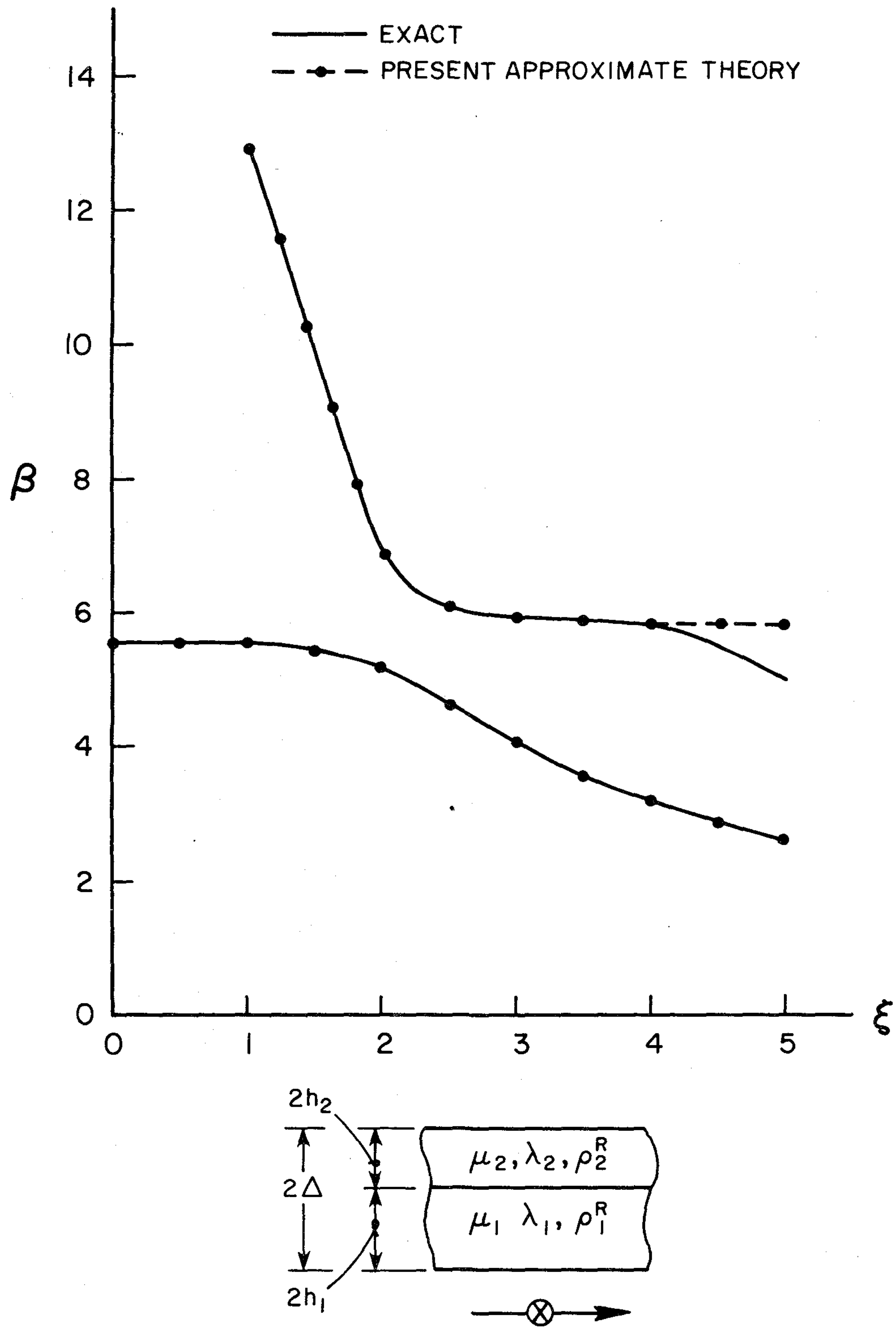

FIG. 5. SPECTRUM FOR SH WAVES PROPAGATING PARALLEL TO LAYERING (SUN'S MATERIAL)

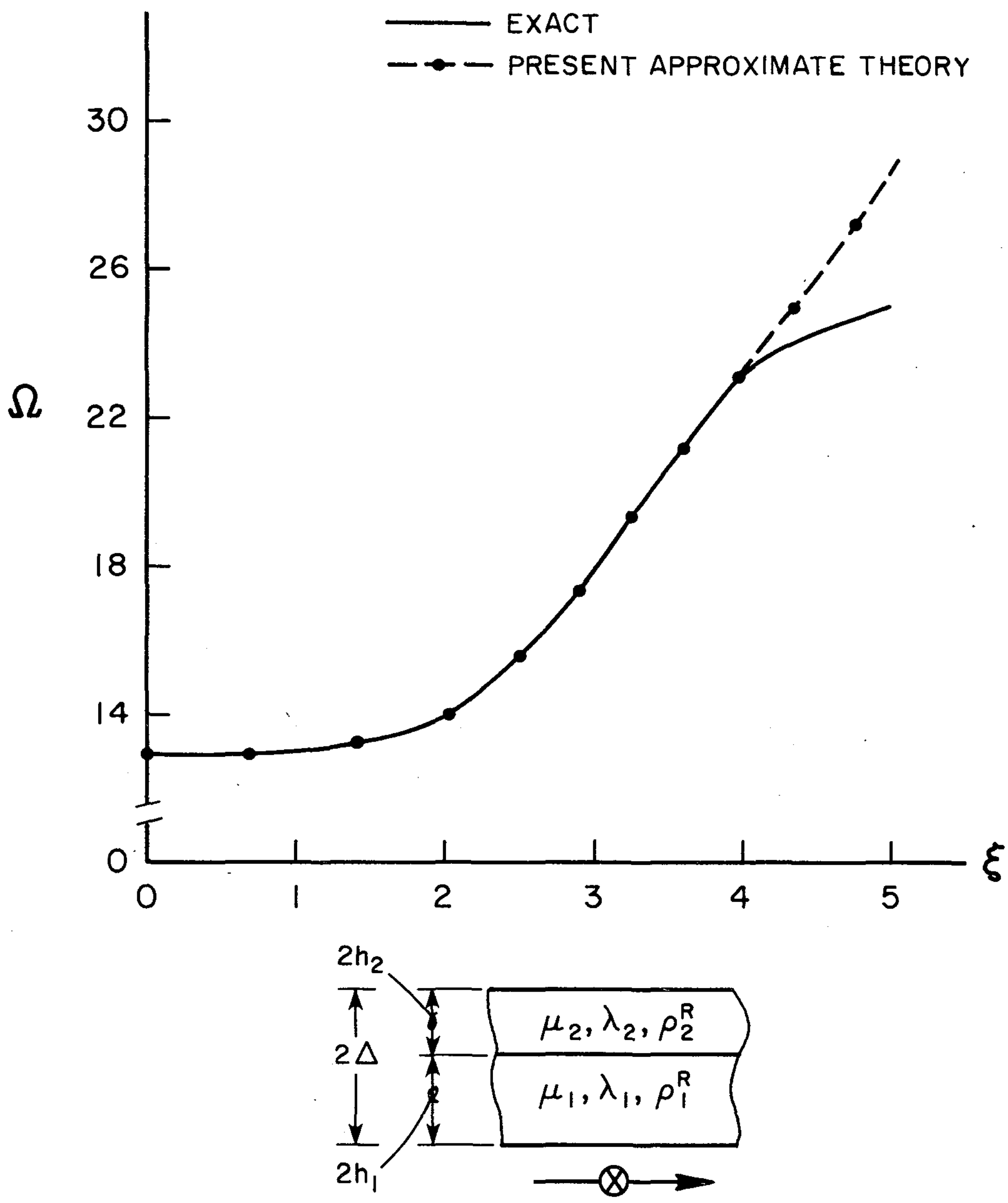

FIG. 6. THE SECOND SPECTRAL LINE ON THE FREQUENCY-WAVE NUMBER PLANE FOR SH WAVES PROPAGATING PARALLEL TO LAYERING (SUN'S MATERIAL)

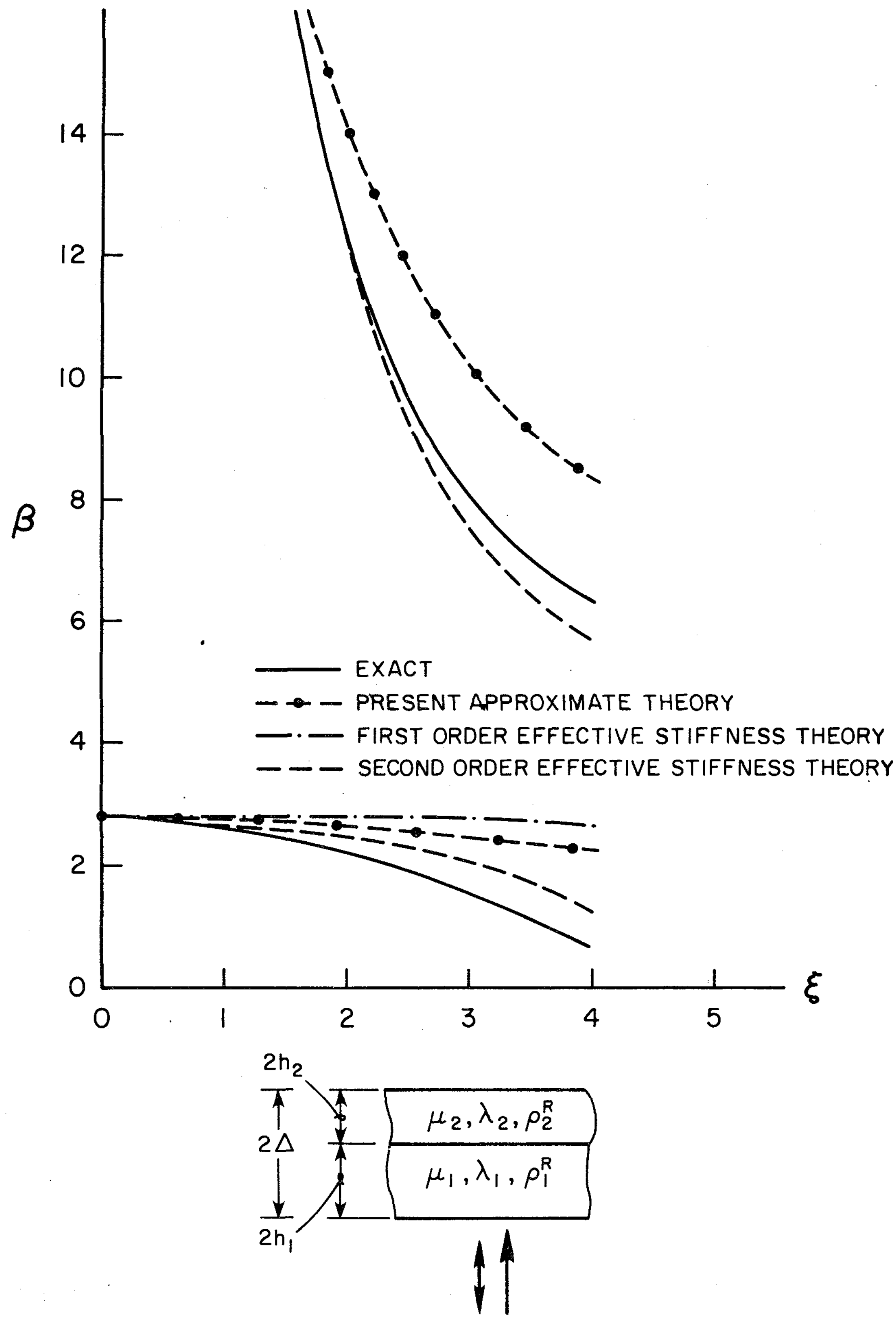

FIG. 7. SPECTRUM FOR DILATATIONAL WAVES PROPAGATING PERPENDICULAR TO LAYERING (SUN'S MATERIAL)

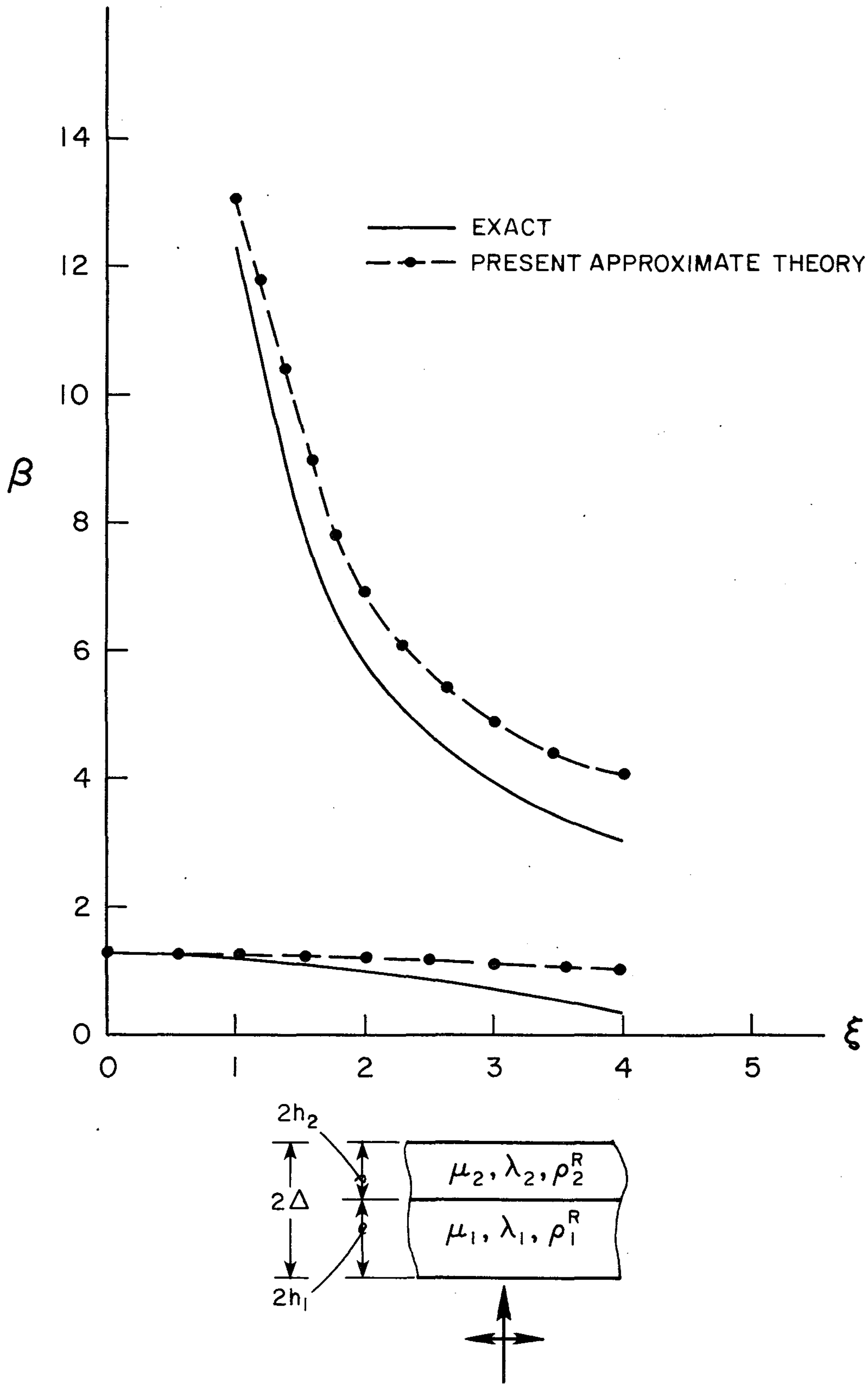

FIG. 8. SPECTRUM FOR TRANSVERSE WAVES PROPAGATING PERPENDICULAR TO LAYERING (SUN'S MATERIAL)

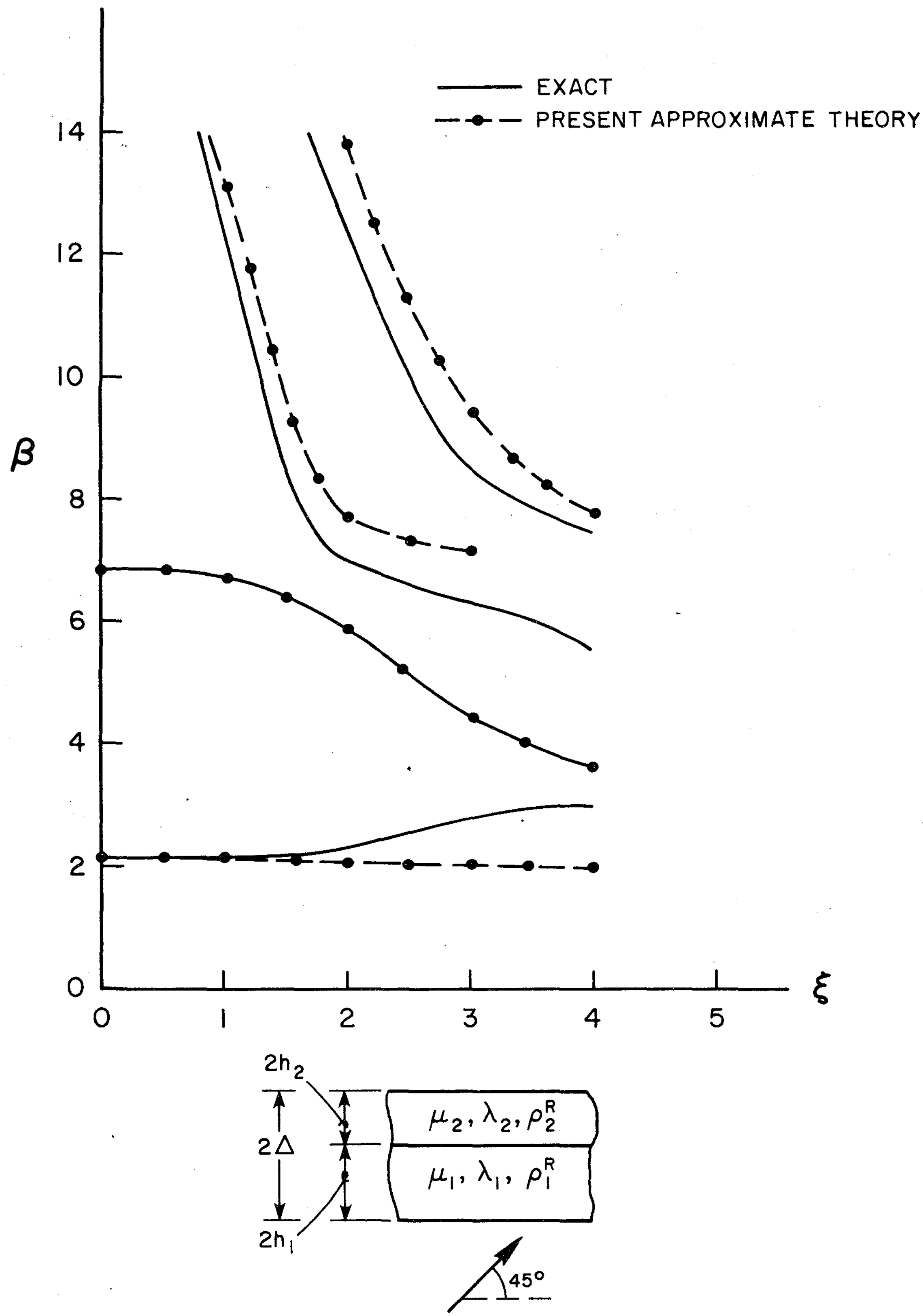

FIG. 9. SPECTRUM FOR WAVES PROPAGATING AT AN ANGLE OF 45° WITH THE x_1 AXIS (SUN'S MATERIAL)

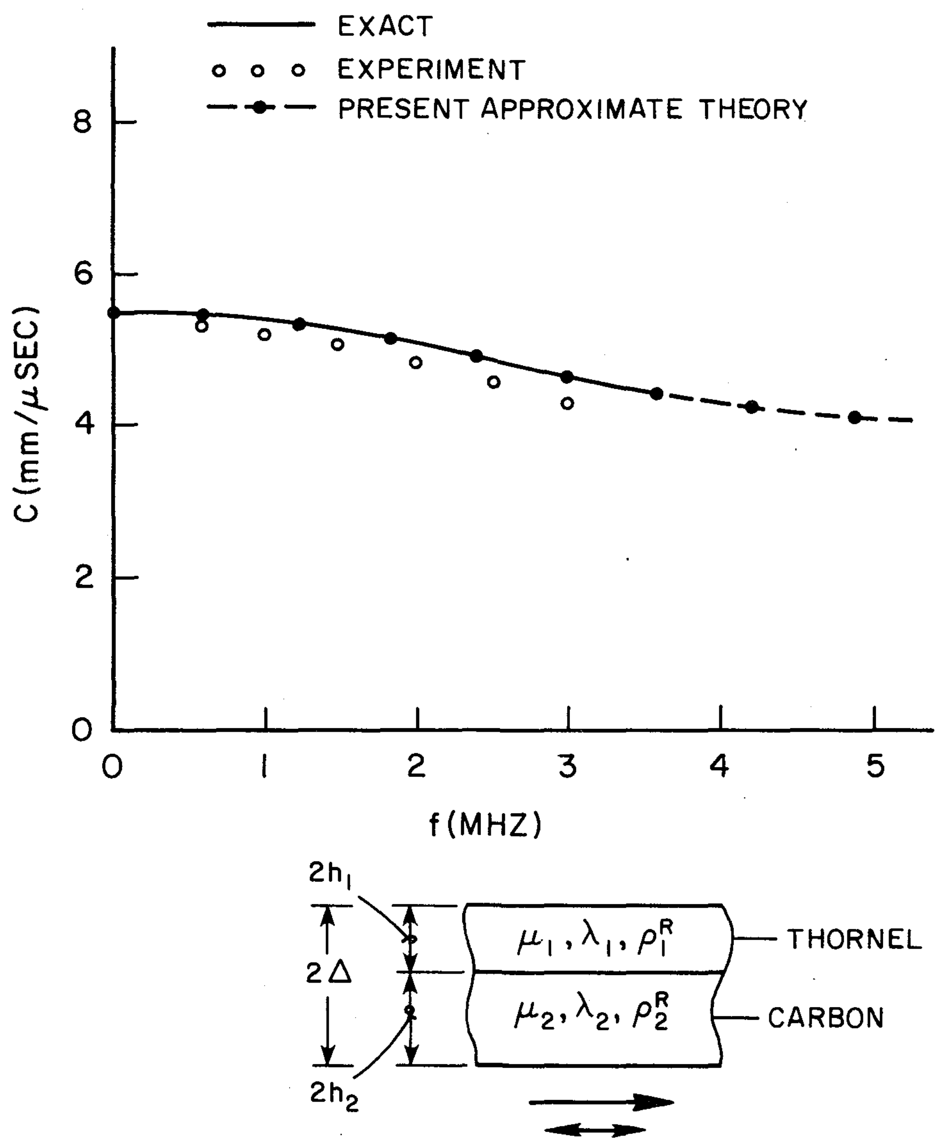

FIG. 10. FIRST SPECTRAL LINE FOR DILATATIONAL WAVES PROPAGATING PARALLEL TO LAYERING (THORNEL REINFORCED CARBON PHENOLIC)

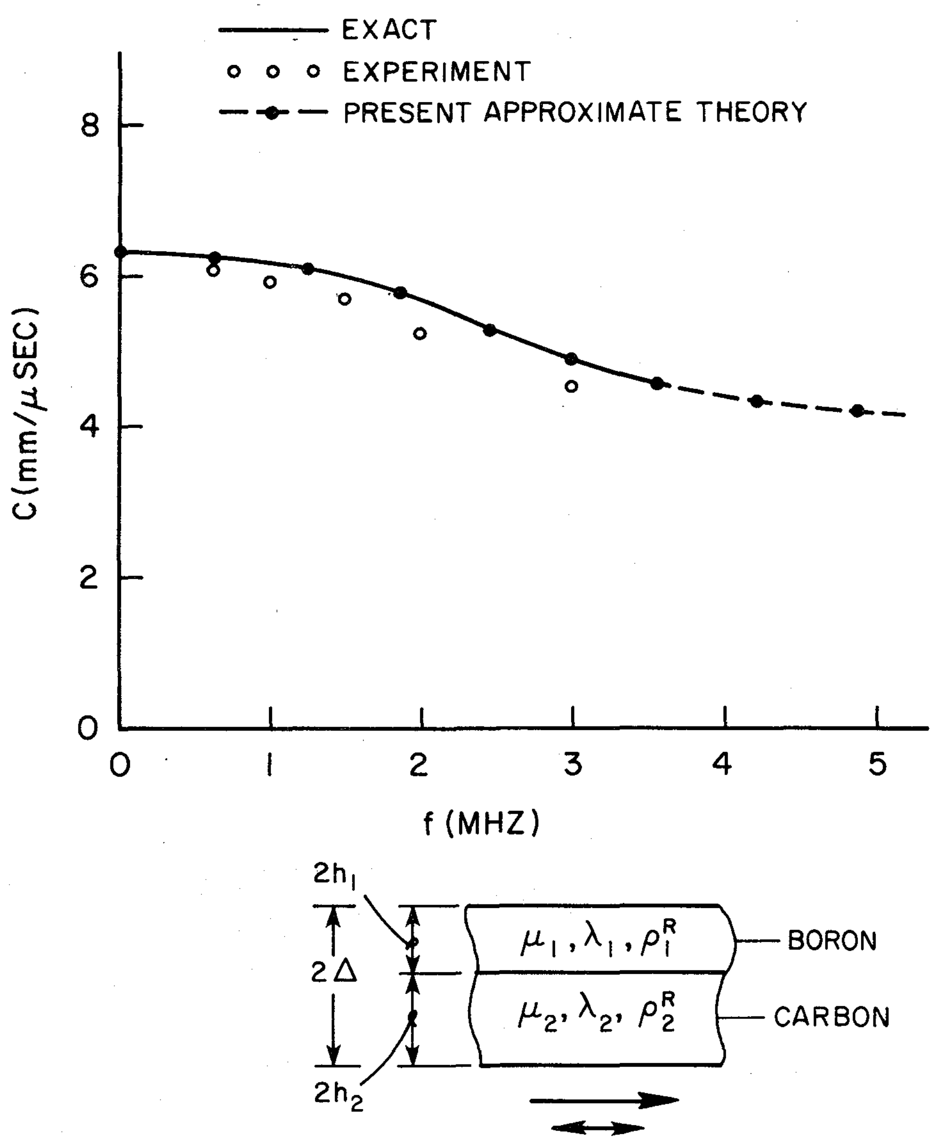

FIG. 11. FIRST SPECTRAL LINE FOR DILATATIONAL WAVES PROPAGATING PARALLEL TO LAYERING
(BORON REINFORCED CARBON PHENOLIC)

CHAPTER 4

PROPAGATION OF TRANSIENT WAVES IN ELASTIC LAMINATED COMPOSITES

In this chapter we appraise the model by comparing the responses predicted by the model for a transient input with those observed experimentally. Experimental data allow us to make comparisons for the behavior of dilatational waves travelling both parallel and perpendicular to the layers in both plates and semi-infinite bodies. Where possible, comparison is also made with responses predicted by the exact theory.

4.1 Formulation of the Problems

The problems that we study are those dictated by the experiments from which we have data for transient responses. They involve either layered half spaces or layered plates; and we study the cases where the layers are parallel to the surface of the half space or one surface of the plate, and the cases where the layers are normal to these surfaces. The time dependent normal pressure is applied to these surfaces so that for the first cases dilatational waves are generated normal to the layers,and for the second cases parallel to them (see Figs.14-20). We assume that the composite slabs or half spaces are initially at rest before the normal pressure is applied.

The symmetry conditions of the problems suggest that the field variables, such as velocities, stresses, etc., depend on time t and the perpendicular distance x measured from the plane surface to which the pressure is applied.

If we denote the normal x-components of phase stresses and strains by σ_α and e_α, the constitutive equations, Eq. (A.1), become

$$\sigma_1 = S_{11}e_1 + S_{12}e_2$$
$$\sigma_2 = S_{12}e_1 + S_{22}e_2 \quad , \tag{4.1}$$

where

$$S_{\alpha\beta} = C_{11}^{\alpha\beta} \text{ , for propagation parallel to layering}$$
$$S_{\alpha\beta} = C_{22}^{\alpha\beta} \text{ , for propagation perpendicular to layering.} \tag{4.2}$$

Then, using Eq.(2.11) the strains, e_α, are related to the x-components of the phase displacements, u_α, by

$$e_\alpha = \frac{\partial u_\alpha}{\partial x} \quad . \tag{4.3}$$

When the weight of the composite material is neglected the equations of linear momentum, Eqs.(3.31), become

$$\frac{\partial \sigma_1}{\partial x} + K(u_2 - u_1) = m_1\dot{v}_1 - q\dot{v}_2$$
$$\frac{\partial \sigma_2}{\partial x} + K(u_1 - u_2) = -q\dot{v}_1 + m_2\dot{v}_2, \tag{4.4}$$

where

$$m_1 = \rho_1 + q \;;\;\; m_2 = \rho_2 + q \tag{4.5}$$

and

$$K = K_1 \;;\;\; q = q_1 \text{ , for propagation parallel to layering}$$
$$K = K_2 \;;\;\; q = q_2 \text{ , for propagation perpendicular to layering,} \tag{4.6}$$

and v_α are the x-components of phase velocity and are related to the displacements by $v_\alpha = \dot{u}_\alpha$.

Since the medium is initially at rest all the field variables (u_α, v_α, etc.) are zero at $t = 0$.

Equations (4.1), (4.3) and (4.4) constitute the governing equations of our problems. Their solutions for appropriate initial and boundary conditions, which will be discussed later, determine the time variations of the field variables (u_α, v_α, σ_α, e_α) at an arbitrary station.

4.2 Solutions of the Problems

The method of characteristics is used because the governing equations are hyperbolic and our problems contain only one space variable; furthermore this method accommodates a variety of boundary conditions.

A full discussion of the method of characteristics is given in [24]. The method of characteristics reduces the governing partial differential equations to an equivalent system of ordinary differential equations, called canonical equations, which are valid along characteristic lines only. The canonical equations are more appropriate for numerical analysis as their solutions are simple to obtain. The method of characteristics also employs decay equations from which the discontinuities across wave fronts can be computed before starting the numerical analysis.

Because of the particular types of time variations chosen for the applied pressure in the numerical analysis, which will be discussed later, the decay equations are not needed in this study. Accordingly, we present the canonical equations only.

Canonical Equations

In order to put the governing partial differential equations, Eqs. (4.1), (4.3) and (4.4), into the form of a system of first order differential equations, we first differentiate Eq. (4.3) with respect to time and obtain the compatibility equations

$$\dot{e}_\alpha = \frac{\partial v_\alpha}{\partial x} \quad . \tag{4.7}$$

Differentiating Eq. (4.1) with respect to time and using Eq. (4.7) we get

$$\begin{aligned} \dot{\sigma}_1 &= S_{11} \frac{\partial v_1}{\partial x} + S_{12} \frac{\partial v_2}{\partial x} \\ \dot{\sigma}_2 &= S_{12} \frac{\partial v_2}{\partial x} + S_{22} \frac{\partial v_2}{\partial x} \quad . \end{aligned} \tag{4.8}$$

Equations (4.4) and (4.8) constitute a system of first order differential equations. In matrix form the system has the form:

$$\underset{-}{A}\, \underset{-}{\bar{u}}_{,t} + \underset{-}{B}\, \underset{-}{\bar{u}}_{,x} + \underset{-}{C} = \underset{-}{0}, \tag{4.9}$$

where

$$\underset{-}{A} = \begin{bmatrix} m_1 & -q & 0 & 0 \\ -q & m_2 & 0 & 0 \\ 0 & 0 & 1 & 0 \\ 0 & 0 & 0 & 1 \end{bmatrix} \; ; \quad \underset{-}{B} = \begin{bmatrix} 0 & 0 & -1 & 0 \\ 0 & 0 & 0 & -1 \\ -S_{11} & -S_{12} & 0 & 0 \\ -S_{12} & -S_{22} & 0 & 0 \end{bmatrix} \; ; \; \underset{-}{C} = \begin{Bmatrix} -K(u_2-u_1) \\ K(u_2-u_1) \\ 0 \\ 0 \end{Bmatrix}, \tag{4.10}$$

$\underset{-}{\bar{u}}$ is the unknown vector defined by

$$\underset{-}{\bar{u}} = \left\{ v_1 \; v_2 \; \sigma_1 \; \sigma_2 \right\}^T , \tag{4.11}$$

and

$$\underset{-}{\bar{u}}_{,t} = \frac{\partial \underset{-}{\bar{u}}}{\partial t} \; ; \quad \underset{-}{\bar{u}}_{,x} = \frac{\partial \underset{-}{\bar{u}}}{\partial x} \; ,$$

and T denotes the transpose of a matrix or vector.

We next find the characteristic lines along which the canonical equations are valid. They are governed by the characteristic equation

$$\det(\underline{B} - V\underline{A}) = 0, \quad (4.12)$$

where $V = \frac{dx}{dt}$ is the wave propagation velocity. The canonical equations are then

$$\underline{\ell}^{(i)T} \underline{A} \frac{d\underline{\bar{u}}}{dt} + \underline{\ell}^{(i)T} \underline{C} = 0, \text{ valid along } \frac{dx}{dt} = V^{(i)} \quad (i = 1\text{-}4), \quad (4.13)$$

where $\frac{d}{dt}$ indicates differentiation along the characteristic line with respect to time, and $\underline{\ell}^{(i)}$ is the left-hand eigen vector satisfying the equation

$$\underline{B}^T \underline{\ell}^{(i)} = V^{(i)} \underline{A}^T \underline{\ell}^{(i)}, \text{ no summation over } i \quad (i = 1\text{-}4). \quad (4.14)$$

In Eqs. (4.13) and (4.14) $V^{(i)}$ is the ith eigenvalue determined by Eq. (4.12). For our problems the four eigenvalues are

$$V^{(1)} = \sqrt{z_1} = C_1;\ V^{(2)} = -\sqrt{z_1} = -C_1;\ V^{(3)} = \sqrt{z_2} = C_2\ \ V^{(4)} = -\sqrt{z_2} = -C_2, \quad (4.15)$$

where z_1 and z_2 are the roots of

$$(m_1 m_2 - q^2)z^2 - [m_2 S_{11} + m_1 S_{22} + 2qS_{12}]z + S_{11}S_{22} - S_{12}^2 = 0 \quad (4.16)$$

Examination of Eq. (4.5) will show that the coefficient $(m_1 m_2 - q^2)$ is positive as $q \geqslant 0$; in addition since the strain energy function is positive definite it follows that z_1 and z_2 are nonnegative. This ensures that the $V^{(i)}$ $(i = 1\text{-}4)$ are real. In the discussions which follow we assume, without loss of generality, that $z_1 > z_2$.

We study separately the cases for waves travelling parallel and perpendicular to layering and ascertain the appropriate wave velocities for each case by studying Eqs. (3.52), (3.56-59), (4.2) and (4.16). For the case of waves propagating parallel to layering, $\frac{dx}{dt} = V^{(i)}$ $(i = 1,2)$ describe two characteristic families of straight lines with slopes (C_1) and $(-C_1)$ on the (x-t) plane; i.e., $x \pm C_1 t$ = const. (see Fig.12). For the same case $\frac{dx}{dt} = V^{(i)}$ (i = 3,4) describe another two families of straight lines $x \pm C_2 t$ = const. For the case of waves propagating perpendicular to layering the first two characteristic families are again governed by $x \pm C_1 t$ = const. (see Fig. 13). The remaining two become vertical lines parallel to the t axis because for this case $C_2 = 0$.

Finally, the canonical equations are obtained from Eqs. (4.9), (4.10) and (4.13). For waves propagating parallel to layering they are

$$(m_1 + q\, V^{(i)} a^{(i)}) \frac{dv_1}{dt} - (q + m_2\, V^{(i)} a^{(i)}) \frac{dv_2}{dt}$$
$$- \frac{1}{V^{(i)}} \frac{d\sigma_1}{dt} + a^{(i)} \frac{d\sigma_2}{dt} - (1 + V^{(i)} a^{(i)})\, K(u_2 - u_1) = 0, \text{ along } \frac{dx}{dt} = V^{(i)} \tag{4.17}$$

(i = 1-4; no summation on i)

where the coefficients $a^{(i)}$ (i = 1-4) are defined by

$$a^{(i)} = \frac{\frac{S_{11}}{V^{(i)}} - m_1 V^{(i)}}{S_{12} + q(V^{(i)})^2} = \frac{\frac{S_{12}}{V^{(i)}} + q\, V^{(i)}}{S_{22} - m_2 (V^{(i)})^2} . \tag{4.18}$$

For waves propagating perpendicular to layering the first two canonical equations valid along the characteristic lines $x \pm C_1 t$ = const. are again given by Eq. (4.17) with i = 1 and 2. The remaining two, which are valid along the vertical lines, are

$$(m_1 + \frac{S_{11}}{S_{12}} q) \frac{dv_1}{dt} - (q + \frac{S_{11}}{S_{12}} m_2) \frac{dv_2}{dt} - K\,(1 + \frac{S_{11}}{S_{12}})(u_2 - u_1) = 0, \text{ along } \frac{dx}{dt} = 0$$
$$- \frac{d\sigma_1}{dt} + \frac{S_{11}}{S_{12}} \frac{d\sigma_2}{dt} = 0, \text{ along } \frac{dx}{dt} = 0. \tag{4.19}$$

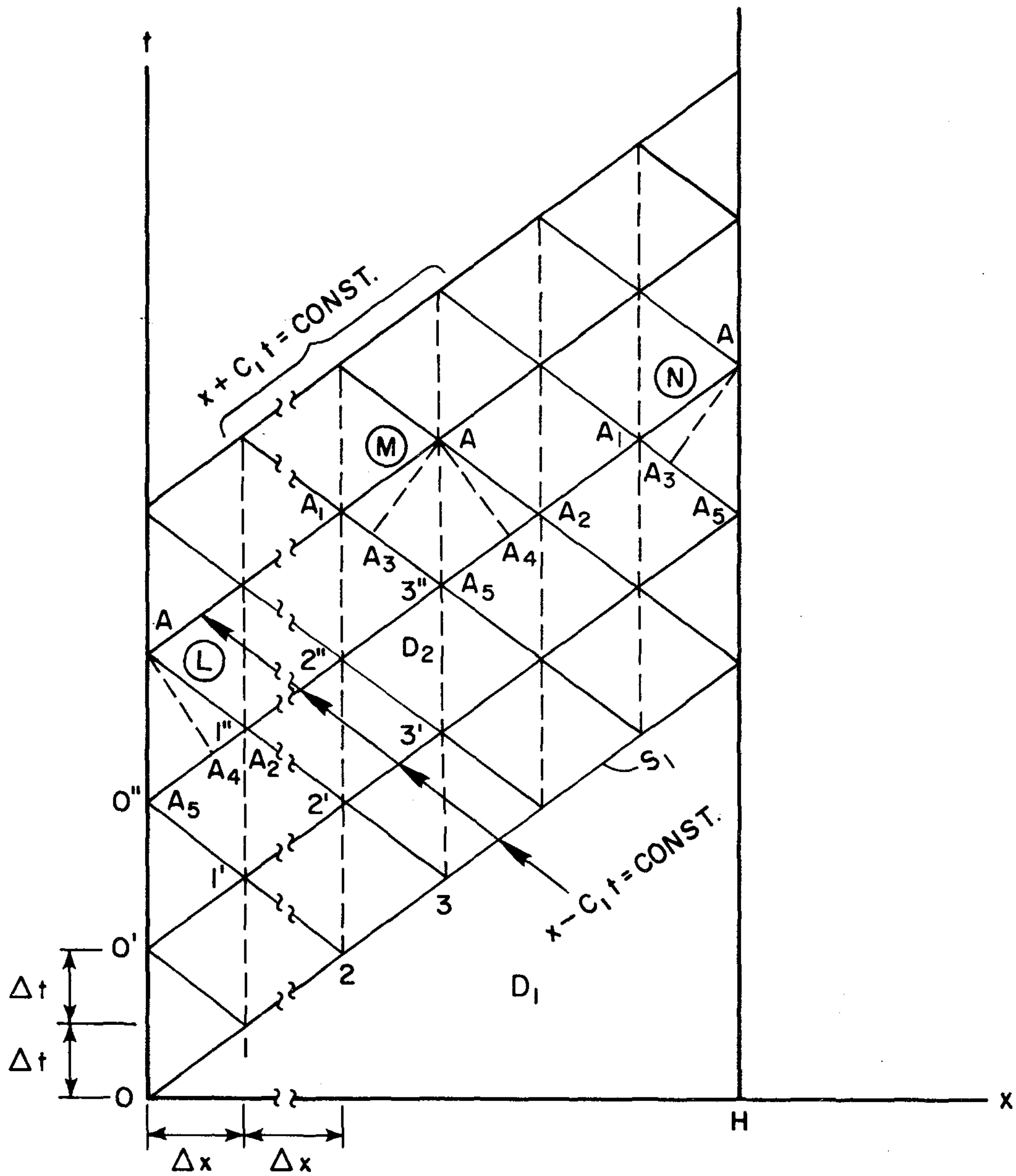

FIG. 12. DESCRIPTION OF CHARACTERISTIC LINES FOR DILATATIONAL WAVES PROPAGATING PARALLEL TO LAYERING IN A LAYERED COMPOSITE SLAB OF THICKNESS H

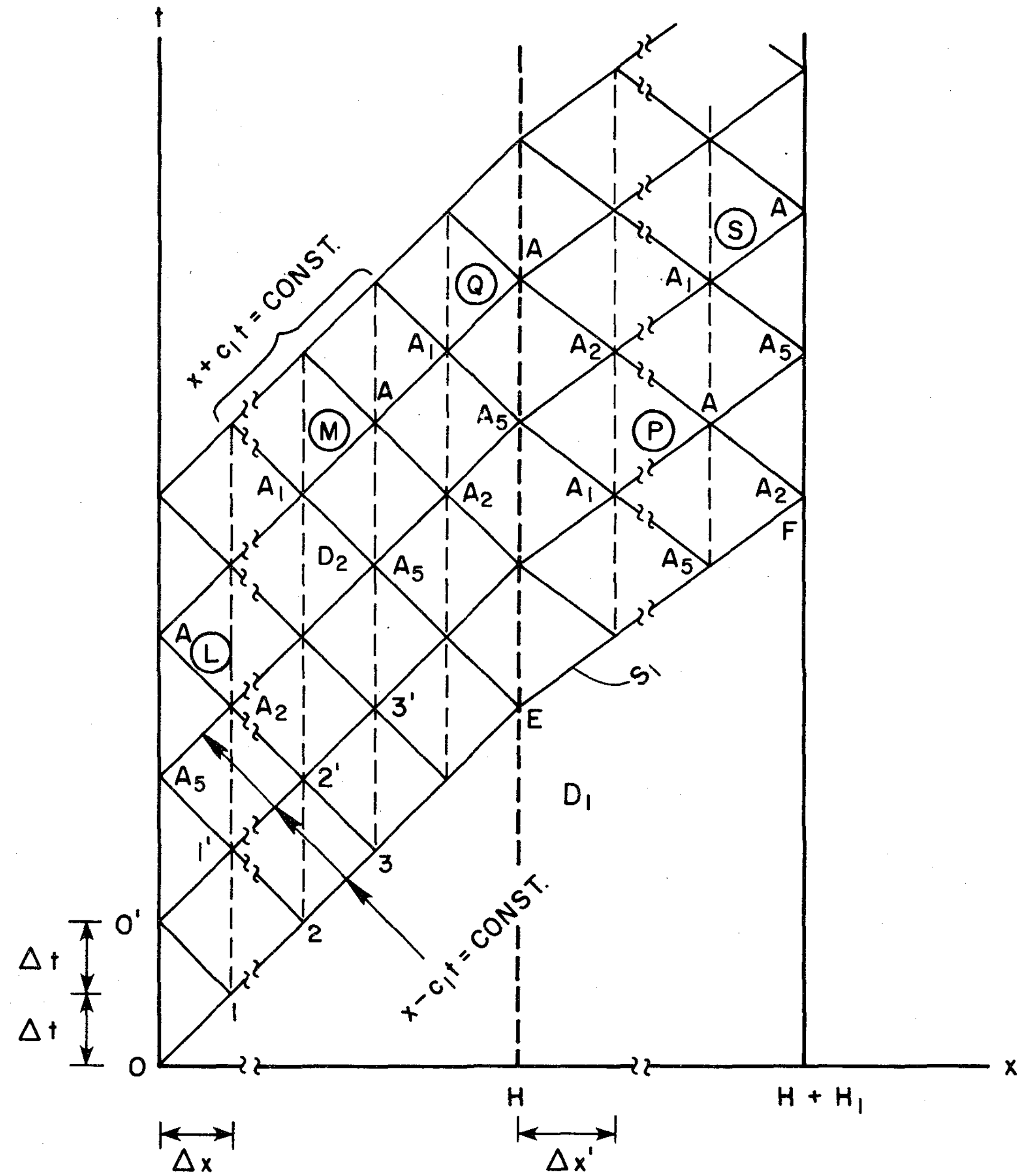

FIG. 13. DESCRIPTION OF CHARACTERISTIC LINES FOR DILATATIONAL WAVES PROPAGATING PERPENDICULAR TO LAYERING IN A LAYERED COMPOSITE SLAB OF THICKNESS H WHICH AT THE RIGHT END IS PERFECTLY BONDED TO A HOMOGENEOUS ELASTIC SLAB OF THICKNESS H_1

4.3 Numerical Analysis

The purpose of this paper is to appraise the ability of the model theory to predict dynamic responses to transient inputs; therefore, the specific problems that we solve are those for which there are experimental data. These consist of four separate problems. Two involve plates of finite thickness, one having the layers parallel to the surfaces and the other perpendicular. The other two problems study the responses in half spaces, again with the two distinguished by whether the layering is parallel or normal to the surface.

The first problem involves a composite slab of thickness H subjected to a uniform dynamic pressure on one surface (see Fig. 14 or 15). The other surface is free of traction. The surfaces of the slab are perpendicular to layering so that the pressure applied generates dilatational waves that propagate parallel to the layers. We seek the solution $(\bar{u}_i) = (u_\alpha, v_\alpha, \sigma_\alpha)$ at a station x and time t. The method of characteristics is best understood by examining Fig. 12 showing the (x-t) plane. On this plane the solution region is bounded by the vertical lines x = 0 and x = H. The portion of the first wave front before reflection is the line S_1 given by $x - C_1 t = 0$. This line divides the solution region into the undisturbed and disturbed regions D_1 and D_2, respectively. The reflected wave fronts are not shown in the figure because they are not needed in the numerical analysis since the time variation chosen for the applied pressure eliminates first order discontinuities across such wave fronts. To find the numerical solution, the disturbed region D_2 is subdivided by means of one primary and one secondary grid. The primary grid is shown by solid lines and formed by two sets of parallel lines $x \pm C_1 t$ = const. so that the space mesh size Δx is related to the time mesh size Δt by $\Delta x = C_1 \Delta t$. The secondary sets of grid lines are members of the families $x \pm C_2 t$ = const. and are shown by dotted lines in Fig. 12. These lines are used when analyzing an individual element. Although we note that the values of $\bar{u}_i$ along S_1 can be

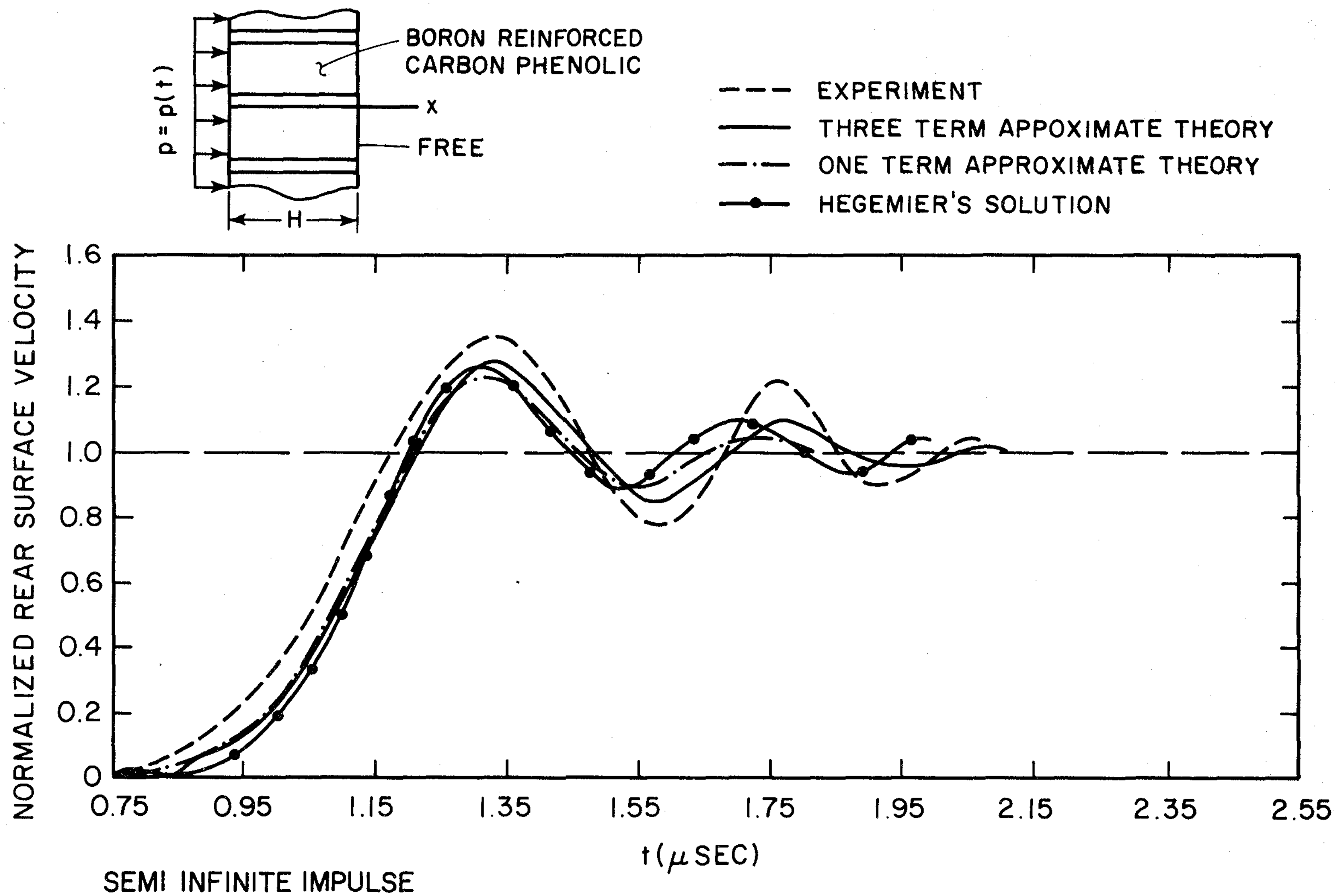

FIG. 14. COMPARISON OF EXPERIMENTAL AND THEORETICAL WAVE PROFILES FOR DILATATIONAL WAVES PROPAGATING PARALLEL TO LAYERING (BORON REINFORCED CARBON PHENOLIC LAMINATE; SEMI INFINITE IMPULSE)

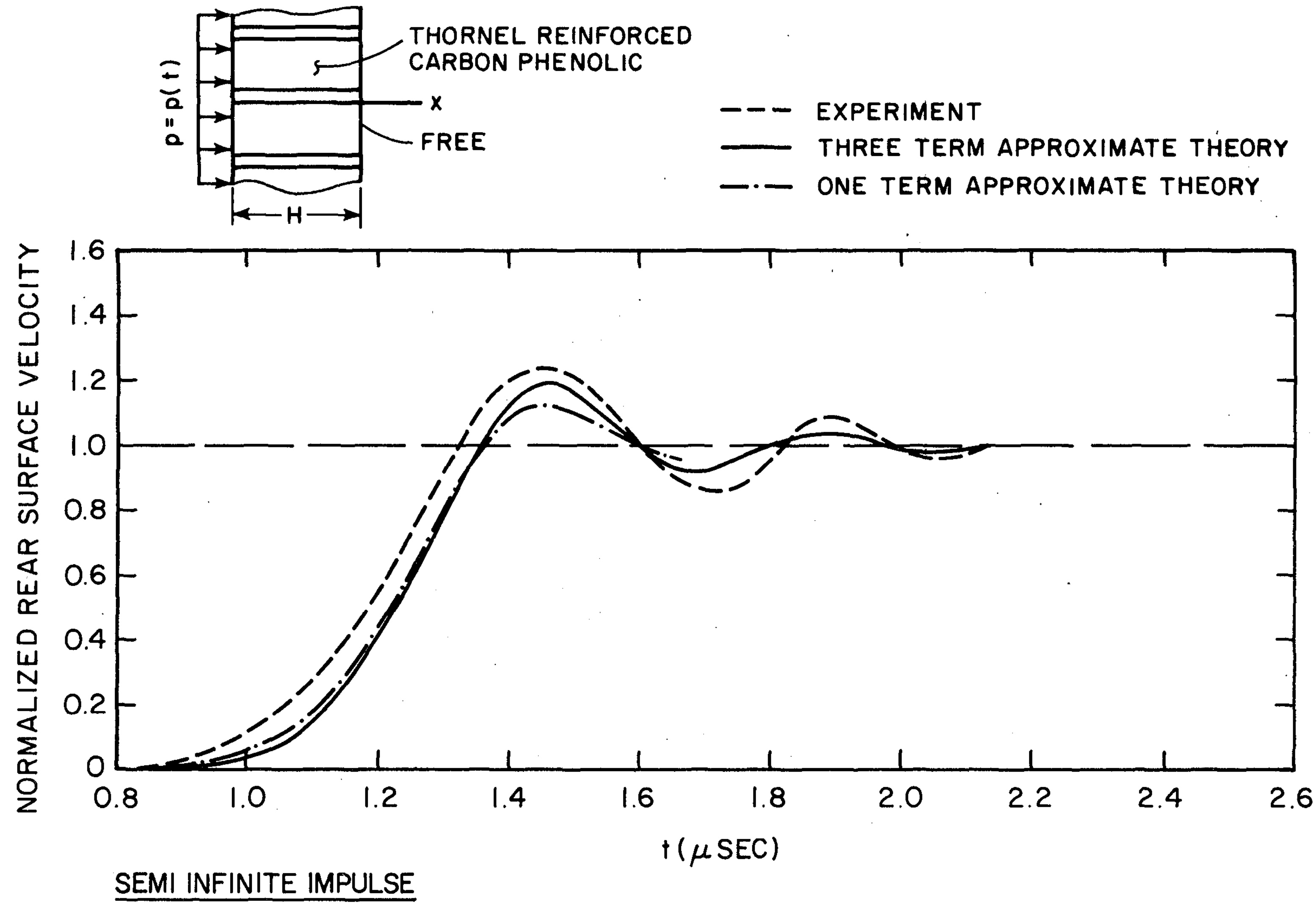

FIG. 15. COMPARISON OF EXPERIMENTAL AND THEORETICAL WAVE PROFILES FOR DILATATIONAL WAVES PROPAGATING PARALLEL TO LAYERING (THORNEL REINFORCED CARBON PHENOLIC LAMINATE; SEMI INFINITE IMPULSE)

determined from decay equations, they are all zero here because the composite slab is initially at rest, and because the applied pressure distribution in our problems has no discontinuity at t = 0. To establish the $\bar{u}_i$ at points of region D_2 we start from the origin and move along S_1 where the $\bar{u}_i$ are known. Using a technique for each element, we advance into the region, element by element, in the order (0', 1', 2', ..., 0", 1", 2",...). The technique depends on the element which can be one of three types on the (x-t) plane, namely, M, L and N (see Fig. 12). For an interior element M we know $\bar{u}_i$ at the points A_1, A_2 and A_5, and wish to determine it at the point A. As $\bar{u}_i$ has six components, we need six equations to establish them. Four equations come from the canonical equations, Eq. (4.17), written along the lines AA_i(i = 1-4). The remaining two are the compatibility equations,

$$v_\alpha = \dot{u}_\alpha \ , \tag{4.20}$$

which relate phase displacements to phase velocities and are valid along the vertical line AA_5. For the values of the $\bar{u}_i$ at the interior points A_3 and A_4 we use linear interpolation between the points A_1 and A_5 or A_2 and A_5. The $\bar{u}_i$ at the point A are found by integrating the six equations using an implicit trapezoidal integration formula.

For the element L, adjacent to the line x = 0, the procedure is the same except that the two equations along the lines AA_1 and AA_3 are replaced by the boundary conditions at x = 0,

$$\sigma_\alpha(A) = -n_\alpha p(A) \ , \tag{4.21}$$

where p is the applied dynamic pressure. Similarly, for the other boundary element N the free traction boundary conditions at x = H,

$$\sigma_\alpha(A) = 0 \tag{4.22}$$

replace the canonical equations along lines AA_2 and AA_4.

The procedure for the problem shown in Fig. 16, involving wave propagation parallel to layering in a composite half space, is the same as that discussed for a composite slab except that the element N is disregarded since H becomes infinite for a half space.

To explain the numerical procedure for the cases for which the direction of propagation is perpendicular to layering, we choose the specific problem described in Fig. 18. The problem involves a composite slab of thickness H subjected to a uniform dynamic pressure on one surface. The other surface of the composite is perfectly bonded to a trailer of thickness H_1, which is made of a homogeneous material. For reasons which will be discussed later, the other surface of the trailer is assumed to be free of traction. We refer to Fig. 13 showing the (x-t) plane and distinguish between two regions on this plane. The first, bounded by the vertical lines $x = 0$ and $x = H$, is the solution domain for the composite slab, while the second bounded by the lines $x = H$ and $x = H + H_1$, is that for the homogeneous trailer. The line S_1 describing the first wave front divides the space-time domain into the undisturbed and disturbed regions D_1 and D_2. The line S_1 is composed of two line segments. The first segment OE has the slope C_1 and represents the wave front before reflection and refraction occur at the interface $x = H$. The second segment EF describes the transmitted wave front and has the slope $C = \sqrt{\frac{2\mu+\lambda}{\bar{\rho}}}$, where C is the dilatational wave propagation velocity in the trailer which is identified by Lamé's constants μ and λ and the mass density $\bar{\rho}$. The primary grid for the numerical analysis is formed by the characteristic lines with slope C_1 in the composite slab region and with slope C in the homogeneous slab region. For the whole solution domain we use a common time mesh size Δt which dictates two different space mesh sizes Δx and $\Delta x'$ in the composite and homogeneous regions.

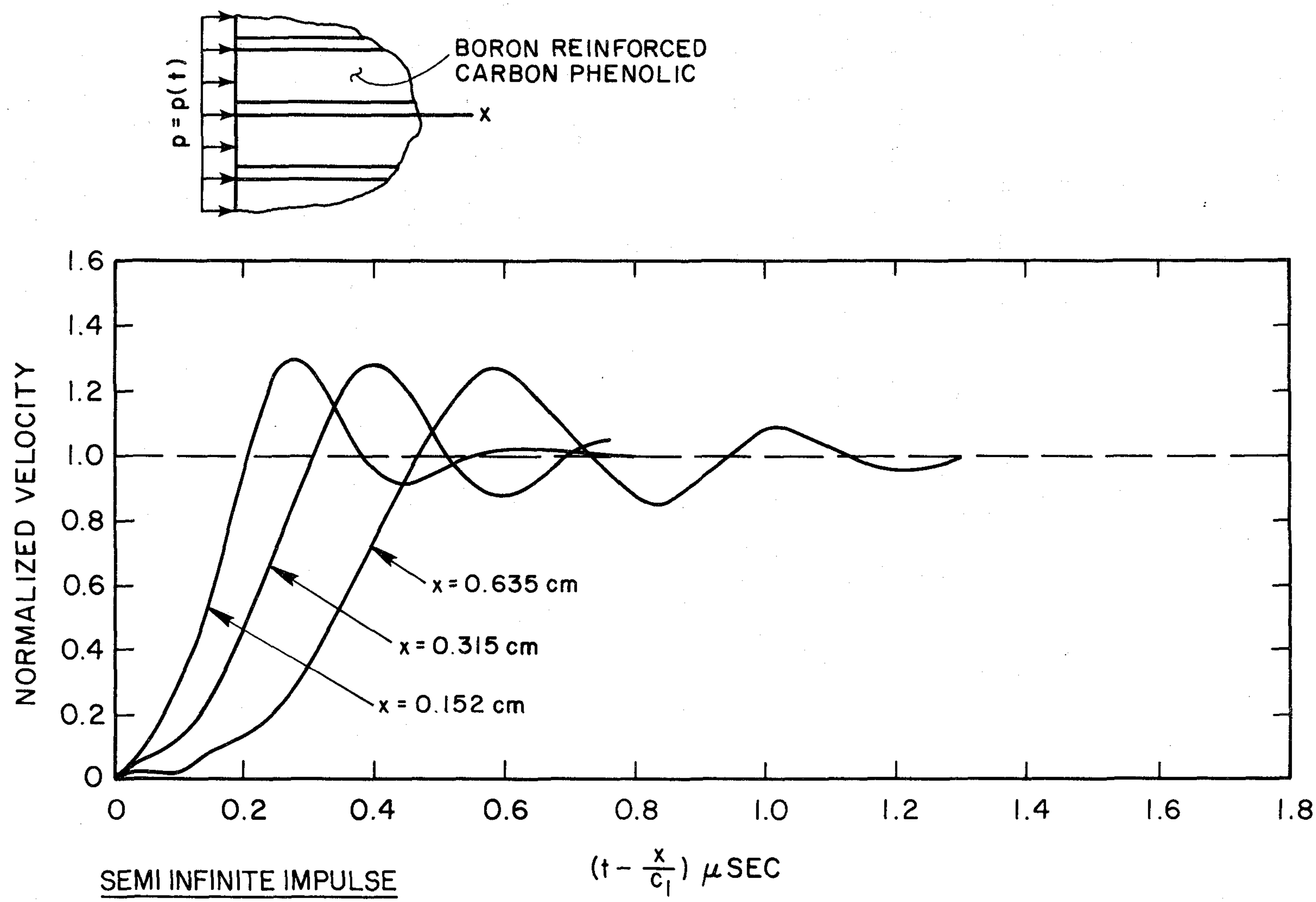

FIG. 16. COMPARISON OF WAVE PROFILES AT VARIOUS STATIONS FOR DILATATIONAL WAVES PROPAGATING PARALLEL TO LAYERING (BORON REINFORCED CARBON PHENOLIC LAMINATE; SEMI INFINITE IMPULSE)

The numerical procedure for this case is basically the same as that discussed for wave propagation parallel to layering. The differences occur in the individual elements, boundary conditions and interface continuity conditions. Accordingly, in what follows, we discuss only these differences. We first note that at points in the composite region the number of unknowns (u_α, v_α, σ_α) is six. On the other hand the unknowns in the homogeneous region are only three, the displacement u, particle velocity v and stress σ. For the interior element M of the composite region two equations come from the canonical equations along AA_1 and AA_2, Eq. (4.17) and i = 1,2, two from the canonical equations along AA_5, Eqs. (4.19), and the remaining two from the compatibility equations along AA_5, Eq. (4.20). For the boundary element L of the composite region, the canonical equation along AA_1 is replaced by the boundary condition at x = 0,

$$\sum_{\alpha=1}^{2} \sigma_\alpha(A) = -p(A) \ . \tag{4.23}$$

For the interior element P of the homogeneous region we need only three equations to find the unknowns at the point A. Two of them are the canonical equations of the homogeneous slab:

$$\begin{aligned} \frac{d\sigma}{dt} - \bar{\rho}\, C \frac{dv}{dt} &= 0 \quad \text{along } AA_1 \\ \frac{d\sigma}{dt} + \bar{\rho}\, C \frac{dv}{dt} &= 0 \quad \text{along } AA_2 \ . \end{aligned} \tag{4.24}$$

The last one is the compatibility equation $v = \dot{u}$ valid along the vertical line AA_5. For the boundary element S, the free traction boundary condition at $x = H + H_1$, $\sigma(A) = 0$, replaces the canonical equation along AA_2. In the analysis of the mixed interface element Q, the interface continuity conditions

$$\sum_{\alpha=1}^{2} \sigma_\alpha(A) = \sigma(A); \quad \sum_{\alpha=1}^{2} n_\alpha v_\alpha(A) = v(A) \; ; \quad \sum_{\alpha=1}^{2} n_\alpha u_\alpha(A) = u(A) \tag{4.25}$$

are used.

We use the same procedure for the problem, shown in Fig.17, involving propagation perpendicular to layering in a half space, except that the width of the composite slab is infinite. Finally for the problem shown in Fig.20 which contains a buffer slab between the applied pressure and composite, the continuity conditions between buffer and composite are taken into account in the analysis.

4.4 Assessment of the Homogeneous Model

We assess the homogeneous, dispersive model, and the theory which governs the propagation of waves in it, by comparing the transient wave behavior in the model with all of the data we have been able to gather describing transient wave response in layered media. Primarily these data are obtained from physical experiments but we have been able to make comparisons, for some of the cases, with the responses predicted by the exact theory and with another approximate theory due to Hegemier, Gurtman and Nayfeh [10].

The first case we study is a plate of thickness H in which the layers are aligned normal to the surfaces (Figs. 14 and 15). The response is generated by a pressure, p(t), applied normal to one surface so that the resulting waves propagate parallel to the layers. The opposite face is free of traction. The response measured is the average particle velocity on the free face. The experiments on these plates were performed by Whittier and Peck [23]. Two different laminates were studied, both having a thickness H = 0.635 cm. The first is composed of alternate layers of thornel and carbon phenolic, the second alternate layers of boron and carbon phenolic. The mechanical properties of these materials and the layer thicknesses are listed in Tables 2 and 3,

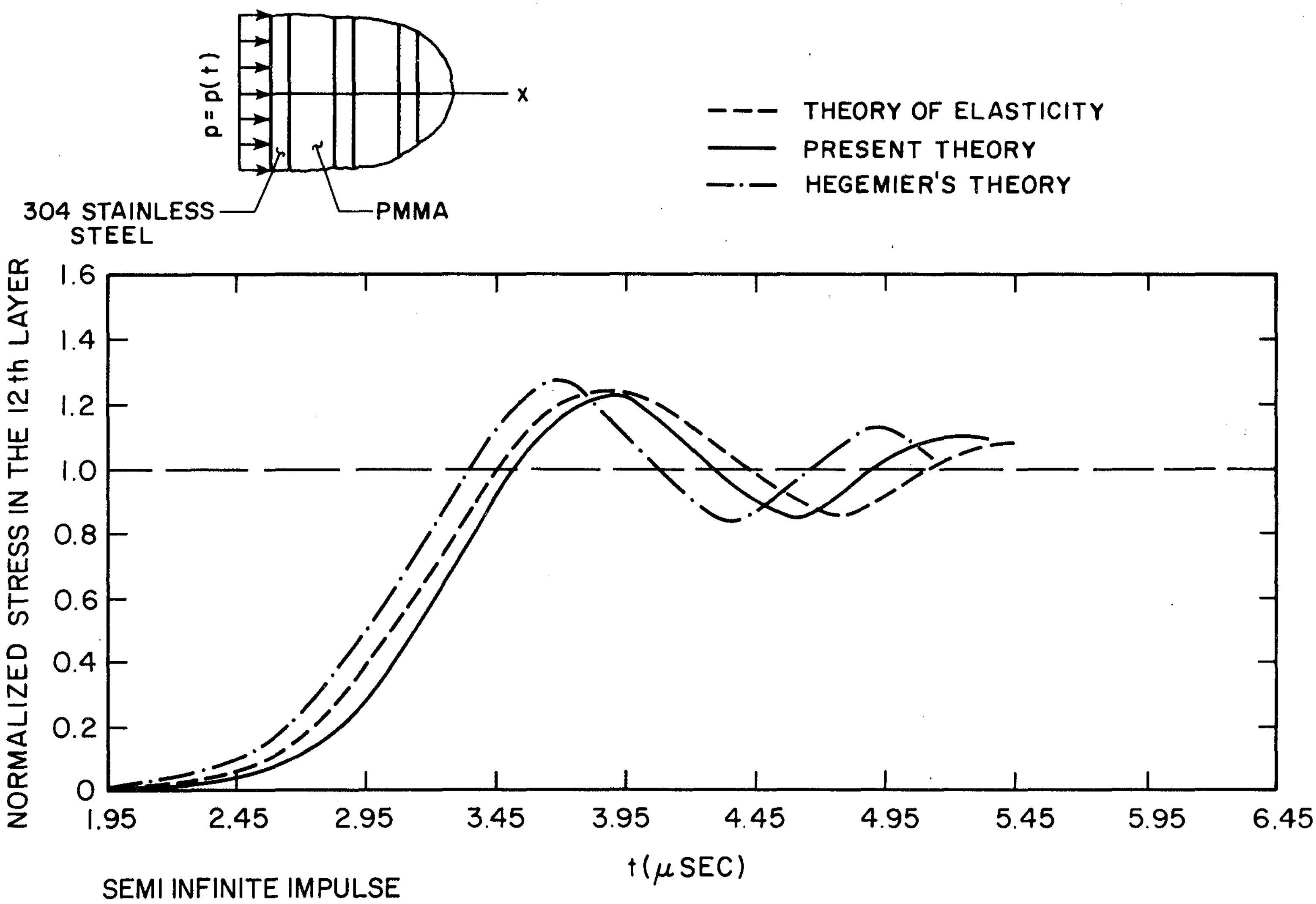

FIG. 17. COMPARISON OF WAVE PROFILES PREDICTED BY THE PRESENT THEORY AND OTHER THEORIES FOR DILATATIONAL WAVES PROPAGATING PERPENDICULAR TO LAYERING (STAINLESS STEEL - PMMA COMPOSITE; SEMI INFINITE IMPULSE)

along with the necessary model constants appropriate to the homogeneous model for each of the layered materials. In accordance with the information presented in [3], the time distribution of the pressure is taken in our analysis to be a quasi step function, which is zero at $t = 0$, rises linearly to a constant value during a rise time of 0.08 μ sec. after which it remains constant.

The numerical analysis is carried out using a mesh size of $\Delta t = 0.005\ \mu$ sec. The responses are the time variations of the average velocity $\overline{v} = \sum_{\alpha=1}^{2} n_\alpha v_\alpha$ at $x = H$.

Some comments on the model theory are in order. In the development of the equations of linear momentum a complicated elastodynamic operator, which appears in the equations, was replaced by a power series expansion. The major theory was obtained by retaining the first three terms of the expansion. It was indicated that a simple cruder theory could also be developed by retaining only the first term. Responses using both of these theories were found for both laminated materials and are displayed in Figs. 14 and 15. For a comparison of these responses with the experimental data, the velocity is normalized with respect to its value at $t = \infty$ and, as the absolute times in the experiments were not measured, the experimental wave profiles are translated parallel to the time axis, so that the times corresponding to the first theoretical and experimental peaks approximately coincide. We are also able to show the response in the second plate (Fig. 14) as it is predicted by the approximate theory due to Hegemier, Gurtman, and Nayfeh [10]. They obtained their numerical results by using the method of finite differences and they took the dynamic input as a step velocity impulse applied to the surface $x = 0$.

A study of Figs. 14 and 15 shows that the responses predicted by the model theory, particularly the three term theory, are close to the experimental responses. Not only are the amplitudes quite accurate, but the responses are in phase with the experimental for large times following the first disturbance. The response predicted by Hegemier in Fig. 14 is quite accurate for short times but quickly falls out of phase with the experimental profile for larger times.

The next case studied is much the same as the first cases except that the body is a half space. The forcing function is the same and alternate layers of boron and carbon phenolic are perpendicular to the surface. We use the three term theory for predicting responses and instead of comparing these with other data, we use response profiles at three stations at successively large distances from the surface to ascertain the nature of the dispersion as the wave profile progresses into the half space. Examination of Fig.16 shows that close to the surface the initial part of the response is steep and the periods of oscillation are small, and as the disturbances move into the material the initial slope lessens and the periods become larger -- phenomena that we would expect.

For the third case, response from the model theory is compared with two responses predicted by other theories. The body is a half space and consists of alternate layers of stainless steel and PMMA parallel to the surface. The response is generated by normal pressure applied to the surface so that the waves generated propagate normal to the layers. The properties of both the stainless steel and PMMA are shown in Table 4, along with the model constants appropriate to the laminate that are needed in finding the response. The pressure p(t) is normal to the surface and has a uniform step distribution in time. To eliminate the complication of having a first order discontinuity in the solution region D_2, the discontinuity in the pressure at $t = 0$ is replaced by a linear distribution that is zero at $t = 0$ and reaches a constant value at $t = 2\Delta t$. In the numerical analysis, $\Delta t = 0.03$ μ sec. is used.

Comparison is made with the responses predicted by the exact theory and the theory due to Hegemier and Nayfeh [6]. The response due to the exact field equations of elasticity is complicated. The lengthy computations are based on tracing out reflected and transmitted components of one-dimensional dilatational waves.

Comparison of the responses can be made by examining Fig.17. For early times the responses from the model and exact theories match accurately and for longer times, after the arrival of the first disturbances, the amplitudes match but the responses grow out of phase.

The final study, Figs.(18-20) is devoted to a comparison of the responses predicted by the model theory with experimental data obtained by Lundergan and Drumheller [25]. Their experiments were performed on a laminated plate of thickness H = 1.009 cm, composed of alternate layers of stainless steel and epon 828 running parallel to the surfaces. The properties of the layers and the values of the constants appearing in the model are given in Table 5. One surface of the plate is subjected to a uniform normal pressure, and the other surface is perfectly bonded to an epon 828 trailer. The time variation of the particle velocity is measured on the outer surface (data plane) of the trailer by using an optical interferometer observed through a PMMA window attached to the trailer at the data plane (see Figs. 18-20). Since the window material has a mechanical impedance of within three percent of that of epon 828 [8], the outer face of the trailer, on which the velocity is measured, is taken as being free of traction in our analysis. The elasticity solutions in the figures correspond to the solutions obtained by using the equations of elasticity and by tracing out the wave components reflected and refracted at interfaces.

The responses shown in Figs.(18-20) all arise from the same type of excitation and differ only in their durations. Figures 18-20 have infinite,

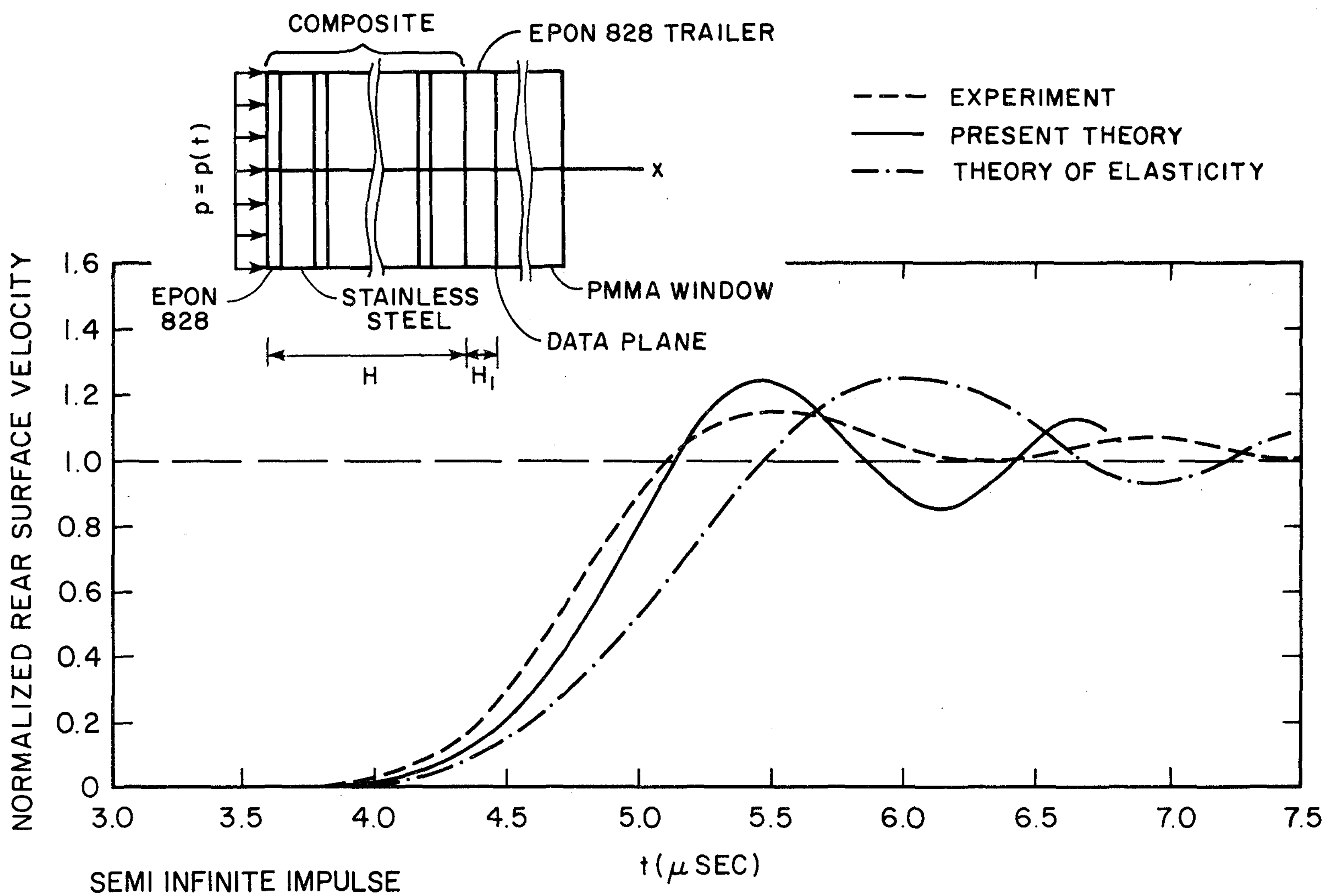

FIG. 18. COMPARISON OF EXPERIMENTAL AND THEORETICAL WAVE PROFILES FOR DILATATIONAL WAVES PROPAGATING PERPENDICULAR TO LAYERING (STAINLESS STEEL - EPON 828 COMPOSITE; SEMI INFINITE IMPULSE)

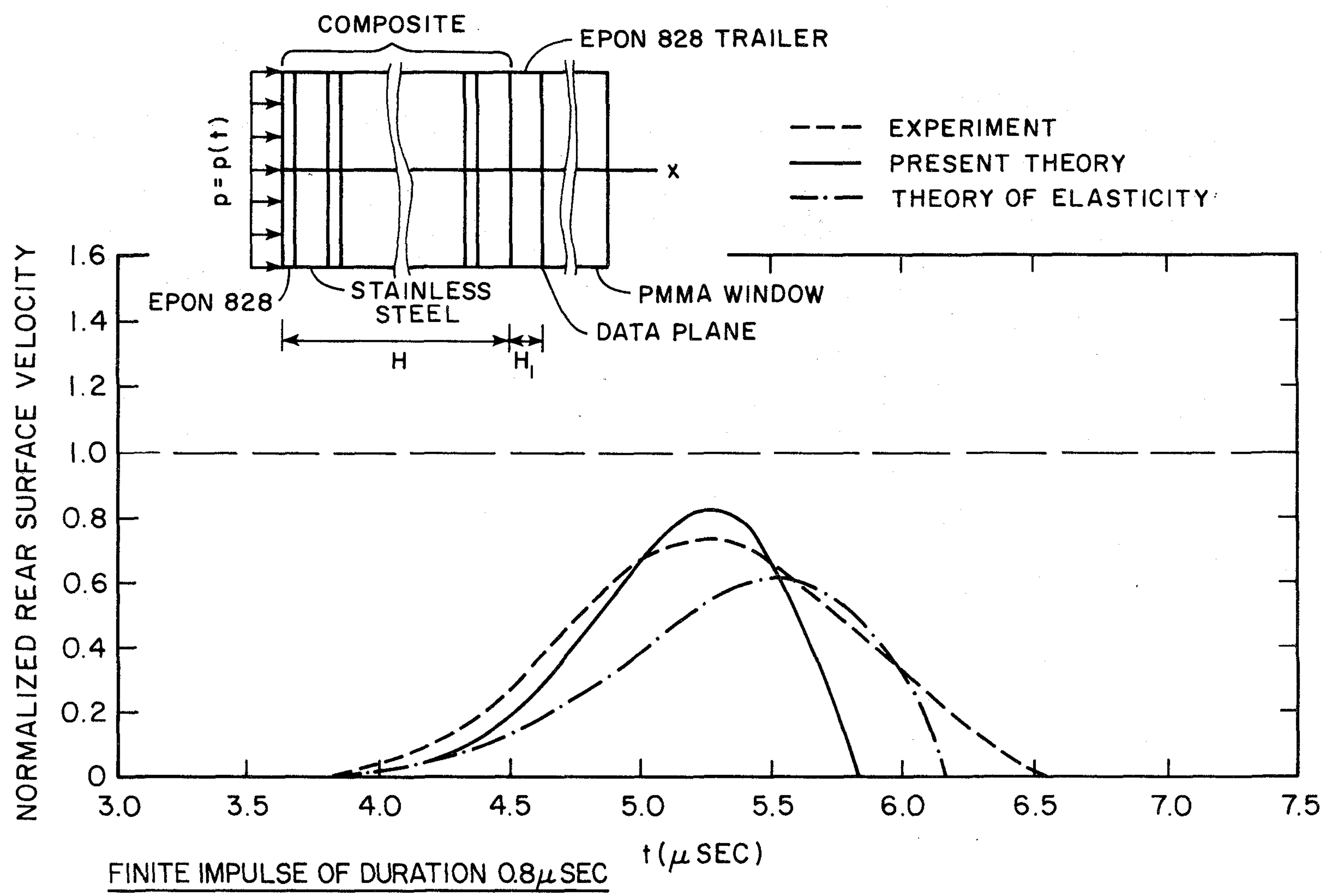

FIG. 19. COMPARISON OF EXPERIMENTAL AND THEORETICAL WAVE PROFILES FOR DILATATIONAL WAVES PROPAGATING PERPENDICULAR TO LAYERING (STAINLESS STEEL - EPON 828 COMPOSITE; FINITE IMPULSE OF DURATION 0.8 μ SEC.)

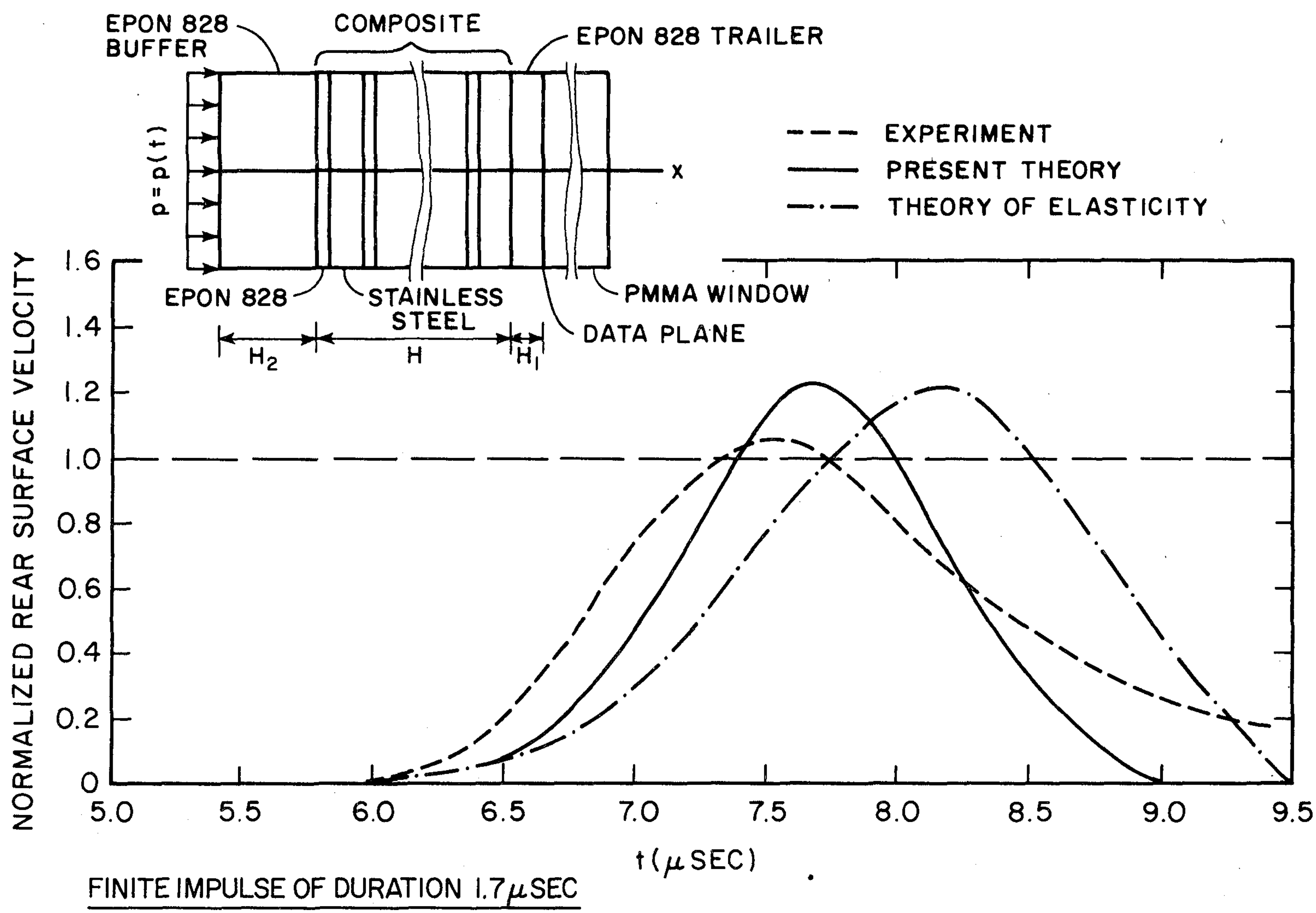

FIG. 20. COMPARISON OF EXPERIMENTAL AND THEORETICAL WAVE PROFILES FOR DILATATIONAL WAVES PROPAGATING PERPENDICULAR TO LAYERING (STAINLESS STEEL - EPON 828 COMPOSITE; FINITE IMPULSE OF DURATION 1.7 μ sec.)

0.8 μ sec. and 1.7 μ sec. durations, respectively. The rise or descent time of the applied pressure is taken in all cases to be $2\Delta t$, when $\Delta t = 0.0175$ μ sec. The problem described in Fig. 20 differs somewhat in that there is an epon 828 buffer between the surface of the laminated plate and the applied pressure.

With Figs.(14-20) we have the basis for a significant assessment of the model. We felt the need for such an assessment for a number of reasons. To review the reasons, it is important to realize that what we have is a set of equations governing the dynamic behavior of a homogeneous, elastic, dispersive material which is used to replace a two phase layered laminate. This model, as do all, consists of two parts, the form of the model, or the form of the governing equations, and the set of values of the parameters that appear in the equations. Both parts need to be assessed.

In the derivation of the equations of the model we used the classical mixture theory rather than the more complicated micromorphic mixture theory. This gave rise to some uneasiness because the classical mixture theory accommodates only the symmetrical distributions of field quantities within the phases. In the same part of the derivation, the elastodynamic operator which resulted was replaced in the final theory by an approximation consisting of the first three terms of a power series expansion.

We arrived at a set of equations for finding the nineteen model constants in terms of the layer constants in an arbitrary way, by using what seemed to us to be the simplest method. In doing so we were aware that a preferable set of parameters could be found using some rational optimization method such as system identification. We also knew that with nineteen unknowns such methods would be formidable.

The most demanding assessment seemed to us to be a comparison of experimental data with transient responses predicted by the model theory

TABLE 4

PROPERTIES OF STAINLESS STEEL-PMMA LAMINATED COMPOSITE

SPECIFIED LAYER PROPERTIES (AFTER HEGEMIER)					
h_1	h_2	ρ_1^R	ρ_2^R	$2\mu_1+\lambda_1$	$2\mu_2+\lambda_2$
cm	cm	$\frac{\text{dyne-}\mu\text{sec}^2}{\text{cm}^4}$	$\frac{\text{dyne-}\mu\text{sec}^2}{\text{cm}^4}$	dyne/cm^2	dyne/cm^2
0.0125	0.0392	7.9 $\times 10^{12}$	1.15 $\times 10^{12}$	1.258 $\times 10^{12}$	0.089 $\times 10^{12}$

COMPUTED MODEL CONSTANTS				
K_2	q_2	C_{22}^{11}	C_{22}^{22}	C_{22}^{12}
dyne/cm^4	$\frac{\text{dyne-}\mu\text{sec}^2}{\text{cm}^4}$	dyne/cm^2	dyne/cm^2	dyne/cm^2
128.4×10^{12}	0.185×10^{12}	0.0014×10^{12}	0.0908×10^{12}	0.0110×10^{12}

TABLE 5

PROPERTIES OF STAINLESS STEEL-EPON 828 LAMINATED COMPOSITE

SPECIFIED LAYER PROPERTIES (AFTER LUNDERGAN)					
h_1	h_2	ρ_1^R	ρ_2^R	$2\mu_1+\lambda_1$	$2\mu_2+\lambda_2$
cm	cm	$\frac{\text{dyne-}\mu\text{sec}^2}{\text{cm}^4}$	$\frac{\text{dyne-}\mu\text{sec}^2}{\text{cm}^4}$	dyne/cm^2	dyne/cm^2
0.0381	0.0123	7.896 $\times 10^{12}$	1.26 $\times 10^{12}$	1.642 $\times 10^{12}$	0.0878 $\times 10^{12}$

COMPUTED MODEL CONSTANTS				
K_2	q_2	C_{22}^{11}	C_{22}^{22}	C_{22}^{12}
dyne/cm^4	$\frac{\text{dyne-}\mu\text{sec}^2}{\text{cm}^4}$	dyne/cm^2	dyne/cm^2	dyne/cm^2
362.331×10^{12}	0.645×10^{12}	0.6962×10^{12}	0.0784×10^{12}	-0.2336×10^{12}

for waves propagating both parallel and perpendicular to the layers. The figures show this comparison to be quite satisfactory; for the relatively simple model with the simple method of finding the parameters, the responses appear to be accurate. Further, the accuracy is not restricted to early arrival times but extends to behavior far behind the head of the pulse.

APPENDIX A

For future use in subsequent studies we write the stress constitutive equations in matrix form

$$\begin{Bmatrix} \underset{-}{\sigma}^1 \\ \underset{-}{\sigma}^2 \end{Bmatrix} = \begin{bmatrix} \underset{-}{C}^{11} & \underset{-}{C}^{12} \\ \underset{-}{C}^{21} & \underset{-}{C}^{22} \end{bmatrix} \begin{Bmatrix} \underset{-}{e}^1 \\ \underset{-}{e}^2 \end{Bmatrix} - \begin{bmatrix} \underset{-}{p}^{11} & \underset{-}{p}^{21} \\ \underset{-}{p}^{12} & \underset{-}{p}^{22} \end{bmatrix} \begin{Bmatrix} \theta^1 \\ \theta^2 \end{Bmatrix}, \qquad \text{(A.1)}$$

where $\underset{-}{\sigma}^\alpha$ and $\underset{-}{e}^\alpha$ are vector representations of stress and strain tensors defined by

$$\underset{-}{\sigma}^\alpha = (\sigma_{11}^\alpha, \sigma_{22}^\alpha, \sigma_{33}^\alpha, \sigma_{12}^\alpha, \sigma_{13}^\alpha, \sigma_{23}^\alpha)$$

$$\underset{-}{e}^\alpha = (e_{11}^\alpha, e_{22}^\alpha, e_{33}^\alpha, 2e_{12}^\alpha, 2e_{13}^\alpha, 2e_{23}^\alpha),$$

$\underset{-}{C}^{\alpha\beta}$ is a 6 x 6 material coefficient matrix of the form

$$\underset{-}{C}^{\alpha\beta} = \begin{bmatrix} C_{11}^{\alpha\beta} & \cdots & C_{16}^{\alpha\beta} \\ \vdots & & \\ C_{61}^{\alpha\beta} & & C_{66}^{\alpha\beta} \end{bmatrix},$$

and $\underset{-}{p}^{\alpha\beta}$ is a six dimensional vector defined by

$$\underset{-}{p}^{\alpha\beta} = (p_{11}^{\alpha\beta}, p_{22}^{\alpha\beta}, p_{33}^{\alpha\beta}, p_{12}^{\alpha\beta}, p_{13}^{\alpha\beta}, p_{23}^{\alpha\beta}).$$

The stress constitutive equations, Eq. (A.1), govern the anisotropic behavior of a given composite. The symmetry conditions, Eq. (2.25), indicate that the matrices $\underset{-}{C}^{11}$ and $\underset{-}{C}^{22}$ are both symmetric, and $\underset{-}{C}^{21}$ is equal to the transpose of $\underline{C}^{12}$ i.e., $\underline{C}^{21} = \underline{C}^{T12}$. This establishes the symmetry of the overall stiffness matrix in Eq. (A.1).

The matrix form of the positive definiteness condition, Eq. (2.36), is

$$\underline{S}^{T} \underline{C} \, \underline{S} \geq 0, \qquad \text{(A.2)}$$

where $\underline{S}$ is an arbitrary twelve dimensional vector and $\underline{C}$ is the 12 x 12 overall stiffness matrix defined by

$$\underline{C} = \begin{bmatrix} \underline{C}^{11} & \underline{C}^{12} \\ \underline{C}^{T12} & \underline{C}^{22} \end{bmatrix} . \qquad \text{(A.3)}$$

From linear algebra we know that the inequality, Eq. (A.2), is satisfied if all of the eigenvalues or principal minors of the symmetric matrix $\underline{C}$ are positive. This explicitly determines the constraints to be satisfied by the model constants.

REFERENCES

1. S. M. Rytov, "Acoustical Properties of a Thinly Laminated Medium," Soviet Physics-Acoustics, Vol. 2, 1955 (68-80).

2. C. T. Sun, J. D. Achenbach and G. Herrmann, "Continuum Theory for a Laminated Medium," Journal of Applied Mechanics, Vol. 35, 1968 (467-475).

3. J. D. Achenbach, C. T. Sun and G. Herrmann, "On the Vibrations of a Laminated Body," Journal of Applied Mechanics, Vol. 35, 1968 (689-696).

4. D. S. Drumheller and A. Bedford, "Wave Propagation in Elastic Laminates using a Second Order Microstructure Theory," Int. J. Solids Structures, Vol. 10, 1974 (61-76).

5. G. A. Hegemier and T. C. Bache, "A General Continuum Theory with Microstructure for Wave Propagation in Elastic Laminated Composites," Journal of Applied Mechanics, Vol. 41, 1974 (101-105).

6. G. A. Hegemier and A. H. Nayfeh, "A Continuum Theory for Wave Propagation in Laminated Composites," Journal of Applied Mechanics, Vol. 40, 1973 (503-510).

7. G. Herrmann, R. K. Kaul and T. J. Delph, "On Continuum Modeling of the Dynamic Behavior of Layered Composites," Archives of Mechanics, Vol. 28, 1976 (405-421).

8. G. Herrmann, T. J. Delph and R. K. Kaul, "New Results on Continuum Modeling of Composites," to be published in the Proceedings of the Second Int'l Symposium on Continuum Models of Discrete Systems.

9. A. Bedford and M. Stern, "Toward a Diffusing Continuum Theory of Composite Materials," Journal of Applied Mechanics, Vol. 38, 1971 (8-14).

10. G. A. Hegemier, G. A. Gurtman and A. H. Nayfeh, "A Continuum Mixture Theory of Wave Propagation in Laminated and Fiber Reinforced Composites," Int. J. Solids Structures, Vol. 9, 1973 (395-414).

11. A. Bedford and M. Stern, "A Multi-Continuum Theory for Composite Elastic Materials, Acta Mechanica, Vol. 14, 1972 (85-102).

12. R. I. Nigmatulin, "Methods of Mechanics of a Continuum Medium for the Description of Multiphase Mixtures," PMM, Vol. 34, 1970 (1097-1112).

13. A. E. Green and P. M. Naghdi, "On Basic Equations for Mixtures," Quarterly Journal of Mechanics and Applied Mathematics, Vol. 22, 1969 (427-438).

14. A. E. Green and P. M. Naghdi, "Entropy Inequalities for Mixtures," Quarterly Journal of Mechanics and Applied Mathematics, Vol. 24, 1971 (474-485).

15. R. J. Atkins and R. E. Craine, "Continuum Theories of Mixtures: Basic Theory and Historical Development," Quarterly Journal of Mechanics and Applied Mathematics, Vol. 29, 1976 (209-244).

16. R. J. Atkins and R. E. Craine, "Continuum Theories of Mixtures: Applications," Journal of the Institute of Mathematics and its Applications," Vol. 17, 1976 (153-207).

17. R. M. Bowen, "Theory of Mixtures," Continuum Physics (Edited by A. C. Eringen), Vol. III, Academic Press, 1976 (1-127).

18. M. A. Biot, "Theory of Propagation of Elastic Waves in a Fluid Saturated Porous Solid, Parts I and II," Journal of the Acoustical Society of America, Vol. 28, 1956 (168-191).

19. M. A. Biot, "Generalized Theory of Acoustic Propagation in Porous Dissipative Media," Journal of the Acoustical Society of America, Vol. 34, 1962 (1254-1264).

20. R. M. Bowen, "Theory of Mixtures," Continuum Physics (Edited by A.C. Eringen), Vol. III, Academic Press, 1976 (1-127).

21. M. Stern and A. Bedford, "Wave Propagation in Elastic Laminates Using a Multi-Continuum Theory," Acta Mechanica, Vol. 15, 1972 (21-38).

22. R. D. Mindlin and H. D. McNiven, "Axially Symmetric Waves in Elastic Rods," Journal of Applied Mechanics, Vol. 82E, 1960 (145-151).

23. J. S. Whittier and J. C. Peck, "Experiments on Dispersive Pulse Propagation in Laminated Composites and Comparison with Theory," Journal of Applied Mechanics, Vol. 36, 1969 (485-490).

24. R. Courant and D. Hilbert, "Methods of Mathematical Physics," Vol. II Interscience 1966.

25. C. D. Lundergan and D. S. Drumheller, "Propagation of Stress Waves in a Laminated Plate Composite," Journal of Applied Physics, Vol. 42, 1971 (669-675).

EARTHQUAKE ENGINEERING RESEARCH CENTER REPORTS

NOTE: Numbers in parenthesis are Accession Numbers assigned by the National Technical Information Service; these are followed by a price code. Copies of the reports may be ordered from the National Technical Information Service, 5285 Port Royal Road, Springfield, Virginia, 22161. Accession Numbers should be quoted on orders for reports (PB --- ---) and remittance must accompany each order. Reports without this information were not available at time of printing. Upon request, EERC will mail inquirers this information when it becomes available.

EERC 67-1 "Feasibility Study Large-Scale Earthquake Simulator Facility," by J. Penzien, J.G. Bouwkamp, R.W. Clough and D. Rea - 1967 (PB 187 905)A07

EERC 68-1 Unassigned

EERC 68-2 "Inelastic Behavior of Beam-to-Column Subassemblages Under Repeated Loading," by V.V. Bertero - 1968 (PB 184 888)A05

EERC 68-3 "A Graphical Method for Solving the Wave Reflection-Refraction Problem," by H.D. McNiven and Y. Mengi - 1968 (PB 187 943)A03

EERC 68-4 "Dynamic Properties of McKinley School Buildings," by D. Rea, J.G. Bouwkamp and R.W. Clough - 1968 (PB 187 902)A07

EERC 68-5 "Characteristics of Rock Motions During Earthquakes," by H.B. Seed, I.M. Idriss and F.W. Kiefer - 1968 (PB 188 338)A03

EERC 69-1 "Earthquake Engineering Research at Berkeley," - 1969 (PB 187 906)A11

EERC 69-2 "Nonlinear Seismic Response of Earth Structures," by M. Dibaj and J. Penzien - 1969 (PB 187 904)A08

EERC 69-3 "Probabilistic Study of the Behavior of Structures During Earthquakes," by R. Ruiz and J. Penzien - 1969 (PB 187 886)A06

EERC 69-4 "Numerical Solution of Boundary Value Problems in Structural Mechanics by Reduction to an Initial Value Formulation," by N. Distefano and J. Schujman - 1969 (PB 187 942)A02

EERC 69-5 "Dynamic Programming and the Solution of the Biharmonic Equation," by N. Distefano - 1969 (PB 187 941)A03

EERC 69-6 "Stochastic Analysis of Offshore Tower Structures," by A.K. Malhotra and J. Penzien - 1969 (PB 187 903)A09

EERC 69-7 "Rock Motion Accelerograms for High Magnitude Earthquakes," by H.B. Seed and I.M. Idriss - 1969 (PB 187 940)A02

EERC 69-8 "Structural Dynamics Testing Facilities at the University of California, Berkeley," by R.M. Stephen, J.G. Bouwkamp, R.W. Clough and J. Penzien - 1969 (PB 189 111)A04

EERC 69-9 "Seismic Response of Soil Deposits Underlain by Sloping Rock Boundaries," by H. Dezfulian and H.B. Seed 1969 (PB 189 114)A03

EERC 69-10 "Dynamic Stress Analysis of Axisymmetric Structures Under Arbitrary Loading," by S. Ghosh and E.L. Wilson 1969 (PB 189 026)A10

EERC 69-11 "Seismic Behavior of Multistory Frames Designed by Different Philosophies," by J.C. Anderson and V. V. Bertero - 1969 (PB 190 662)A10

EERC 69-12 "Stiffness Degradation of Reinforcing Concrete Members Subjected to Cyclic Flexural Moments," by V.V. Bertero, B. Bresler and H. Ming Liao - 1969 (PB 202 942)A07

EERC 69-13 "Response of Non-Uniform Soil Deposits to Travelling Seismic Waves," by H. Dezfulian and H.B. Seed - 1969 (PB 191 023)A03

EERC 69-14 "Damping Capacity of a Model Steel Structure," by D. Rea, R.W. Clough and J.G. Bouwkamp - 1969 (PB 190 663)A06

EERC 69-15 "Influence of Local Soil Conditions on Building Damage Potential during Earthquakes," by H.B. Seed and I.M. Idriss - 1969 (PB 191 036)A03

EERC 69-16 "The Behavior of Sands Under Seismic Loading Conditions," by M.L. Silver and H.B. Seed - 1969 (AD 714 982)A07

EERC 70-1 "Earthquake Response of Gravity Dams," by A.K. Chopra - 1970 (AD 709 640)A03

EERC 70-2 "Relationships between Soil Conditions and Building Damage in the Caracas Earthquake of July 29, 1967," by H.B. Seed, I.M. Idriss and H. Dezfulian - 1970 (PB 195 762)A05

EERC 70-3 "Cyclic Loading of Full Size Steel Connections," by E.P. Popov and R.M. Stephen - 1970 (PB 213 545)A04

EERC 70-4 "Seismic Analysis of the Charaima Building, Caraballeda, Venezuela," by Subcommittee of the SEAONC Research Committee: V.V. Bertero, P.F. Fratessa, S.A. Mahin, J.H. Sexton, A.C. Scordelis, E.L. Wilson, L.A. Wyllie, H.B. Seed and J. Penzien, Chairman - 1970 (PB 201 455)A06

EERC 70-5 "A Computer Program for Earthquake Analysis of Dams," by A.K. Chopra and P. Chakrabarti - 1970 (AD 723 994)A05

EERC 70-6 "The Propagation of Love Waves Across Non-Horizontally Layered Structures," by J. Lysmer and L.A. Drake 1970 (PB 197 896)A03

EERC 70-7 "Influence of Base Rock Characteristics on Ground Response," by J. Lysmer, H.B. Seed and P.B. Schnabel 1970 (PB 197 897)A03

EERC 70-8 "Applicability of Laboratory Test Procedures for Measuring Soil Liquefaction Characteristics under Cyclic Loading," by H.B. Seed and W.H. Peacock - 1970 (PB 198 016)A03

EERC 70-9 "A Simplified Procedure for Evaluating Soil Liquefaction Potential," by H.B. Seed and I.M. Idriss - 1970 (PB 198 009)A03

EERC 70-10 "Soil Moduli and Damping Factors for Dynamic Response Analysis," by H.B. Seed and I.M. Idriss - 1970 (PB 197 869)A03

EERC 71-1 "Koyna Earthquake of December 11, 1967 and the Performance of Koyna Dam," by A.K. Chopra and P. Chakrabarti 1971 (AD 731 496)A06

EERC 71-2 "Preliminary In-Situ Measurements of Anelastic Absorption in Soils Using a Prototype Earthquake Simulator," by R.D. Borcherdt and P.W. Rodgers - 1971 (PB 201 454)A03

EERC 71-3 "Static and Dynamic Analysis of Inelastic Frame Structures," by F.L. Porter and G.H. Powell - 1971 (PB 210 135)A06

EERC 71-4 "Research Needs in Limit Design of Reinforced Concrete Structures," by V.V. Bertero - 1971 (PB 202 943)A04

EERC 71-5 "Dynamic Behavior of a High-Rise Diagonally Braced Steel Building," by D. Rea, A.A. Shah and J.G. Bouwkamp 1971 (PB 203 584)A06

EERC 71-6 "Dynamic Stress Analysis of Porous Elastic Solids Saturated with Compressible Fluids," by J. Ghaboussi and E. L. Wilson - 1971 (PB 211 396)A06

EERC 71-7 "Inelastic Behavior of Steel Beam-to-Column Subassemblages," by H. Krawinkler, V.V. Bertero and E.P. Popov 1971 (PB 211 335)A14

EERC 71-8 "Modification of Seismograph Records for Effects of Local Soil Conditions," by P. Schnabel, H.B. Seed and J. Lysmer - 1971 (PB 214 450)A03

EERC 72-1 "Static and Earthquake Analysis of Three Dimensional Frame and Shear Wall Buildings," by E.L. Wilson and H.H. Dovey - 1972 (PB 212 904)A05

EERC 72-2 "Accelerations in Rock for Earthquakes in the Western United States," by P.B. Schnabel and H.B. Seed - 1972 (PB 213 100)A03

EERC 72-3 "Elastic-Plastic Earthquake Response of Soil-Building Systems," by T. Minami - 1972 (PB 214 868)A08

EERC 72-4 "Stochastic Inelastic Response of Offshore Towers to Strong Motion Earthquakes," by M.K. Kaul - 1972 (PB 215 713)A05

EERC 72-5 "Cyclic Behavior of Three Reinforced Concrete Flexural Members with High Shear," by E.P. Popov, V.V. Bertero and H. Krawinkler - 1972 (PB 214 555)A05

EERC 72-6 "Earthquake Response of Gravity Dams Including Reservoir Interaction Effects," by P. Chakrabarti and A.K. Chopra - 1972 (AD 762 330)A08

EERC 72-7 "Dynamic Properties of Pine Flat Dam," by D. Rea, C.Y. Liaw and A.K. Chopra - 1972 (AD 763 928)A05

EERC 72-8 "Three Dimensional Analysis of Building Systems," by E.L. Wilson and H.H. Dovey - 1972 (PB 222 438)A06

EERC 72-9 "Rate of Loading Effects on Uncracked and Repaired Reinforced Concrete Members," by S. Mahin, V.V. Bertero, D. Rea and M. Atalay - 1972 (PB 224 520)A08

EERC 72-10 "Computer Program for Static and Dynamic Analysis of Linear Structural Systems," by E.L. Wilson, K.-J. Bathe, J.E. Peterson and H.H.Dovey - 1972 (PB 220 437)A04

EERC 72-11 "Literature Survey - Seismic Effects on Highway Bridges," by T. Iwasaki, J. Penzien and R.W. Clough - 1972 (PB 215 613)A19

EERC 72-12 "SHAKE-A Computer Program for Earthquake Response Analysis of Horizontally Layered Sites," by P.B. Schnabel and J. Lysmer - 1972 (PB 220 207)A06

EERC 73-1 "Optimal Seismic Design of Multistory Frames," by V.V. Bertero and H. Kamil - 1973

EERC 73-2 "Analysis of the Slides in the San Fernando Dams During the Earthquake of February 9, 1971," by H.B. Seed, K.L. Lee, I.M. Idriss and F. Makdisi - 1973 (PB 223 402)A14

EERC 73-3 "Computer Aided Ultimate Load Design of Unbraced Multistory Steel Frames," by M.B. El-Hafez and G.H. Powell 1973 (PB 248 315)A09

EERC 73-4 "Experimental Investigation into the Seismic Behavior of Critical Regions of Reinforced Concrete Components as Influenced by Moment and Shear," by M. Celebi and J. Penzien - 1973 (PB 215 884)A09

EERC 73-5 "Hysteretic Behavior of Epoxy-Repaired Reinforced Concrete Beams," by M. Celebi and J. Penzien - 1973 (PB 239 568)A03

EERC 73-6 "General Purpose Computer Program for Inelastic Dynamic Response of Plane Structures," by A. Kanaan and G.H. Powell - 1973 (PB 221 260)A08

EERC 73-7 "A Computer Program for Earthquake Analysis of Gravity Dams Including Reservoir Interaction," by P. Chakrabarti and A.K. Chopra - 1973 (AD 766 271)A04

EERC 73-8 "Behavior of Reinforced Concrete Deep Beam-Column Subassemblages Under Cyclic Loads," by O. Küstü and J.G. Bouwkamp - 1973 (PB 246 117)A12

EERC 73-9 "Earthquake Analysis of Structure-Foundation Systems," by A.K. Vaish and A.K. Chopra - 1973 (AD 766 272)A07

EERC 73-10 "Deconvolution of Seismic Response for Linear Systems," by R.B. Reimer - 1973 (PB 227 179)A08

EERC 73-11 "SAP IV: A Structural Analysis Program for Static and Dynamic Response of Linear Systems," by K.-J. Bathe, E.L. Wilson and F.E. Peterson - 1973 (PB 221 967)A09

EERC 73-12 "Analytical Investigations of the Seismic Response of Long, Multiple Span Highway Bridges," by W.S. Tseng and J. Penzien - 1973 (PB 227 816)A10

EERC 73-13 "Earthquake Analysis of Multi-Story Buildings Including Foundation Interaction," by A.K. Chopra and J.A. Gutierrez - 1973 (PB 222 970)A03

EERC 73-14 "ADAP: A Computer Program for Static and Dynamic Analysis of Arch Dams," by R.W. Clough, J.M. Raphael and S. Mojtahedi - 1973 (PB 223 763)A09

EERC 73-15 "Cyclic Plastic Analysis of Structural Steel Joints," by R.B. Pinkney and R.W. Clough - 1973 (PB 226 843)A08

EERC 73-16 "QUAD-4: A Computer Program for Evaluating the Seismic Response of Soil Structures by Variable Damping Finite Element Procedures," by I.M. Idriss, J. Lysmer, R. Hwang and H.B. Seed - 1973 (PB 229 424)A05

EERC 73-17 "Dynamic Behavior of a Multi-Story Pyramid Shaped Building," by R.M. Stephen, J.P. Hollings and J.G. Bouwkamp - 1973 (PB 240 718)A06

EERC 73-18 "Effect of Different Types of Reinforcing on Seismic Behavior of Short Concrete Columns," by V.V. Bertero, J. Hollings, O. Küstü, R.M. Stephen and J.G. Bouwkamp - 1973

EERC 73-19 "Olive View Medical Center Materials Studies, Phase I," by B. Bresler and V.V. Bertero - 1973 (PB 235 986)A06

EERC 73-20 "Linear and Nonlinear Seismic Analysis Computer Programs for Long Multiple-Span Highway Bridges," by W.S. Tseng and J. Penzien - 1973

EERC 73-21 "Constitutive Models for Cyclic Plastic Deformation of Engineering Materials," by J.M. Kelly and P.P. Gillis 1973 (PB 226 024)A03

EERC 73-22 "DRAIN - 2D User's Guide," by G.H. Powell - 1973 (PB 227 016)A05

EERC 73-23 "Earthquake Engineering at Berkeley - 1973," (PB 226 033)A11

EERC 73-24 Unassigned

EERC 73-25 "Earthquake Response of Axisymmetric Tower Structures Surrounded by Water," by C.Y. Liaw and A.K. Chopra 1973 (AD 773 052)A09

EERC 73-26 "Investigation of the Failures of the Olive View Stairtowers During the San Fernando Earthquake and Their Implications on Seismic Design," by V.V. Bertero and R.G. Collins - 1973 (PB 235 106)A13

EERC 73-27 "Further Studies on Seismic Behavior of Steel Beam-Column Subassemblages," by V.V. Bertero, H. Krawinkler and E.P. Popov - 1973 (PB 234 172)A06

EERC 74-1 "Seismic Risk Analysis," by C.S. Oliveira - 1974 (PB 235 920)A06

EERC 74-2 "Settlement and Liquefaction of Sands Under Multi-Directional Shaking," by R. Pyke, C.K. Chan and H.B. Seed 1974

EERC 74-3 "Optimum Design of Earthquake Resistant Shear Buildings," by D. Ray, K.S. Pister and A.K. Chopra - 1974 (PB 231 172)A06

EERC 74-4 "LUSH - A Computer Program for Complex Response Analysis of Soil-Structure Systems," by J. Lysmer, T. Udaka, H.B. Seed and R. Hwang - 1974 (PB 236 796)A05

EERC 74-5 "Sensitivity Analysis for Hysteretic Dynamic Systems: Applications to Earthquake Engineering," by D. Ray 1974 (PB 233 213)A06

EERC 74-6 "Soil Structure Interaction Analyses for Evaluating Seismic Response," by H.B. Seed, J. Lysmer and R. Hwang 1974 (PB 236 519)A04

EERC 74-7 Unassigned

EERC 74-8 "Shaking Table Tests of a Steel Frame - A Progress Report," by R.W. Clough and D. Tang - 1974 (PB 240 869)A03

EERC 74-9 "Hysteretic Behavior of Reinforced Concrete Flexural Members with Special Web Reinforcement," by V.V. Bertero, E.P. Popov and T.Y. Wang - 1974 (PB 236 797)A07

EERC 74-10 "Applications of Reliability-Based, Global Cost Optimization to Design of Earthquake Resistant Structures," by E. Vitiello and K.S. Pister - 1974 (PB 237 231)A06

EERC 74-11 "Liquefaction of Gravelly Soils Under Cyclic Loading Conditions," by R.T. Wong, H.B. Seed and C.K. Chan 1974 (PB 242 042)A03

EERC 74-12 "Site-Dependent Spectra for Earthquake-Resistant Design," by H.B. Seed, C. Ugas and J. Lysmer - 1974 (PB 240 953)A03

EERC 74-13 "Earthquake Simulator Study of a Reinforced Concrete Frame," by P. Hidalgo and R.W. Clough - 1974 (PB 241 944)A13

EERC 74-14 "Nonlinear Earthquake Response of Concrete Gravity Dams," by N. Pal - 1974 (AD/A 006 583)A06

EERC 74-15 "Modeling and Identification in Nonlinear Structural Dynamics - I. One Degree of Freedom Models," by N. Distefano and A. Rath - 1974 (PB 241 548)A06

EERC 75-1 "Determination of Seismic Design Criteria for the Dumbarton Bridge Replacement Structure, Vol. I: Description, Theory and Analytical Modeling of Bridge and Parameters," by F. Baron and S.-H. Pang - 1975 (PB 259 407)A15

EERC 75-2 "Determination of Seismic Design Criteria for the Dumbarton Bridge Replacement Structure, Vol. II: Numerical Studies and Establishment of Seismic Design Criteria," by F. Baron and S.-H. Pang - 1975 (PB 259 408)A11 (For set of EERC 75-1 and 75-2 (PB 259 406))

EERC 75-3 "Seismic Risk Analysis for a Site and a Metropolitan Area," by C.S. Oliveira - 1975 (PB 248 134)A09

EERC 75-4 "Analytical Investigations of Seismic Response of Short, Single or Multiple-Span Highway Bridges," by M.-C. Chen and J. Penzien - 1975 (PB 241 454)A09

EERC 75-5 "An Evaluation of Some Methods for Predicting Seismic Behavior of Reinforced Concrete Buildings," by S.A. Mahin and V.V. Bertero - 1975 (PB 246 306)A16

EERC 75-6 "Earthquake Simulator Study of a Steel Frame Structure, Vol. I: Experimental Results," by R.W. Clough and D.T. Tang - 1975 (PB 243 981)A13

EERC 75-7 "Dynamic Properties of San Bernardino Intake Tower," by D. Rea, C.-Y. Liaw and A.K. Chopra - 1975 (AD/A008 406) A05

EERC 75-8 "Seismic Studies of the Articulation for the Dumbarton Bridge Replacement Structure, Vol. I: Description, Theory and Analytical Modeling of Bridge Components," by F. Baron and R.E. Hamati - 1975 (PB 251 539)A07

EERC 75-9 "Seismic Studies of the Articulation for the Dumbarton Bridge Replacement Structure, Vol. 2: Numerical Studies of Steel and Concrete Girder Alternates," by F. Baron and R.E. Hamati - 1975 (PB 251 540)A10

EERC 75-10 "Static and Dynamic Analysis of Nonlinear Structures," by D.P. Mondkar and G.H. Powell - 1975 (PB 242 434)A08

EERC 75-11 "Hysteretic Behavior of Steel Columns," by E.P. Popov, V.V. Bertero and S. Chandramouli - 1975 (PB 252 365)A11

EERC 75-12 "Earthquake Engineering Research Center Library Printed Catalog," - 1975 (PB 243 711)A26

EERC 75-13 "Three Dimensional Analysis of Building Systems (Extended Version)," by E.L. Wilson, J.P. Hollings and H.H. Dovey - 1975 (PB 243 989)A07

EERC 75-14 "Determination of Soil Liquefaction Characteristics by Large-Scale Laboratory Tests," by P. De Alba, C.K. Chan and H.B. Seed - 1975 (NUREG 0027)A08

EERC 75-15 "A Literature Survey - Compressive, Tensile, Bond and Shear Strength of Masonry," by R.L. Mayes and R.W. Clough - 1975 (PB 246 292)A10

EERC 75-16 "Hysteretic Behavior of Ductile Moment Resisting Reinforced Concrete Frame Components," by V.V. Bertero and E.P. Popov - 1975 (PB 246 388)A05

EERC 75-17 "Relationships Between Maximum Acceleration, Maximum Velocity, Distance from Source, Local Site Conditions for Moderately Strong Earthquakes," by H.B. Seed, R. Murarka, J. Lysmer and I.M. Idriss - 1975 (PB 248 172)A03

EERC 75-18 "The Effects of Method of Sample Preparation on the Cyclic Stress-Strain Behavior of Sands," by J. Mulilis, C.K. Chan and H.B. Seed - 1975 (Summarized in EERC 75-28)

EERC 75-19 "The Seismic Behavior of Critical Regions of Reinforced Concrete Components as Influenced by Moment, Shear and Axial Force," by M.B. Atalay and J. Penzien - 1975 (PB 258 842)A11

EERC 75-20 "Dynamic Properties of an Eleven Story Masonry Building," by R.M. Stephen, J.P. Hollings, J.G. Bouwkamp and D. Jurukovski - 1975 (PB 246 945)A04

EERC 75-21 "State-of-the-Art in Seismic Strength of Masonry - An Evaluation and Review," by R.L. Mayes and R.W. Clough 1975 (PB 249 040)A07

EERC 75-22 "Frequency Dependent Stiffness Matrices for Viscoelastic Half-Plane Foundations," by A.K. Chopra, P. Chakrabarti and G. Dasgupta - 1975 (PB 248 121)A07

EERC 75-23 "Hysteretic Behavior of Reinforced Concrete Framed Walls," by T.Y. Wong, V.V. Bertero and E.P. Popov - 1975

EERC 75-24 "Testing Facility for Subassemblages of Frame-Wall Structural Systems," by V.V. Bertero, E.P. Popov and T. Endo - 1975

EERC 75-25 "Influence of Seismic History on the Liquefaction Characteristics of Sands," by H.B. Seed, K. Mori and C.K. Chan - 1975 (Summarized in EERC 75-28)

EERC 75-26 "The Generation and Dissipation of Pore Water Pressures during Soil Liquefaction," by H.B. Seed, P.P. Martin and J. Lysmer - 1975 (PB 252 648)A03

EERC 75-27 "Identification of Research Needs for Improving Aseismic Design of Building Structures," by V.V. Bertero 1975 (PB 248 136)A05

EERC 75-28 "Evaluation of Soil Liquefaction Potential during Earthquakes," by H.B. Seed, I. Arango and C.K. Chan - 1975 (NUREG 0026)A13

EERC 75-29 "Representation of Irregular Stress Time Histories by Equivalent Uniform Stress Series in Liquefaction Analyses," by H.B. Seed, I.M. Idriss, F. Makdisi and N. Banerjee - 1975 (PB 252 635)A03

EERC 75-30 "FLUSH - A Computer Program for Approximate 3-D Analysis of Soil-Structure Interaction Problems," by J. Lysmer, T. Udaka, C.-F. Tsai and H.B. Seed - 1975 (PB 259 332)A07

EERC 75-31 "ALUSH - A Computer Program for Seismic Response Analysis of Axisymmetric Soil-Structure Systems," by E. Berger, J. Lysmer and H.B. Seed - 1975

EERC 75-32 "TRIP and TRAVEL - Computer Programs for Soil-Structure Interaction Analysis with Horizontally Travelling Waves," by T. Udaka, J. Lysmer and H.B. Seed - 1975

EERC 75-33 "Predicting the Performance of Structures in Regions of High Seismicity," by J. Penzien - 1975 (PB 248 130)A03

EERC 75-34 "Efficient Finite Element Analysis of Seismic Structure - Soil - Direction," by J. Lysmer, H.B. Seed, T. Udaka, R.N. Hwang and C.-F. Tsai - 1975 (PB 253 570)A03

EERC 75-35 "The Dynamic Behavior of a First Story Girder of a Three-Story Steel Frame Subjected to Earthquake Loading," by R.W. Clough and L.-Y. Li - 1975 (PB 248 841)A05

EERC 75-36 "Earthquake Simulator Study of a Steel Frame Structure, Volume II - Analytical Results," by D.T. Tang - 1975 (PB 252 926)A10

EERC 75-37 "ANSR-I General Purpose Computer Program for Analysis of Non-Linear Structural Response," by D.P. Mondkar and G.H. Powell - 1975 (PB 252 386)A08

EERC 75-38 "Nonlinear Response Spectra for Probabilistic Seismic Design and Damage Assessment of Reinforced Concrete Structures," by M. Murakami and J. Penzien - 1975 (PB 259 530)A05

EERC 75-39 "Study of a Method of Feasible Directions for Optimal Elastic Design of Frame Structures Subjected to Earthquake Loading," by N.D. Walker and K.S. Pister - 1975 (PB 257 781)A06

EERC 75-40 "An Alternative Representation of the Elastic-Viscoelastic Analogy," by G. Dasgupta and J.L. Sackman - 1975 (PB 252 173)A03

EERC 75-41 "Effect of Multi-Directional Shaking on Liquefaction of Sands," by H.B. Seed, R. Pyke and G.R. Martin - 1975 (PB 258 781)A03

EERC 76-1 "Strength and Ductility Evaluation of Existing Low-Rise Reinforced Concrete Buildings - Screening Method," by T. Okada and B. Bresler - 1976 (PB 257 906)A11

EERC 76-2 "Experimental and Analytical Studies on the Hysteretic Behavior of Reinforced Concrete Rectangular and T-Beams," by S.-Y.M. Ma, E.P. Popov and V.V. Bertero - 1976 (PB 260 843)A12

EERC 76-3 "Dynamic Behavior of a Multistory Triangular-Shaped Building," by J. Petrovski, R.M. Stephen, E. Gartenbaum and J.G. Bouwkamp - 1976

EERC 76-4 "Earthquake Induced Deformations of Earth Dams," by N. Serff and H.B. Seed - 1976

EERC 76-5 "Analysis and Design of Tube-Type Tall Building Structures," by H. de Clercq and G.H. Powell - 1976 (PB 252 220) A10

EERC 76-6 "Time and Frequency Domain Analysis of Three-Dimensional Ground Motions, San Fernando Earthquake," by T. Kubo and J. Penzien (PB 260 556)A11

EERC 76-7 "Expected Performance of Uniform Building Code Design Masonry Structures," by R.L. Mayes, Y. Omote, S.W. Chen and R.W. Clough - 1976

EERC 76-8 "Cyclic Shear Tests on Concrete Masonry Piers," Part I - Test Results," by R.L. Mayes, Y. Omote and R.W. Clough - 1976 (PB 264 424)A06

EERC 76-9 "A Substructure Method for Earthquake Analysis of Structure - Soil Interaction," by J.A. Gutierrez and A.K. Chopra - 1976 (PB 257 783)A08

EERC 76-10 "Stabilization of Potentially Liquefiable Sand Deposits using Gravel Drain Systems," by H.B. Seed and J.R. Booker - 1976 (PB 258 820)A04

EERC 76-11 "Influence of Design and Analysis Assumptions on Computed Inelastic Response of Moderately Tall Frames," by G.H. Powell and D.G. Row - 1976

EERC 76-12 "Sensitivity Analysis for Hysteretic Dynamic Systems: Theory and Applications," by D. Ray, K.S. Pister and E. Polak - 1976 (PB 262 859)A04

EERC 76-13 "Coupled Lateral Torsional Response of Buildings to Ground Shaking," by C.L. Kan and A.K. Chopra - 1976 (PB 257 907)A09

EERC 76-14 "Seismic Analyses of the Banco de America," by V.V. Bertero, S.A. Mahin and J.A. Hollings - 1976

EERC 76-15 "Reinforced Concrete Frame 2: Seismic Testing and Analytical Correlation," by R.W. Clough and J. Gidwani - 1976 (PB 261 323)A08

EERC 76-16 "Cyclic Shear Tests on Masonry Piers, Part II - Analysis of Test Results," by R.L. Mayes, Y. Omote and R.W. Clough - 1976

EERC 76-17 "Structural Steel Bracing Systems: Behavior Under Cyclic Loading," by E.P. Popov, K. Takanashi and C.W. Roeder - 1976 (PB 260 715)A05

EERC 76-18 "Experimental Model Studies on Seismic Response of High Curved Overcrossings," by D. Williams and W.G. Godden - 1976

EERC 76-19 "Effects of Non-Uniform Seismic Disturbances on the Dumbarton Bridge Replacement Structure," by F. Baron and R.E. Hamati - 1976

EERC 76-20 "Investigation of the Inelastic Characteristics of a Single Story Steel Structure Using System Identification and Shaking Table Experiments," by V.C. Matzen and H.D. McNiven - 1976 (PB 258 453)A07

EERC 76-21 "Capacity of Columns with Splice Imperfections," by E.P. Popov, R.M. Stephen and R. Philbrick - 1976 (PB 260 378)A04

EERC 76-22 "Response of the Olive View Hospital Main Building during the San Fernando Earthquake," by S. A. Mahin, R. Collins, A.K. Chopra and V.V. Bertero - 1976

EERC 76-23 "A Study on the Major Factors Influencing the Strength of Masonry Prisms," by N.M. Mostaghel, R.L. Mayes, R. W. Clough and S.W. Chen - 1976

EERC 76-24 "GADFLEA - A Computer Program for the Analysis of Pore Pressure Generation and Dissipation during Cyclic or Earthquake Loading," by J.R. Booker, M.S. Rahman and H.B. Seed - 1976 (PB 263 947)A04

EERC 76-25 "Rehabilitation of an Existing Building: A Case Study," by B. Bresler and J. Axley - 1976

EERC 76-26 "Correlative Investigations on Theoretical and Experimental Dynamic Behavior of a Model Bridge Structure," by K. Kawashima and J. Penzien - 1976 (PB 263 388)A11

EERC 76-27 "Earthquake Response of Coupled Shear Wall Buildings," by T. Srichatrapimuk - 1976 (PB 265 157)A07

EERC 76-28 "Tensile Capacity of Partial Penetration Welds," by E.P. Popov and R.M. Stephen - 1976 (PB 262 899)A03

EERC 76-29 "Analysis and Design of Numerical Integration Methods in Structural Dynamics," by H.M. Hilber - 1976 (PB 264 410)A06

EERC 76-30 "Contribution of a Floor System to the Dynamic Characteristics of Reinforced Concrete Buildings," by L.J. Edgar and V.V. Bertero - 1976

EERC 76-31 "The Effects of Seismic Disturbances on the Golden Gate Bridge," by F. Baron, M. Arikan and R.E. Hamati - 1976

EERC 76-32 "Infilled Frames in Earthquake Resistant Construction," by R.E. Klingner and V.V. Bertero - 1976 (PB 265 892)A13

UCB/EERC-77/01 "PLUSH - A Computer Program for Probabilistic Finite Element Analysis of Seismic Soil-Structure Interaction," by M.P. Romo Organista, J. Lysmer and H.B. Seed - 1977

UCB/EERC-77/02 "Soil-Structure Interaction Effects at the Humboldt Bay Power Plant in the Ferndale Earthquake of June 7, 1975," by J.E. Valera, H.B. Seed, C.F. Tsai and J. Lysmer - 1977 (PB 265 795)A04

UCB/EERC-77/03 "Influence of Sample Disturbance on Sand Response to Cyclic Loading," by K. Mori, H.B. Seed and C.K. Chan - 1977 (PB 267 352)A04

UCB/EERC-77/04 "Seismological Studies of Strong Motion Records," by J. Shoja-Taheri - 1977 (PB 269 655)A10

UCB/EERC-77/05 "Testing Facility for Coupled-Shear Walls," by L. Li-Hyung, V.V. Bertero and E.P. Popov - 1977

UCB/EERC-77/06 "Developing Methodologies for Evaluating the Earthquake Safety of Existing Buildings," by No. 1 - B. Bresler; No. 2 - B. Bresler, T. Okada and D. Zisling; No. 3 - T. Okada and B. Bresler; No. 4 - V.V. Bertero and B. Bresler - 1977 (PB 267 354)A08

UCB/EERC-77/07 "A Literature Survey - Transverse Strength of Masonry Walls," by Y. Omote, R.L. Mayes, S.W. Chen and R.W. Clough - 1977 (PB 277 933)A07

UCB/EERC-77/08 "DRAIN-TABS: A Computer Program for Inelastic Earthquake Response of Three Dimensional Buildings," by R. Guendelman-Israel and G.H. Powell - 1977 (PB 270 693)A07

UCB/EERC-77/09 "SUBWALL: A Special Purpose Finite Element Computer Program for Practical Elastic Analysis and Design of Structural Walls with Substructure Option," by D.Q. Le, H. Peterson and E.P. Popov - 1977 (PB 270 567)A05

UCB/EERC-77/10 "Experimental Evaluation of Seismic Design Methods for Broad Cylindrical Tanks," by D.P. Clough (PB 272 280)A13

UCB/EERC-77/11 "Earthquake Engineering Research at Berkeley - 1976," - 1977 (PB 273 507)A09

UCB/EERC-77/12 "Automated Design of Earthquake Resistant Multistory Steel Building Frames," by N.D. Walker, Jr. - 1977 (PB 276 526)A09

UCB/EERC-77/13 "Concrete Confined by Rectangular Hoops Subjected to Axial Loads," by J. Vallenas, V.V. Bertero and E.P. Popov - 1977 (PB 275 165)A06

UCB/EERC-77/14 "Seismic Strain Induced in the Ground During Earthquakes," by Y. Sugimura - 1977 (PB 284 201)A04

UCB/EERC-77/15 "Bond Deterioration under Generalized Loading," by V.V. Bertero, E.P. Popov and S. Viwathanatepa - 1977

UCB/EERC-77/16 "Computer Aided Optimum Design of Ductile Reinforced Concrete Moment Resisting Frames," by S.W. Zagajeski and V.V. Bertero - 1977 (PB 280 137)A07

UCB/EERC-77/17 "Earthquake Simulation Testing of a Stepping Frame with Energy-Absorbing Devices," by J.M. Kelly and D.F. Tsztoo - 1977 (PB 273 506)A04

UCB/EERC-77/18 "Inelastic Behavior of Eccentrically Braced Steel Frames under Cyclic Loadings," by C.W. Roeder and E.P. Popov - 1977 (PB 275 526)A15

UCB/EERC-77/19 "A Symplified Procedure for Estimating Earthquake-Induced Deformations in Dams and Embankments," by F.I. Makdisi and H.B. Seed - 1977 (PB 276 820) A04

UCB/EERC-77/20 "The Performance of Earth Dams during Earthquakes," by H.B. Seed, F.I. Makdisi and P. de Alba - 1977 (PB 276 821)A04

UCB/EERC-77/21 "Dynamic Plastic Analysis Using Stress Resultant Finite Element Formulation," by P. Lukkunapvasit and J.M. Kelly - 1977 (PB 275 453)A04

UCB/EERC-77/22 "Preliminary Experimental Study of Seismic Uplift of a Steel Frame," by R.W. Clough and A.A. Huckelbridge 1977 (PB 278 769)A08

UCB/EERC-77/23 "Earthquake Simulator Tests of a Nine-Story Steel Frame with Columns Allowed to Uplift," by A.A. Huckelbridge - 1977 (PB 277 944)A09

UCB/EERC-77/24 "Nonlinear Soil-Structure Interaction of Skew Highway Bridges," by M.-C. Chen and J. Penzien - 1977 (PB 276 176)A07

UCB/EERC-77/25 "Seismic Analysis of an Offshore Structure Supported on Pile Foundations," by D.D.-N. Liou and J. Penzien 1977 (PB 283 180)A06

UCB/EERC-77/26 "Dynamic Stiffness Matrices for Homogeneous Viscoelastic Half-Planes," by G. Dasgupta and A.K. Chopra - 1977 (PB 279 654)A06

UCB/EERC-77/27 "A Practical Soft Story Earthquake Isolation System," by J.M. Kelly and J.M. Eidinger - 1977 (PB 276 814)A07

UCB/EERC-77/28 "Seismic Safety of Existing Buildings and Incentives for Hazard Mitigation in San Francisco: An Exploratory Study," by A.J. Meltsner - 1977 (PB 281 970)A05

UCB/EERC-77/29 "Dynamic Analysis of Electrohydraulic Shaking Tables," by D. Rea, S. Abedi-Hayati and Y. Takahashi 1977 (PB 282 569)A04

UCB/EERC-77/30 "An Approach for Improving Seismic - Resistant Behavior of Reinforced Concrete Interior Joints," by B. Galunic, V.V. Bertero and E.P. Popov - 1977

UCB/EERC-78/01 "The Development of Energy-Absorbing Devices for Aseismic Base Isolation Systems," by J.M. Kelly and D.F. Tsztoo 1978 (PB 284 978)A04

UCB/EERC-78/02 "Effect of Tensile Prestrain on the Cyclic Response of Structural Steel Connections," by J.G. Bouwkamp and A. Mukhopadhyay - 1978

UCB/EERC-78/03 "Experimental Results of an Earthquake Isolation System using Natural Rubber Bearings," by J.M. Eidinger and J.M. Kelly - 1978

UCB/EERC-78/04 "Seismic Behavior of Tall Liquid Storage Tanks," by A. Niwa 1978

UCB/EERC-78/05 "Hysteretic Behavior of Reinforced Concrete Columns Subjected to High Axial and Cyclic Shear Forces," by S.W. Zagajeski, V.V. Bertero and J.G. Bouwkamp - 1978

UCB/EERC-78/06 "Inelastic Beam-Column Elements for the ANSR-I Program," by A. Riahi, D.G. Row and G.H. Powell - 1978

UCB/EERC-78/07 "Studies of Structural Response to Earthquake Ground Motion," by O.A. Lopez and A.K. Chopra - 1978

UCB/EERC-78/08 "A Laboratory Study of the Fluid-Structure Interaction of Submerged Tanks and Caissons in Earthquakes," by R.C. Byrd - 1978 (PB 284 957)A08

UCB/EERC-78/09 "Models for Evaluating Damageability of Structures," by I. Sakamoto and B. Bresler - 1978

UCB/EERC-78/10 "Seismic Performance of Secondary Structural Elements," by I. Sakamoto - 1978

UCB/EERC-78/11 Case Study--Seismic Safety Evaluation of a Reinforced Concrete School Building," by J. Axley and B. Bresler 1978

UCB/EERC-78/12 "Potential Damageability in Existing Buildings," by T. Blejwas and B. Bresler - 1978

UCB/EERC-78/13 "Dynamic Behavior of a Pedestal Base Multistory Building," by R. M. Stephen, E. L. Wilson, J. G. Bouwkamp and M. Button - 1978

UCB/EERC-78/14 "Seismic Response of Bridges - Case Studies," by R.A. Imbsen, V. Nutt and J. Penzien - 1978

UCB/EERC-78/15 "A Substructure Technique for Nonlinear Static and Dynamic Analysis," by D.G. Row and G.H. Powell - 1978

UCB/EERC-78/16 "Seismic Performance of Nonstructural and Secondary Structural Elements," by Isao Sakamoto - 1978

UCB/EERC-78/17 "Model for Evaluating Damageability of Structures," by Isao Sakamoto and B. Bresler - 1978

UCB/EERC-78/18 "Response of K-Braced Steel Frame Models to Lateral Loads," by J.G. Bouwkamp, R.M. Stephen and E.P. Popov - 1978

UCB/EERC-78/19 "Rational Design Methods for Light Equipment in Structures Subjected to Ground Motion," by Jerome L. Sackman and James M. Kelly - 1978

UCB/EERC-78/20 "Testing of a Wind Restraint for Aseismic Base Isolation," by James M. Kelly and Daniel E. Chitty - 1978

UCB/EERC-78/21 "APOLLO A Computer Program for the Analysis of Pore Pressure Generation and Dissipation in Horizontal Sand Layers During Cyclic or Earthquake Loading," by Philippe P. Martin and H. Bolton Seed - 1978

UCB/EERC-78/22 "Optimal Design of an Earthquake Isolation System," by M.A. Bhatti, K.S. Pister and E. Polak - 1978

UCB/EERC-78/23 "MASH A Computer Program for the Non-Linear Analysis of Vertically Propagating Shear Waves in Horizontally Layered Deposits," by Philippe P. Martin and H. Bolton Seed - 1978

UCB/EERC-78/24 "Investigation of the Elastic Characteristics of a Three Story Steel Frame Using System Identification," by Izak Kaya and Hugh D. McNiven - 1978

UCB/EERC-78/25 "Investigation of the Nonlinear Characteristics of a Three-Story Steel Frame Using System Identification," by I. Kaya and H.D. McNiven - 1978

UCB/EERC-78/26 "Studies of Strong Ground Motion in Taiwan," by Y.M. Hsiung, B.A. Bolt and J. Penzien - 1978

UCB/EERC-78/27 "Cyclic Loading Tests of Masonry Single Piers Volume 1 - Height to Width Ratio of 2," by P.A. Hidalgo, R.L. Mayes, H.D. McNiven & R.W. Clough - 1978

UCB/EERC-78/28 "Cyclic Loading Tests of Masonry Single Piers Volume 2 - Height to Width Radio of 1," by S.-W.J.Chen, P.A. Hidalgo, R.L. Mayes, R.W. Clough & H.D. McNiven - 1978

UCB/EERC-78/29 "Analytical Procedures in Soil Dynamics," by J. Lysmer - 1978

UCB/EERC-79/01 "Hysteretic Behavior of Lightweight Reinforced Concrete Beam-Column Subassemblages," by B. Forzani, E.P. Popov, and V.V. Bertero - 1979

UCB/EERC-79/02 "The Development of a Mathematical Model to Predict the Flexural Response of Reinforced Concrete Beams to Cyclic Loads, Using System Identification," by J.F. Stanton and H.D. McNiven - 1979

UCB/EERC-79/03 "Linear and Nonlinear Earthquake Response of Simple Torsionally Coupled Systems," by C.L. Kan and A.K. Chopra - 1979

UCB/EERC-79/04 "A Mathematical Model of Masonry For Predicting Its Linear Seismic Response Characteristics," by Y. Mengi and H.D. McNiven - 1979